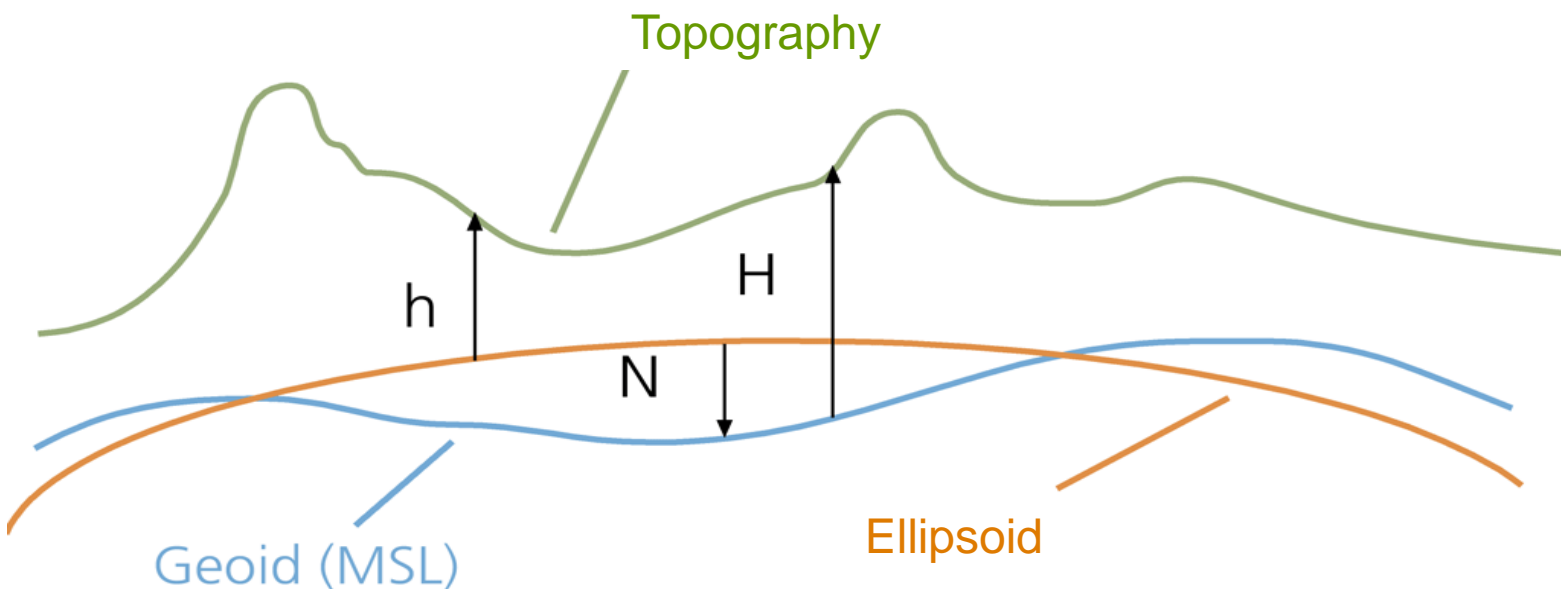

SIND WIR FÜR ZUKÜNFTIGE SCHWEREFELDMISSIONEN GERÜSTET?

Aspekte aus der Schwerefeldforschung am
Geodätischen Institut Stuttgart

Matthias Weigelt

Objective: determination of the gravity field of the Earth

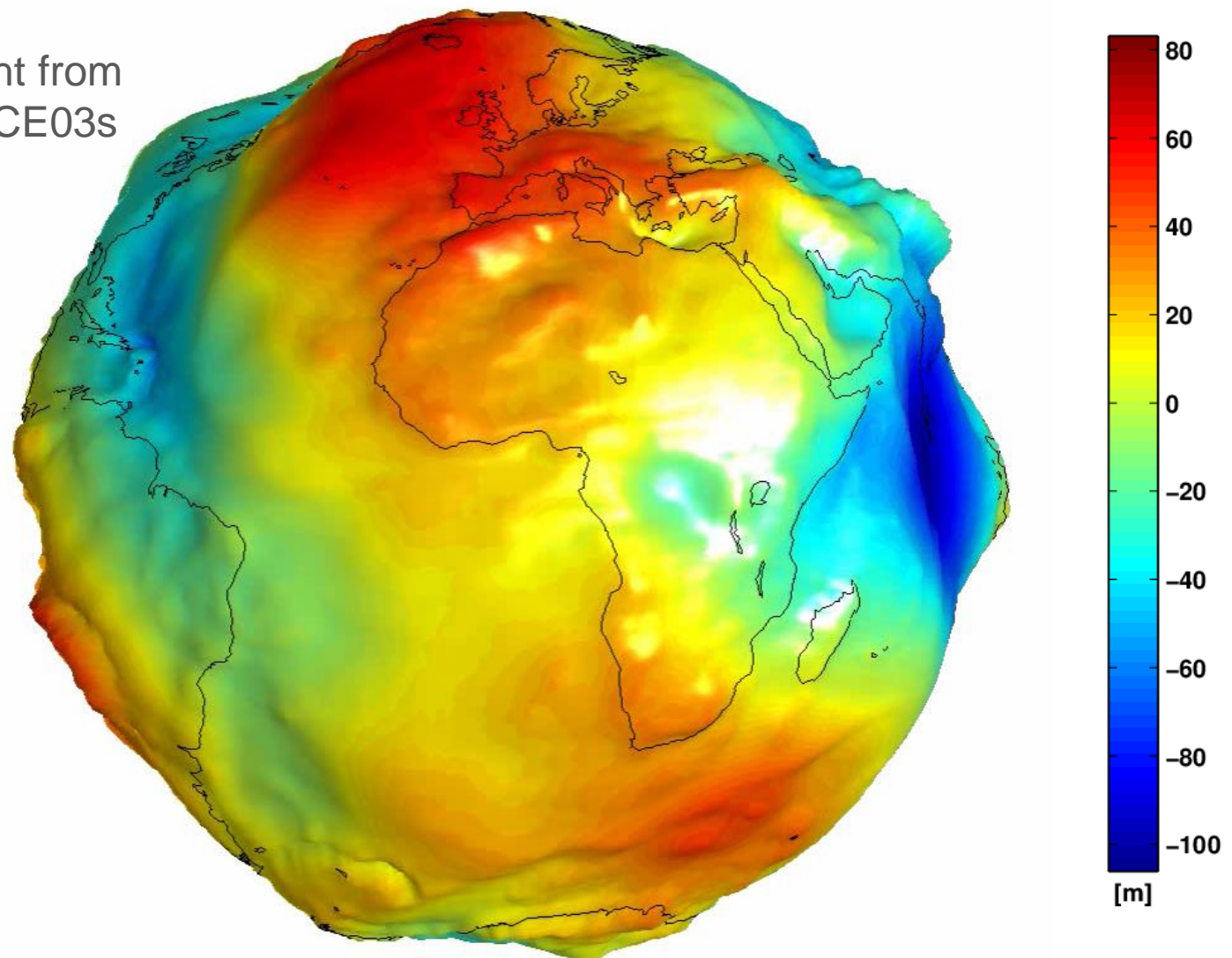
- Almost every geodetic measurement is connected to the plumb-line and/or the geoid.
- The geoid is a equipotential surface at mean sea level:
 - a. Every mass has the same potential energy at this level.
 - b. It indicates the flow of water (higher \rightarrow lower potential).
 - c. It connects GPS-heights (h) with leveled heights (H).



Determination of the potatoid

Geoid height from
AIUB-GRACE03s

Jäggi et al, 2011



$$V = \frac{GM}{R} \sum_{l=0}^{\infty} \left(\frac{R}{r} \right)^{l+1} \sum_{m=0}^l \bar{P}_{lm} (\sin \phi) (\bar{C}_{lm} \cos m\lambda + \bar{S}_{lm} \sin m\lambda)$$

with GM gravitational constant times mass of the Earth

R radius of the Earth

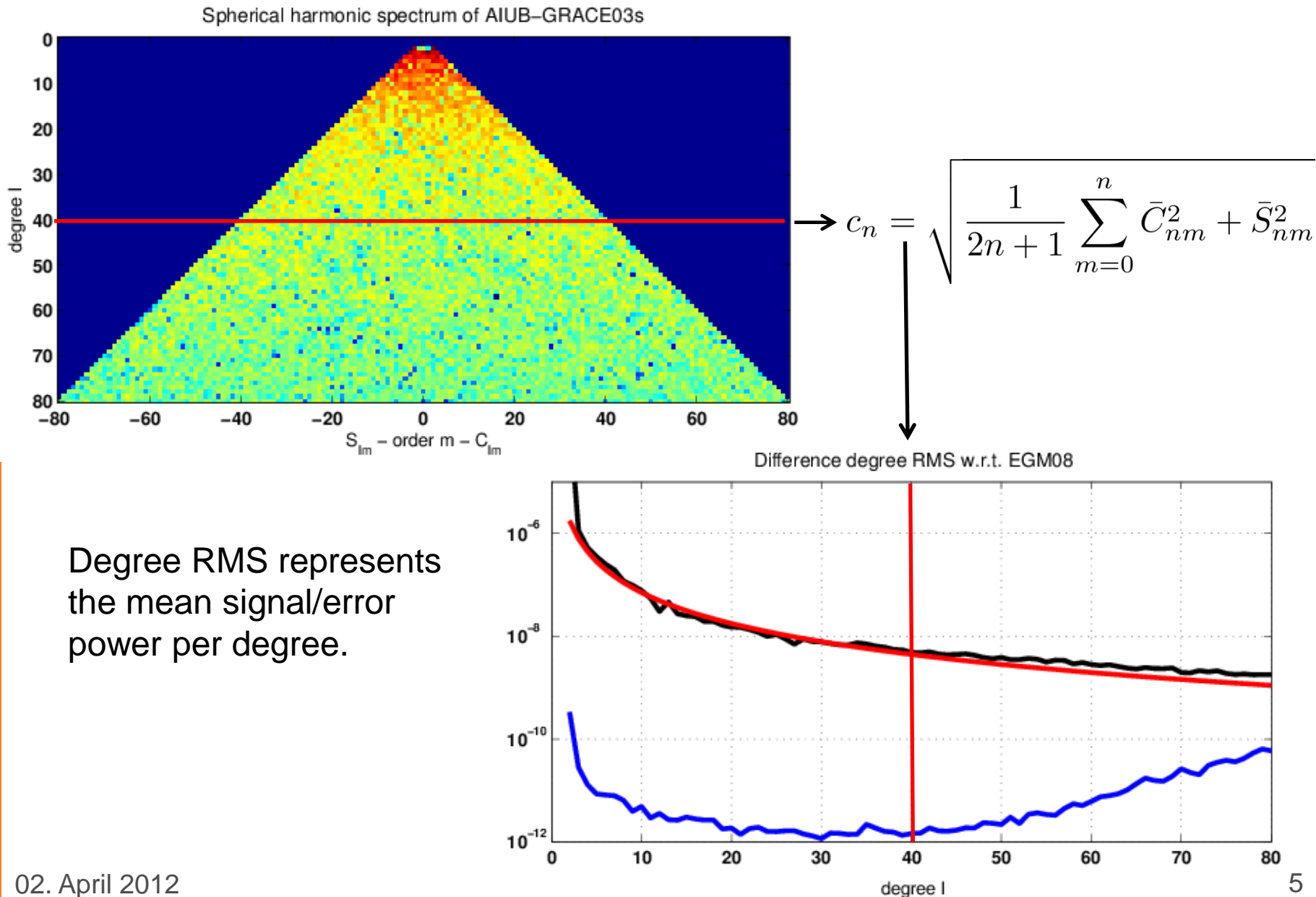
r, ϕ, λ spherical coordinates of the calculation point

\bar{P}_{lm} Legendre function

l, m degree, order

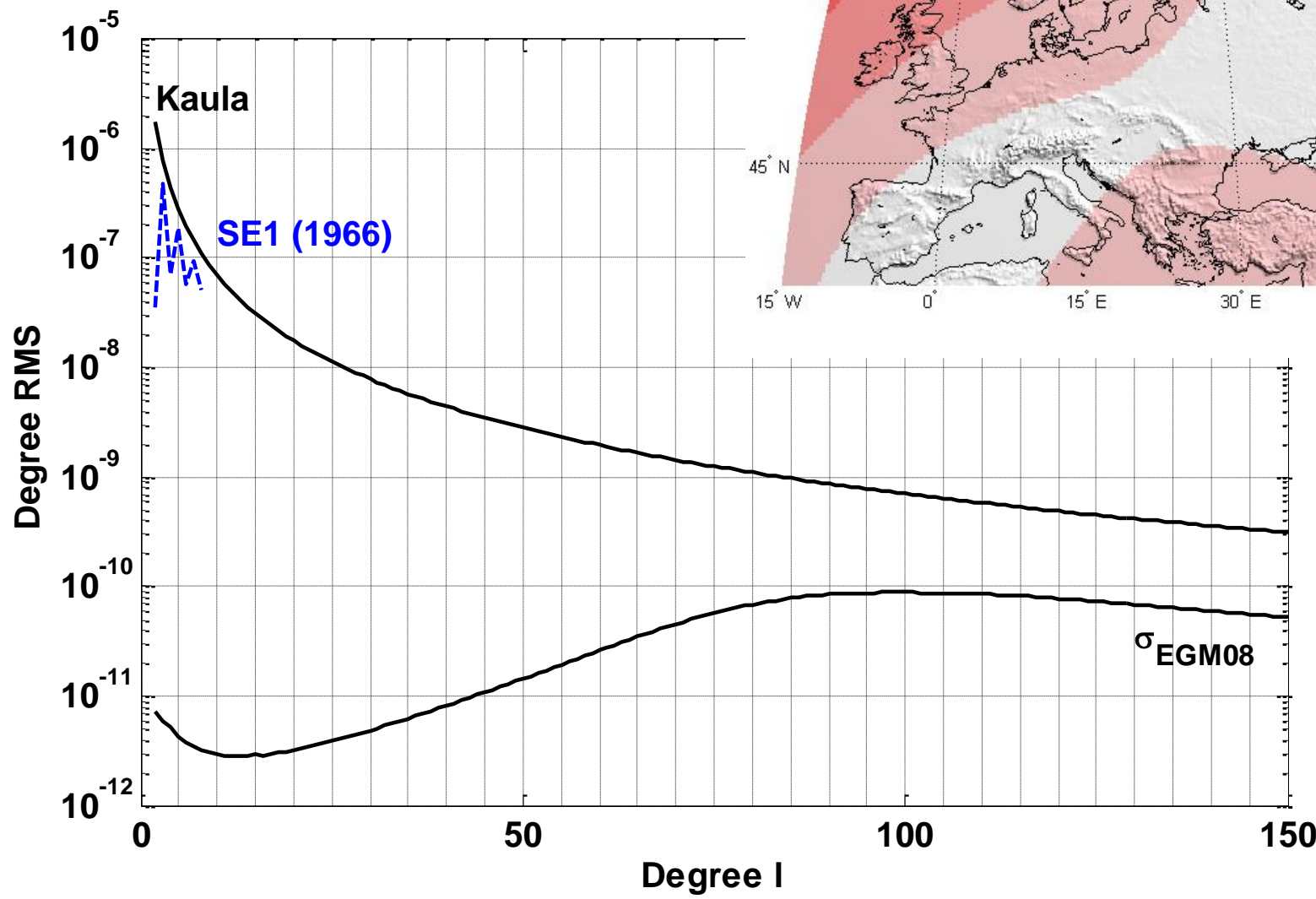
$\bar{C}_{lm}, \bar{S}_{lm}$ (unknown) spherical harmonic coefficients

Spectral representation



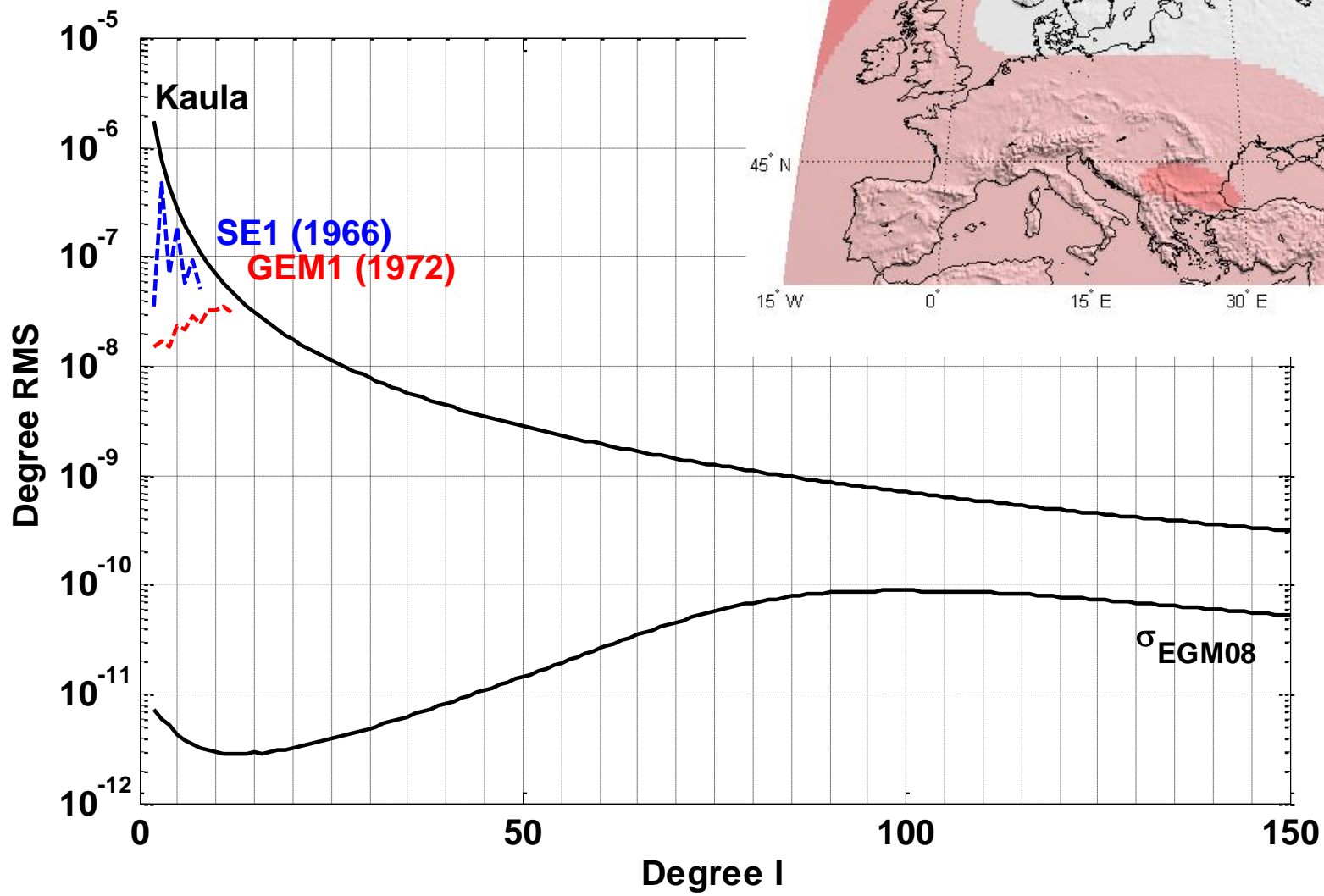
Spatial resolution

$$1966: L_{Max} = 8 \quad \frac{\lambda}{2} = 2500 \text{ km}$$



Spatial resolution

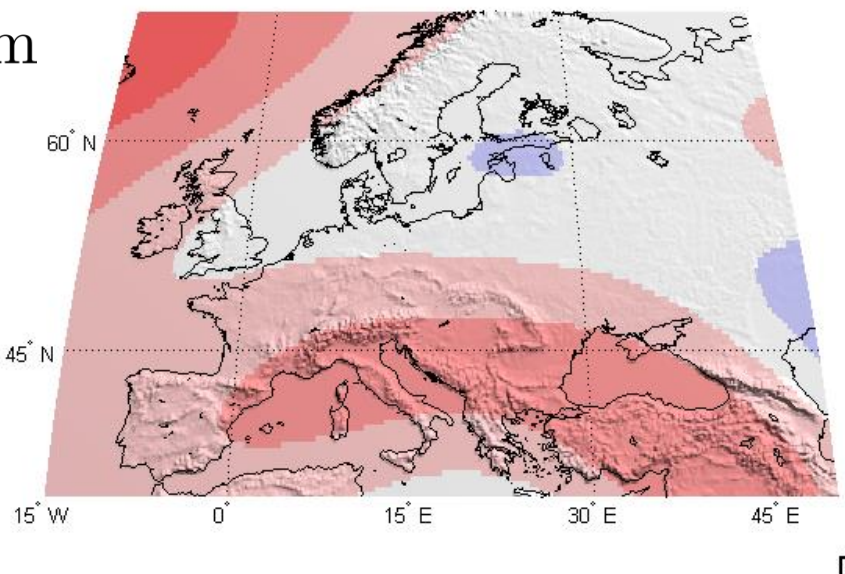
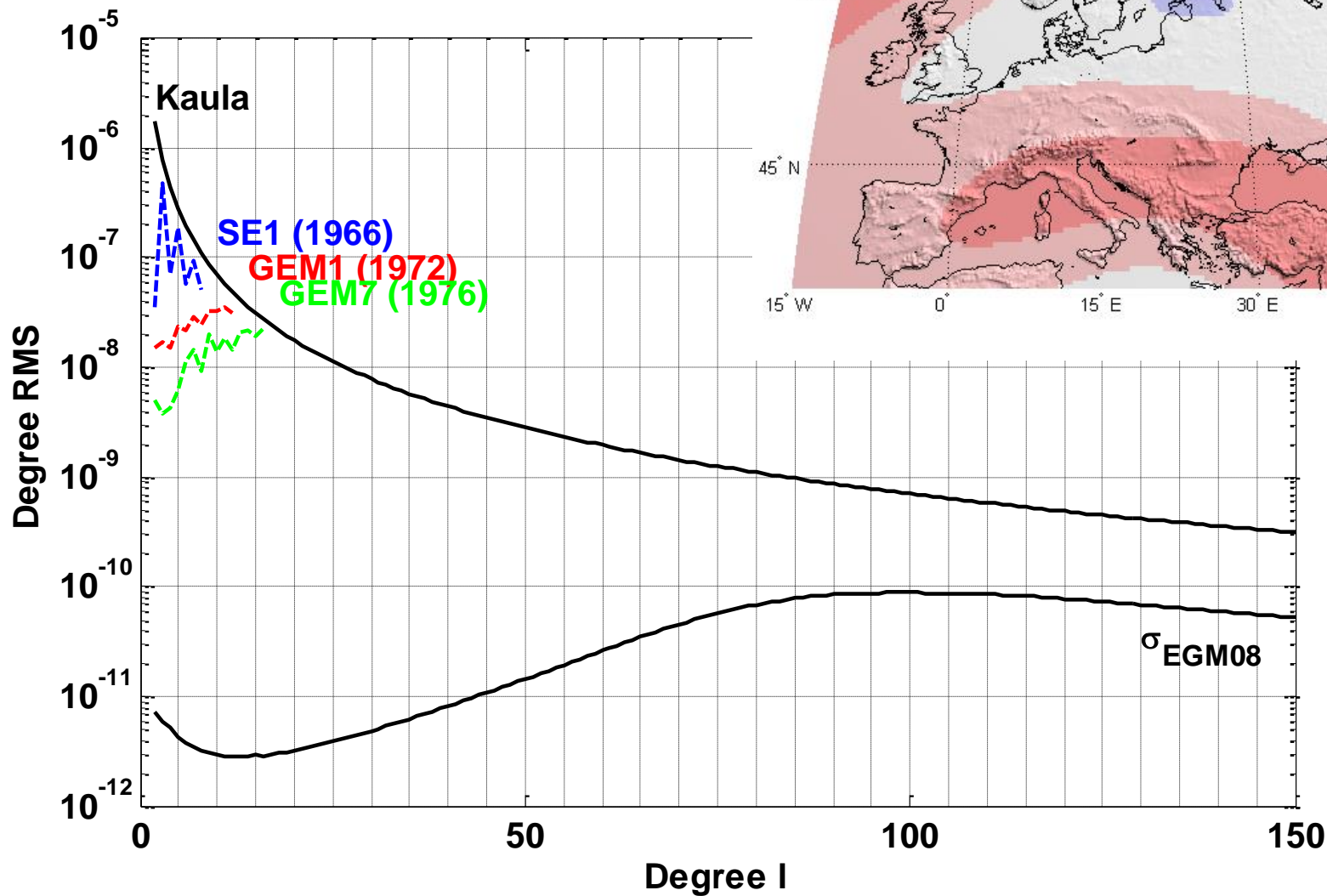
$$1972: L_{Max} = 12 \quad \frac{\lambda}{2} = 1600 \text{ km}$$



75
60
45
30
15
0
-15
-30
-45
-60
-75
[mGal]

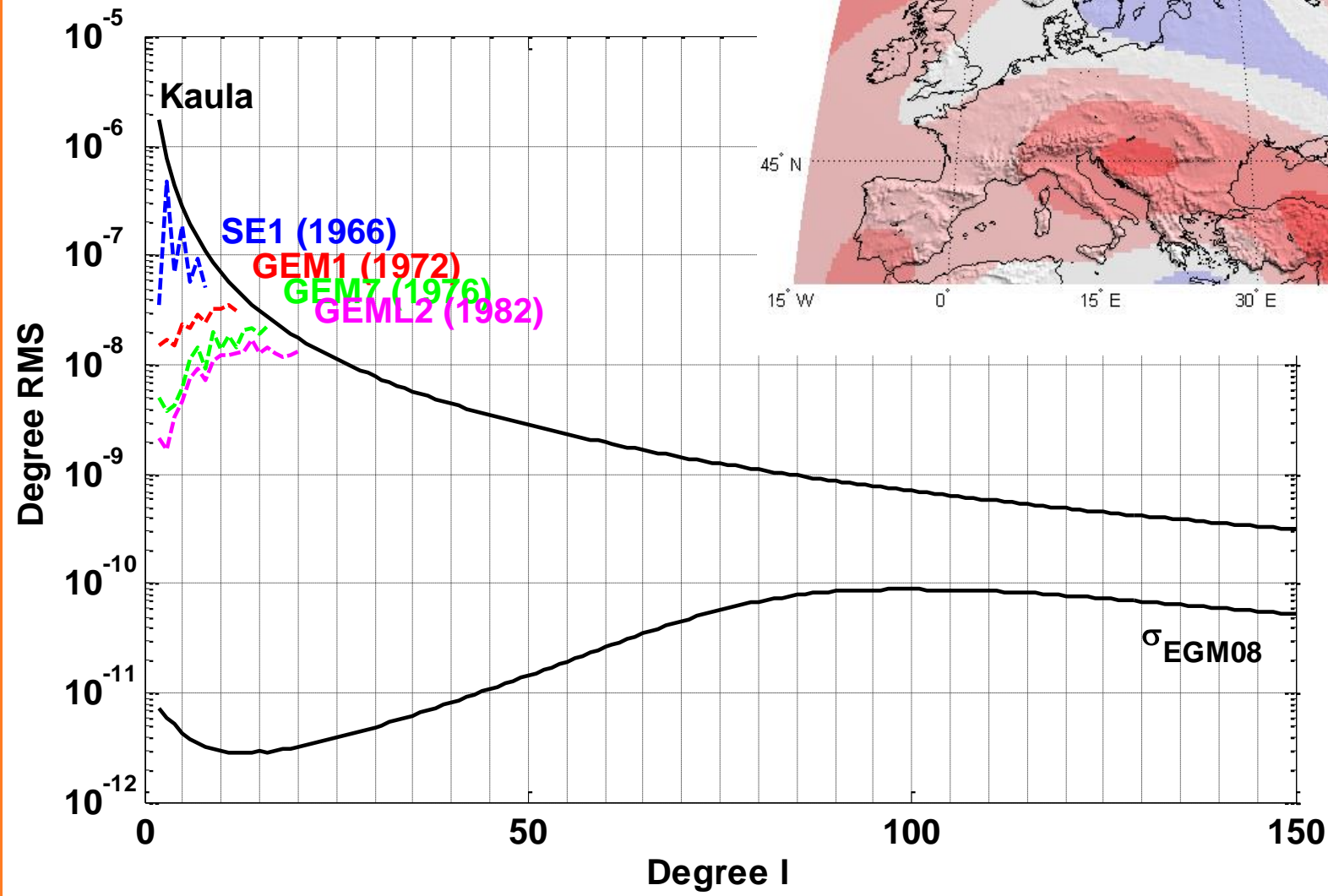
Spatial resolution

$$1976: L_{Max} = 16 \quad \frac{\lambda}{2} = 1250 \text{ km}$$



Spatial resolution

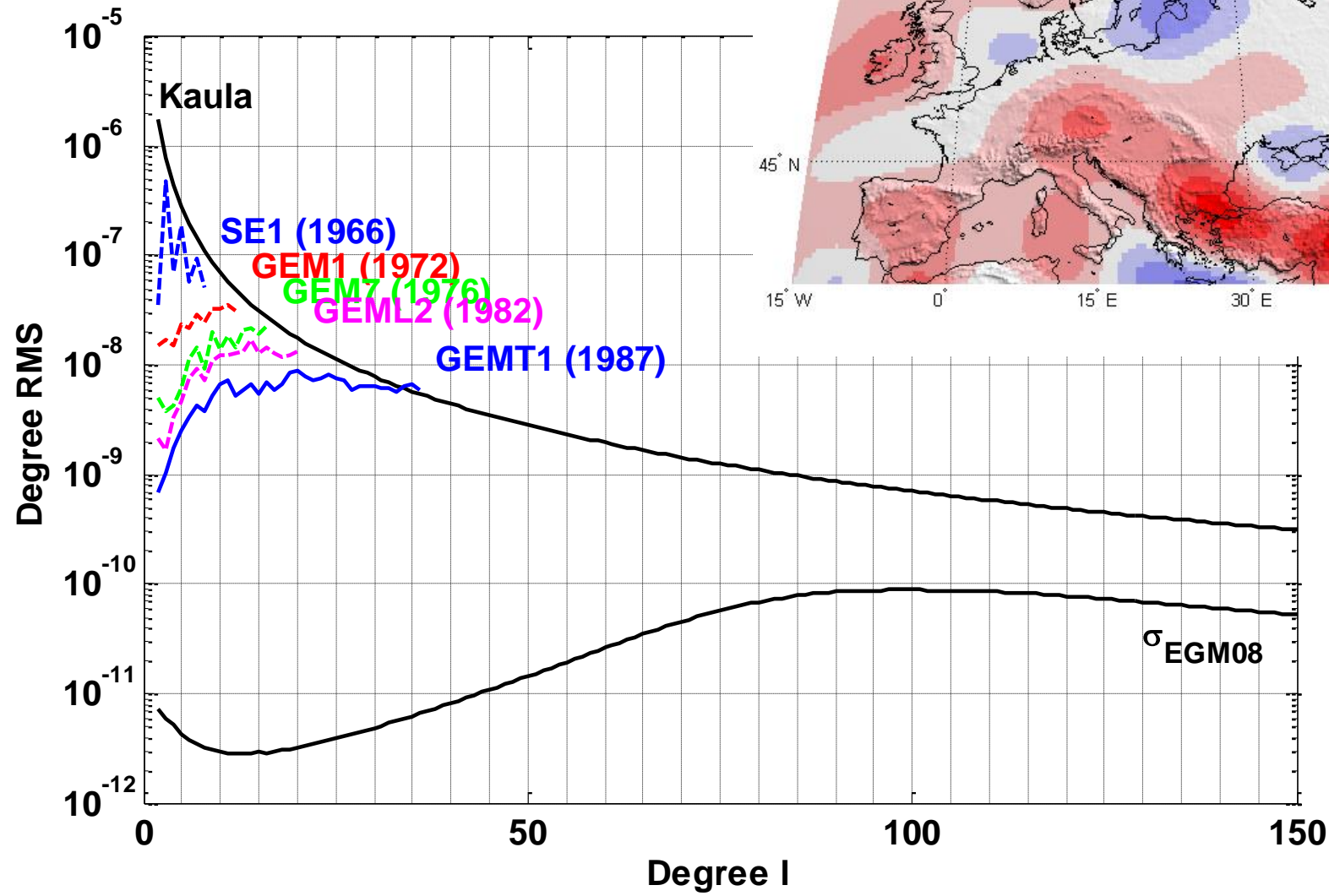
$$1982: L_{Max} = 20 \quad \frac{\lambda}{2} = 1000 \text{ km}$$



75
60
45
30
15
0
-15
-30
-45
-60
-75
[mGal]

Spatial resolution

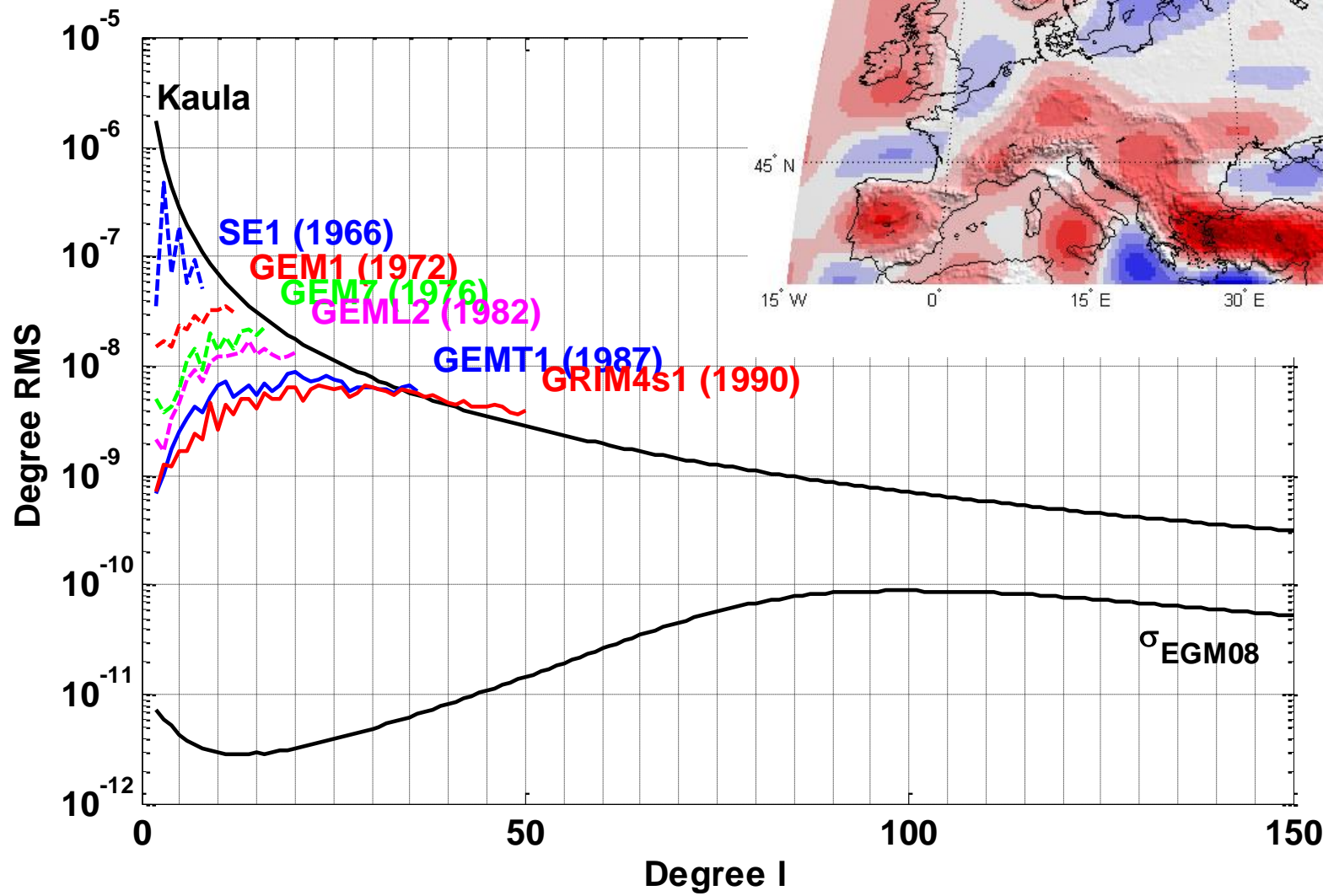
$$1987: L_{Max} = 36 \quad \frac{\lambda}{2} = 555 \text{ km}$$



75
60
45
30
15
0
-15
-30
-45
-60
-75
[mGal]

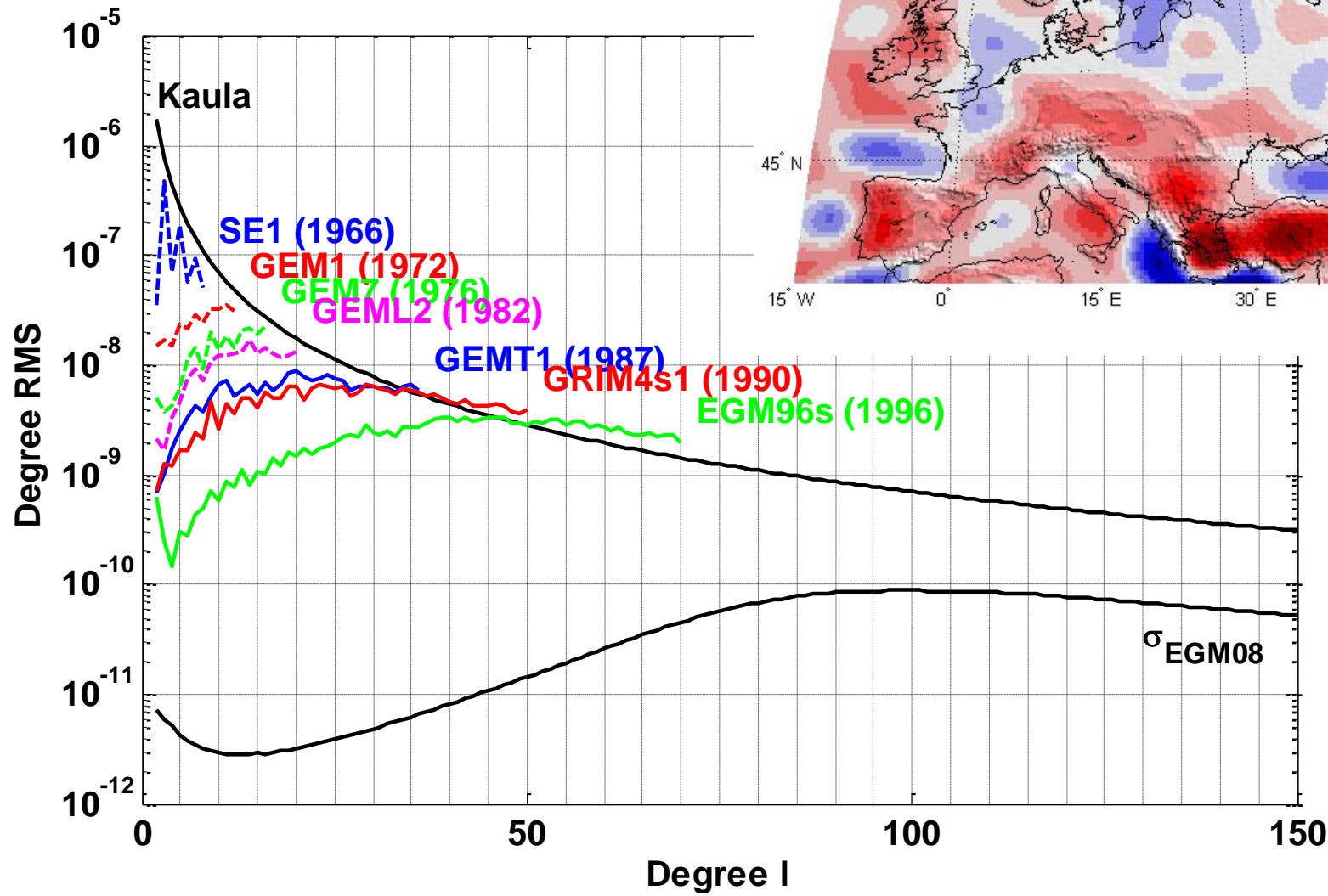
Spatial resolution

$$1990: L_{Max} = 50 \quad \frac{\lambda}{2} = 400 \text{ km}$$

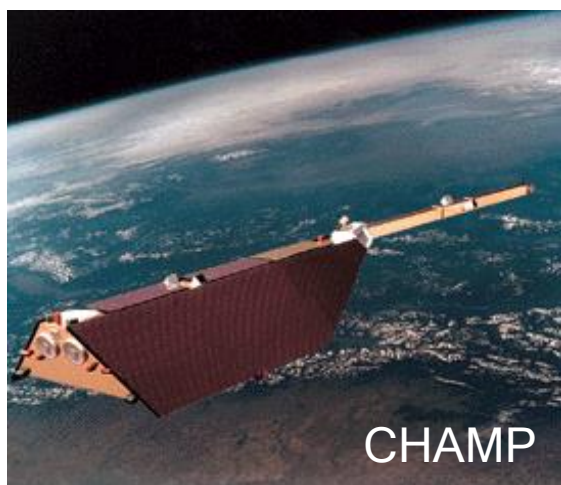
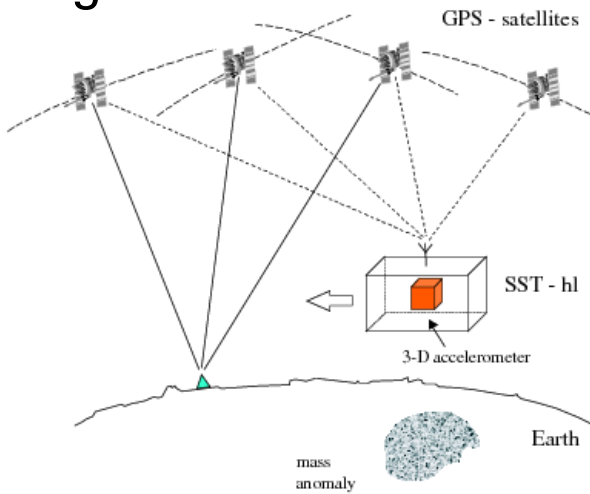


Spatial resolution

$$1996: L_{Max} = 70 \quad \frac{\lambda}{2} = 285 \text{ km}$$

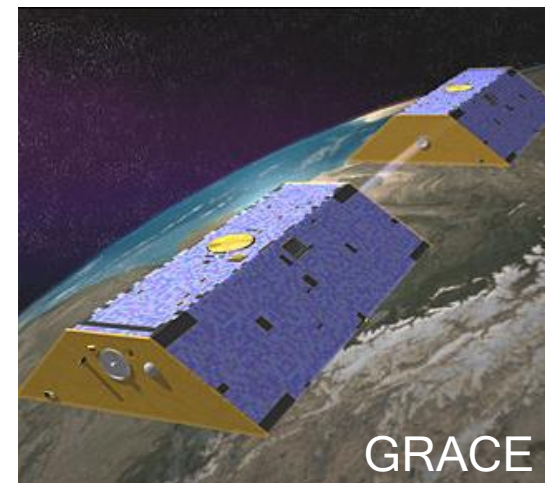
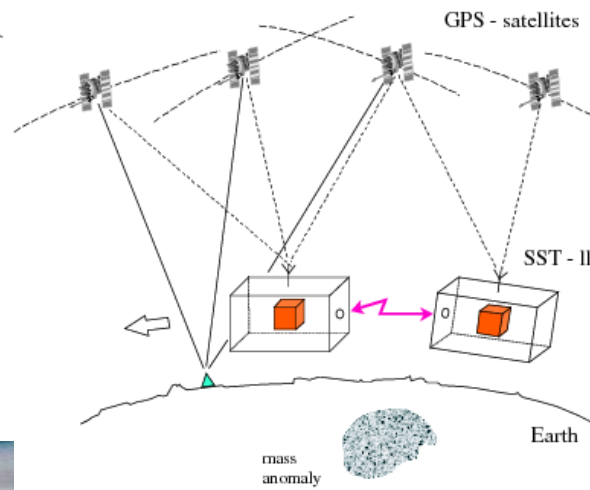


High-low SST



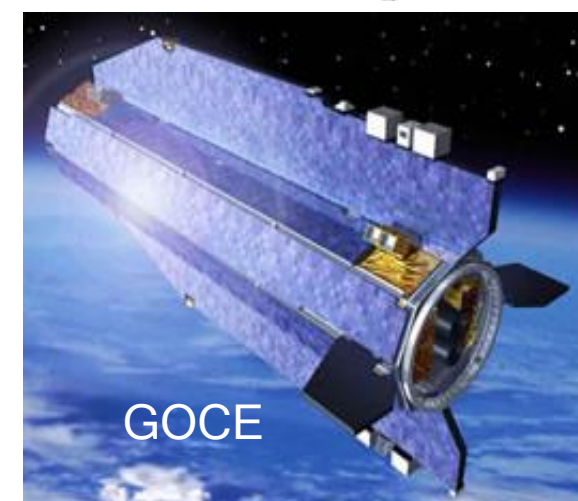
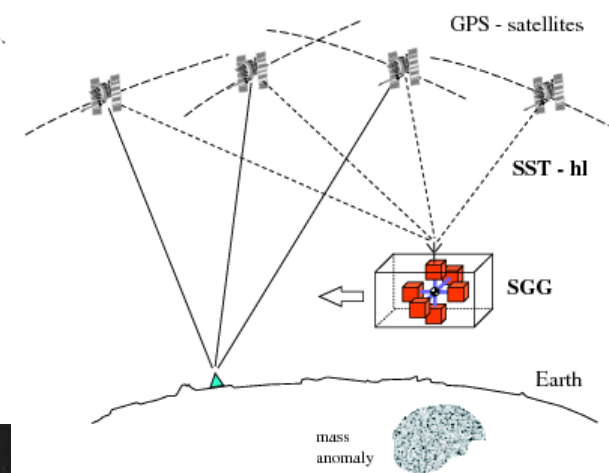
© GFZ-Potsdam

Low-low SST



© CSR Texas

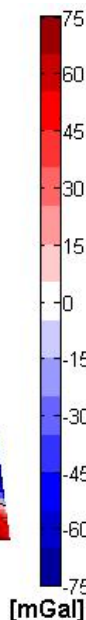
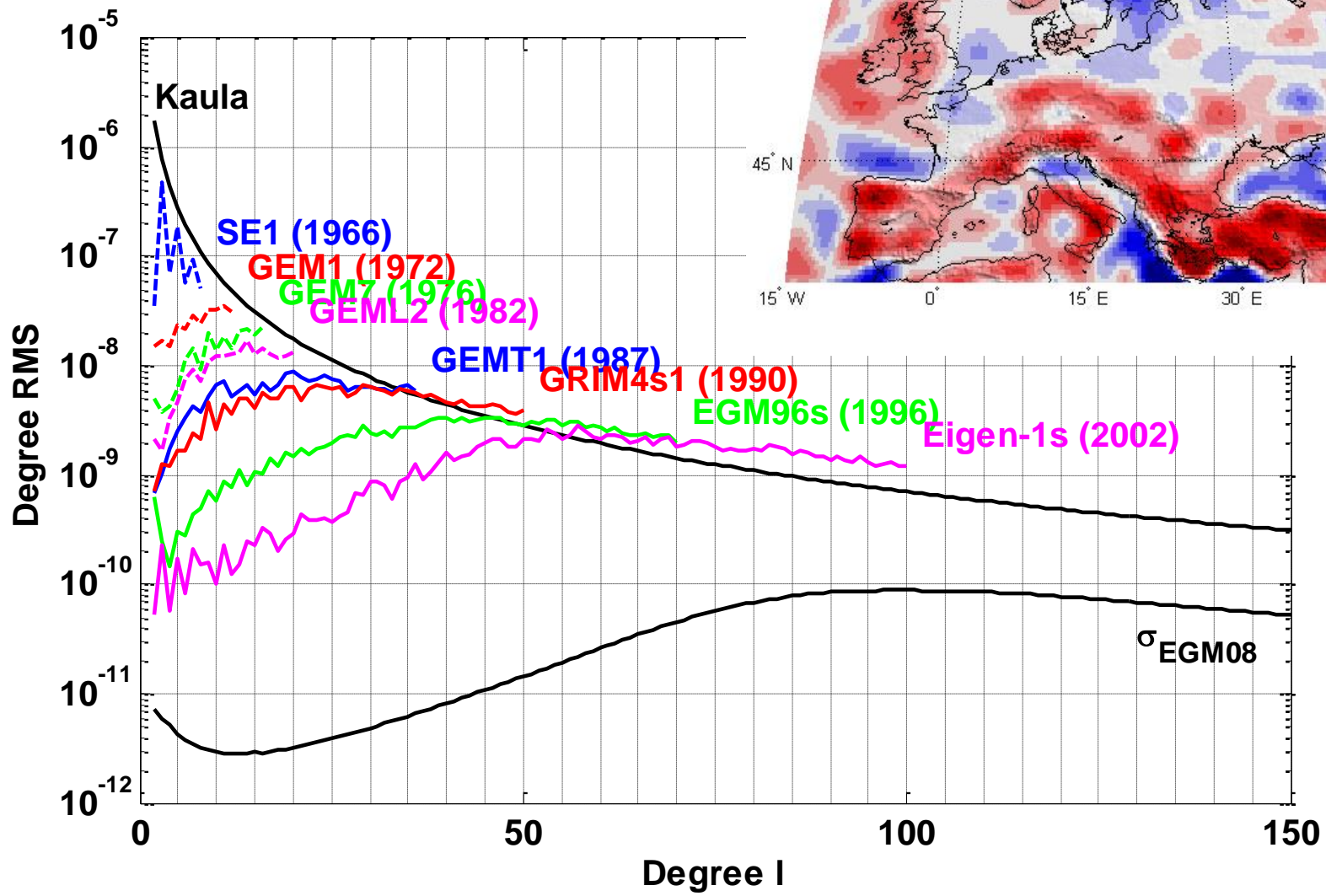
Gradiometry



© ESA

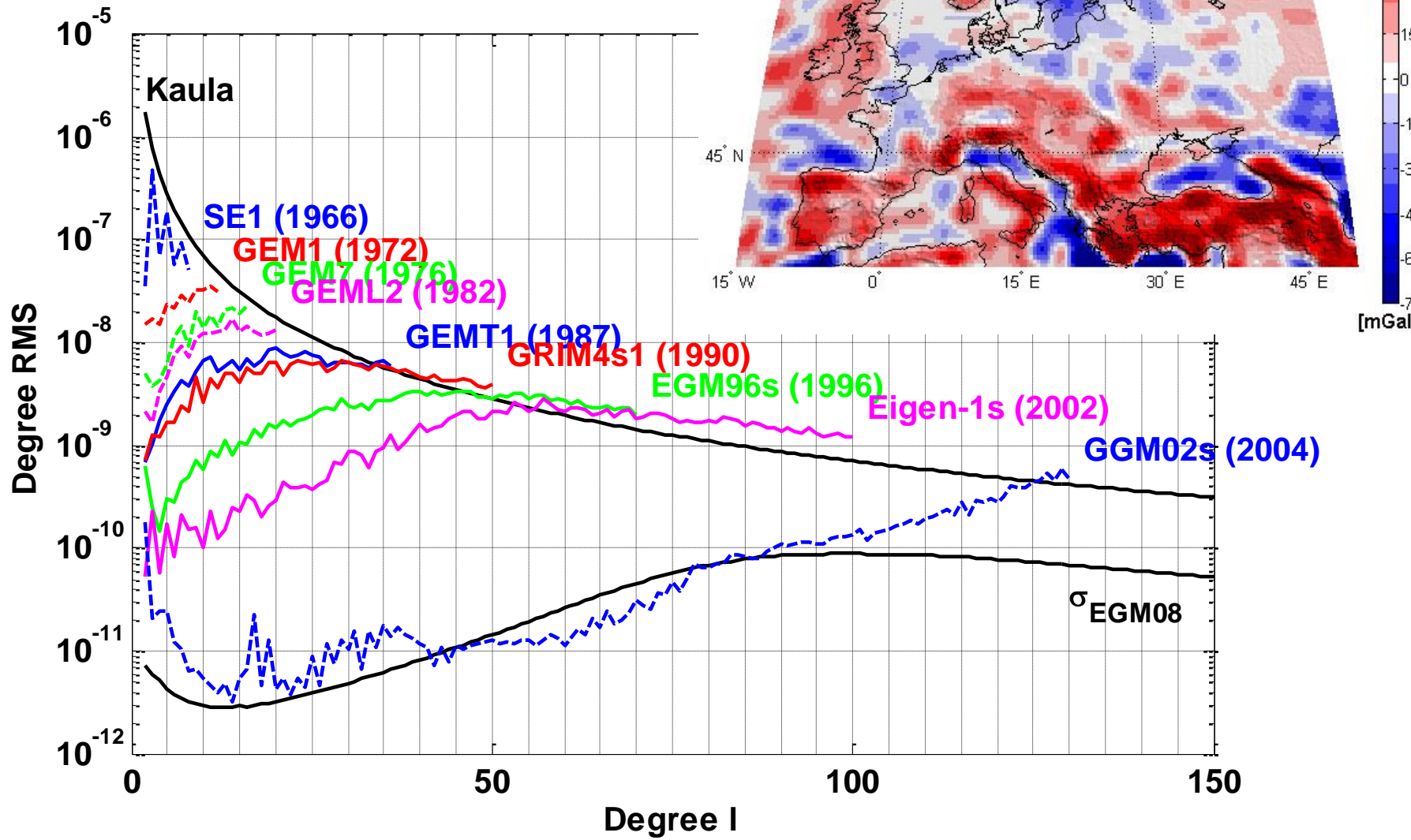
Spatial resolution

$$2002: L_{Max} = 100 \quad \frac{\lambda}{2} = 200 \text{ km}$$

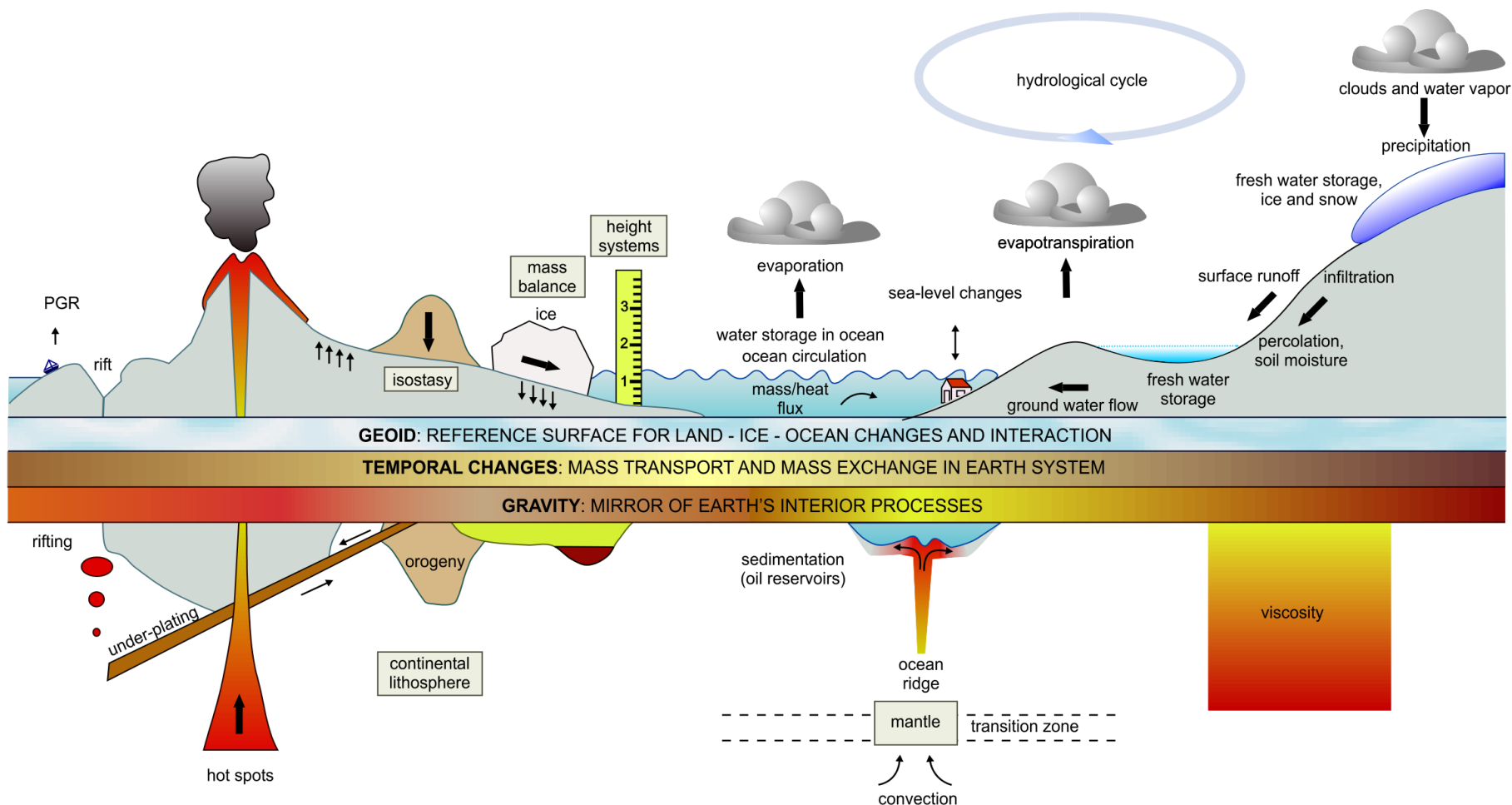


Spatial resolution

$$2004: L_{Max} = 130 \quad \frac{\lambda}{2} = 155 \text{ km}$$



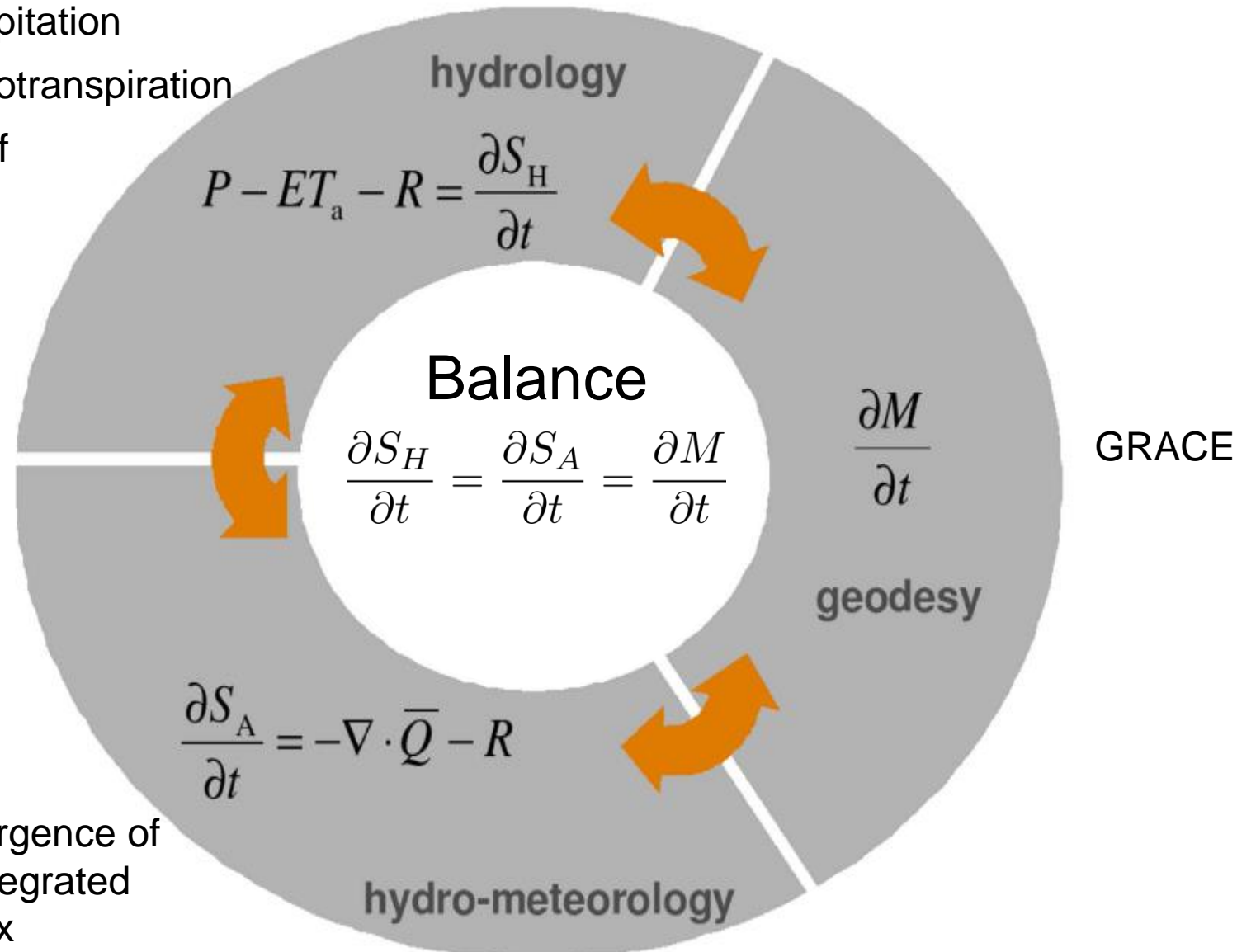
Geophysical implications of the gravity field



P = precipitation

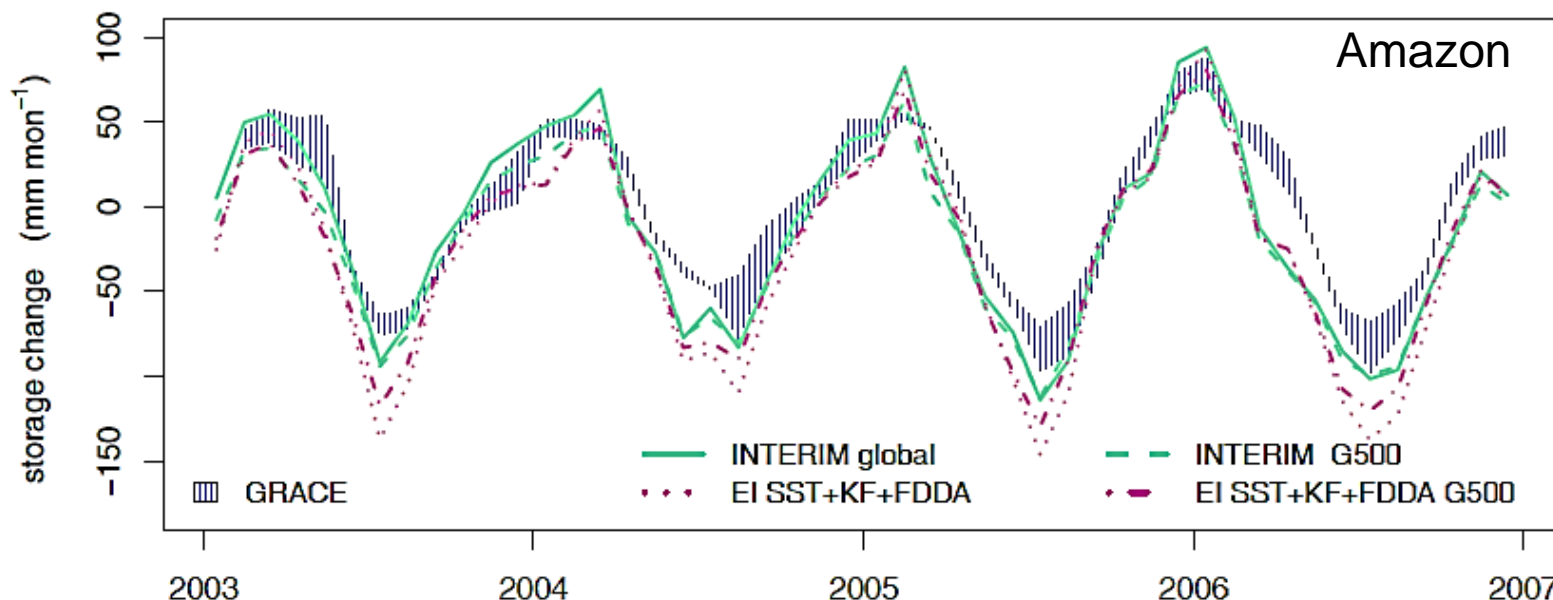
ET_a = evapotranspiration

R = runoff

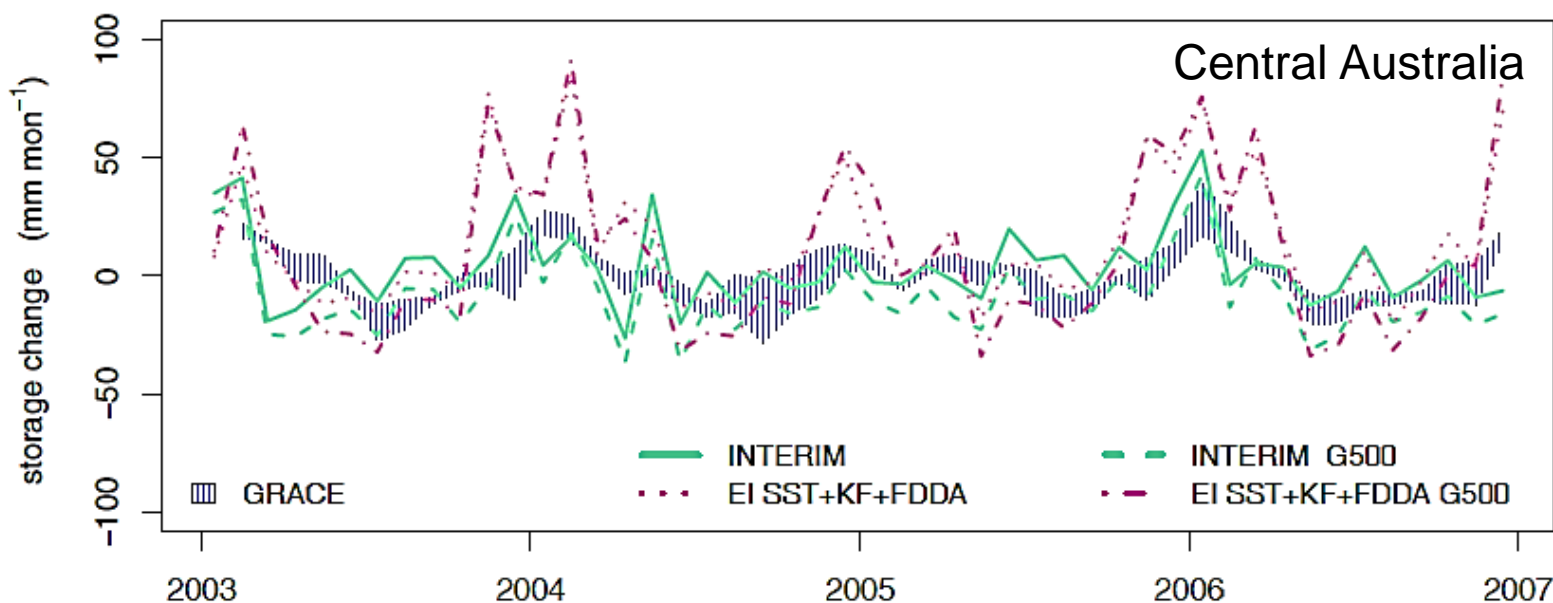


$\nabla \cdot \bar{Q}$ = divergence of
vertically integrated
moisture flux

Examples of the comparisons



Fersch, KIT



Fersch, KIT

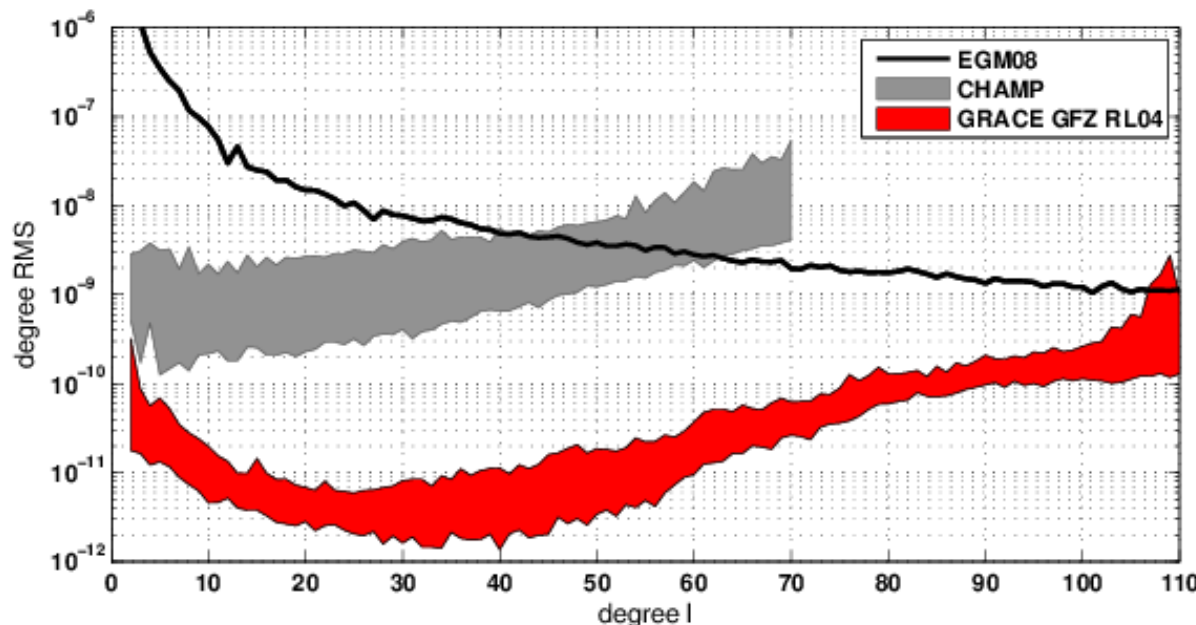
Some aspects in detail:

- CHAMP: time variability
- Spatial aliasing
- GRACE and GRACE Follow-on

PART I: CHAMP

Motivation

- Did we make use of the full potential of the CHAMP data?
- Single satellite scenario: sampling investigations
- Is the time variable gravity field really out of reach?



- What do we learn for future satellite missions?
- Can high-low SST serve as a transitory technology?

METHODOLOGY

Approach

- Acceleration approach:

$$\nabla V = \ddot{\vec{x}} - \vec{f}_{\text{3rdBody}} - \vec{f}_{\text{Tides}} - \vec{f}_{\text{Rel}} - \vec{f}_{\text{Grav}}$$

- accelerations by numerical differentiation
- three dimensional (pseudo-) observations
- evaluation in the LNOF (local North-oriented frame)

- Least-squares adjustment: $\vec{l} = A\vec{x} - \vec{\epsilon}$ $\Sigma_{ll} = \sigma_0^2 Q_{ll}$

- Covariance information:

- unit matrix
- epochwise covariance information (only correlations between coordinates)
- empirical covariance information (only correlations between epochs)
- scaled empirical covariance information (only correlations between epochs)
- full error propagation (numerical stability ?)

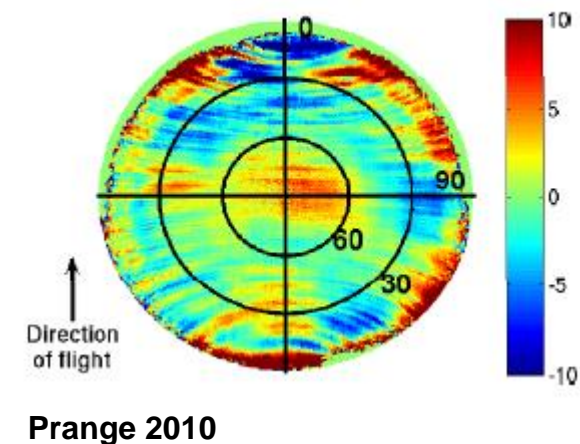
GPS positions: **AIUB**

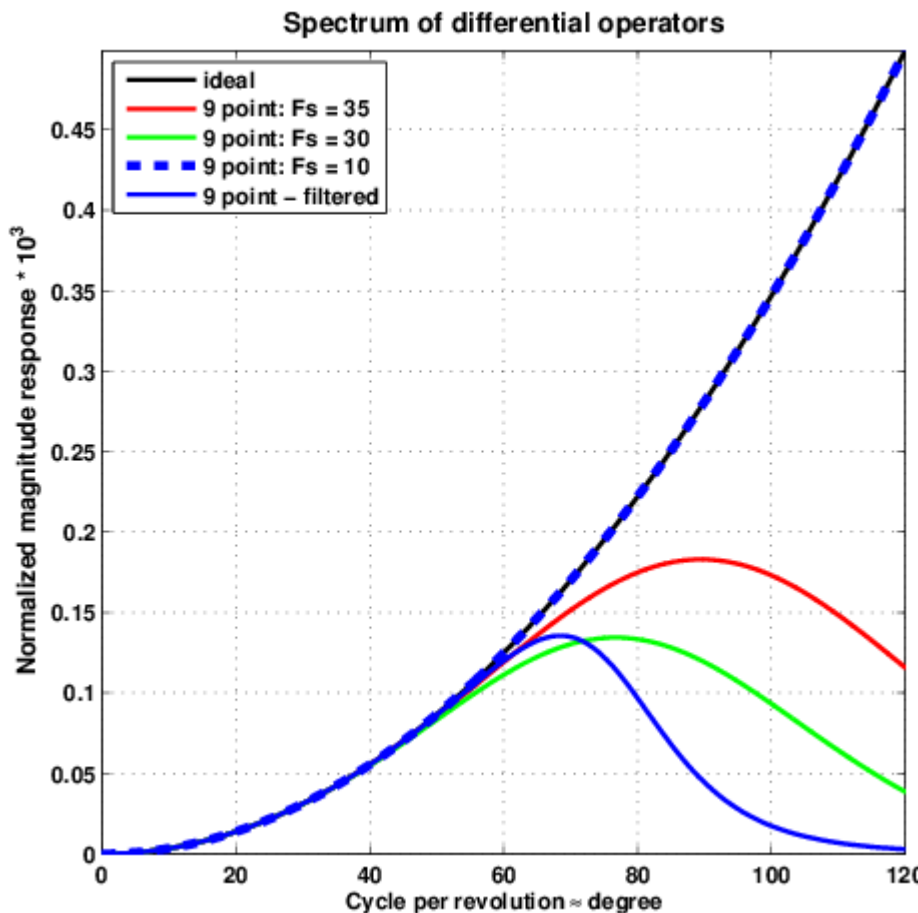
- 10 s sampling
- estimated absolute antenna phase center model
- new IGS standards
- ...

Background models:

- JPL ephemeris DE405
- Solid Earth tides (IERS conventions)
- Solid Earth pole tides (IERS conventions)
- Ocean tides (FES 2004)
- Ocean pole tides (IERS conventions, Desai 2002)
- Atmospheric tides (N1-model, Biancale and Bode 2006)
- Relativistic corrections (IERS conventions)
- AOD1B-product (Flechtner 2008)

No accelerometer data needed!





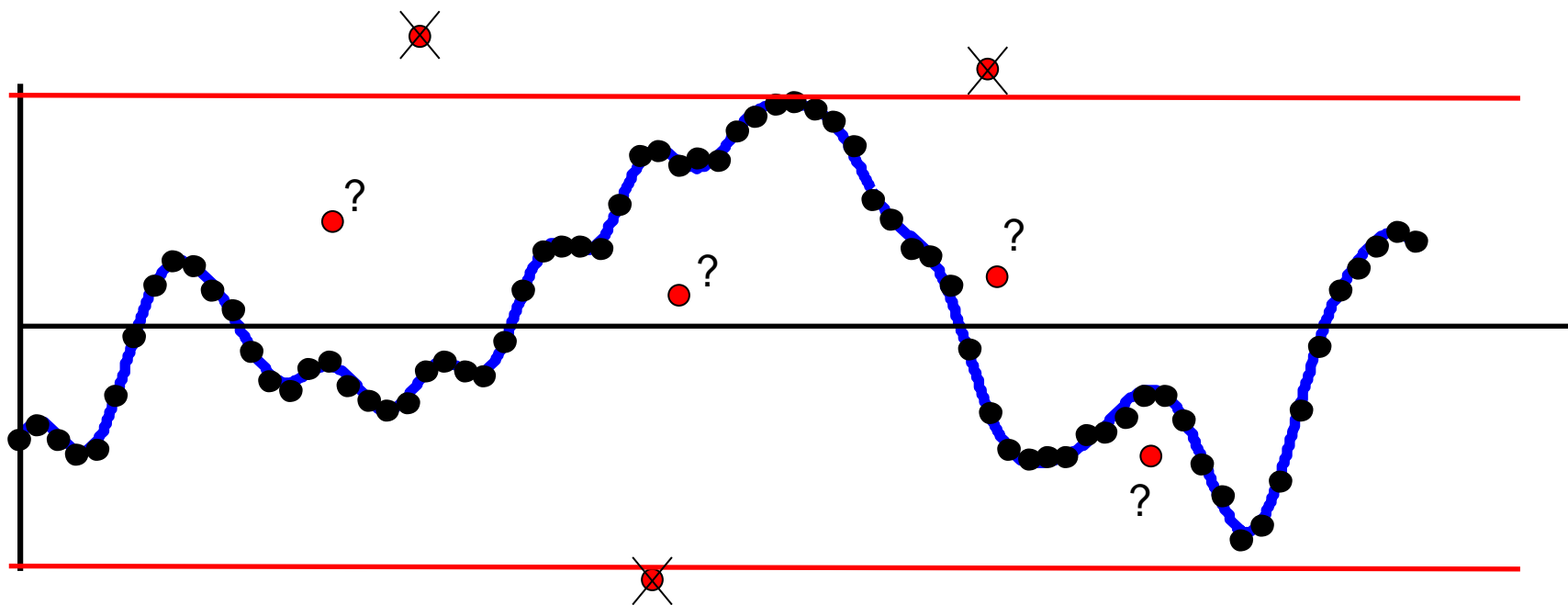
- Ideal differentiator: $|H(\omega)| = \omega^2$
- Numerical approximation by n-point central difference differentiator

$$\frac{\partial^j f_i}{\partial t^j} = \frac{1}{T} \sum_{k=-(n-1)/2}^{(n-1)/2} g_k^{(j)} f_{k+i}$$

- Filtering of high frequency noise
 - by lowpass filtering (warmup!)
 - inherently by the differentiator (varying the step size)

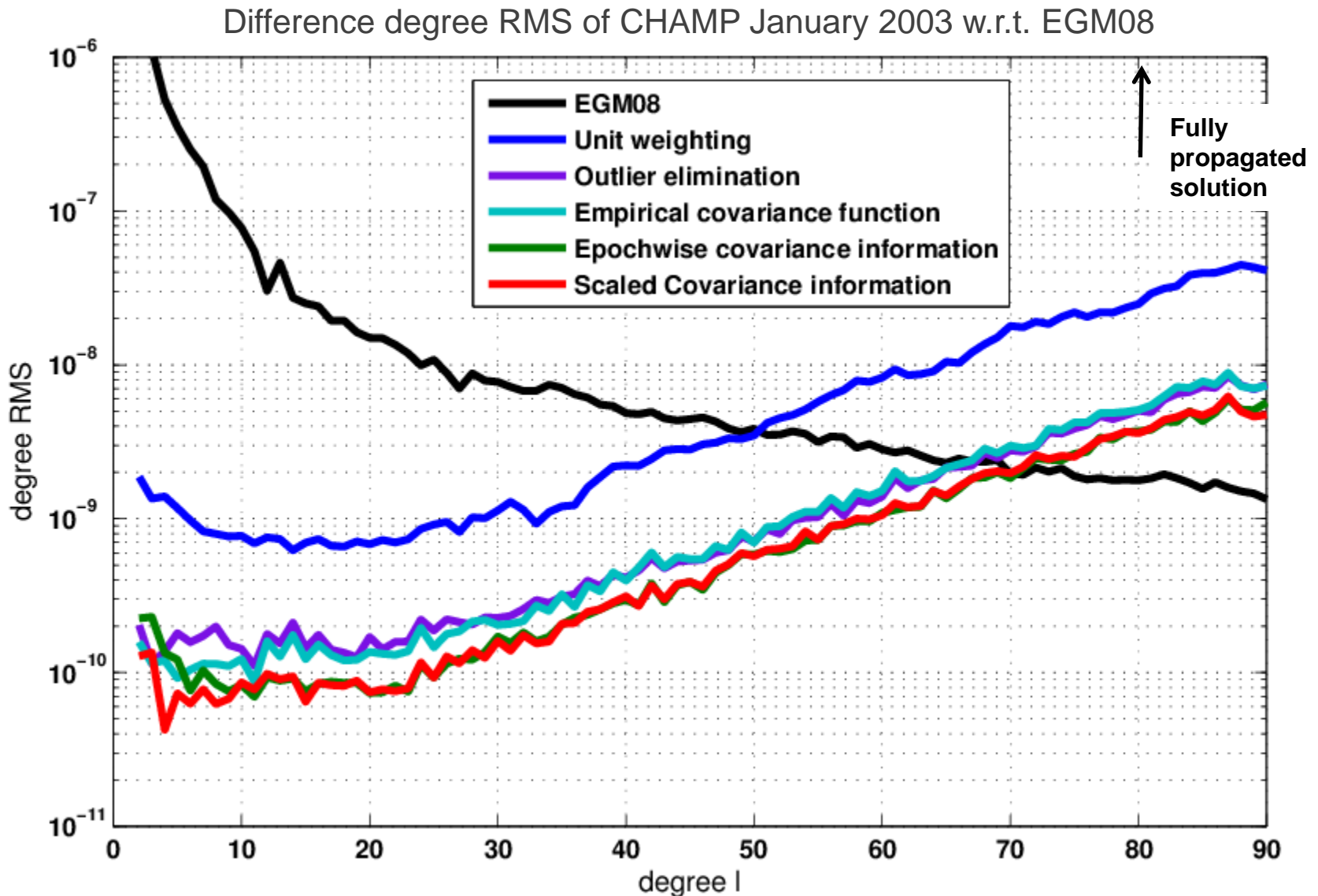
Outliers vs. poor observations

- Typically threshold based outlier detection based on residuals:



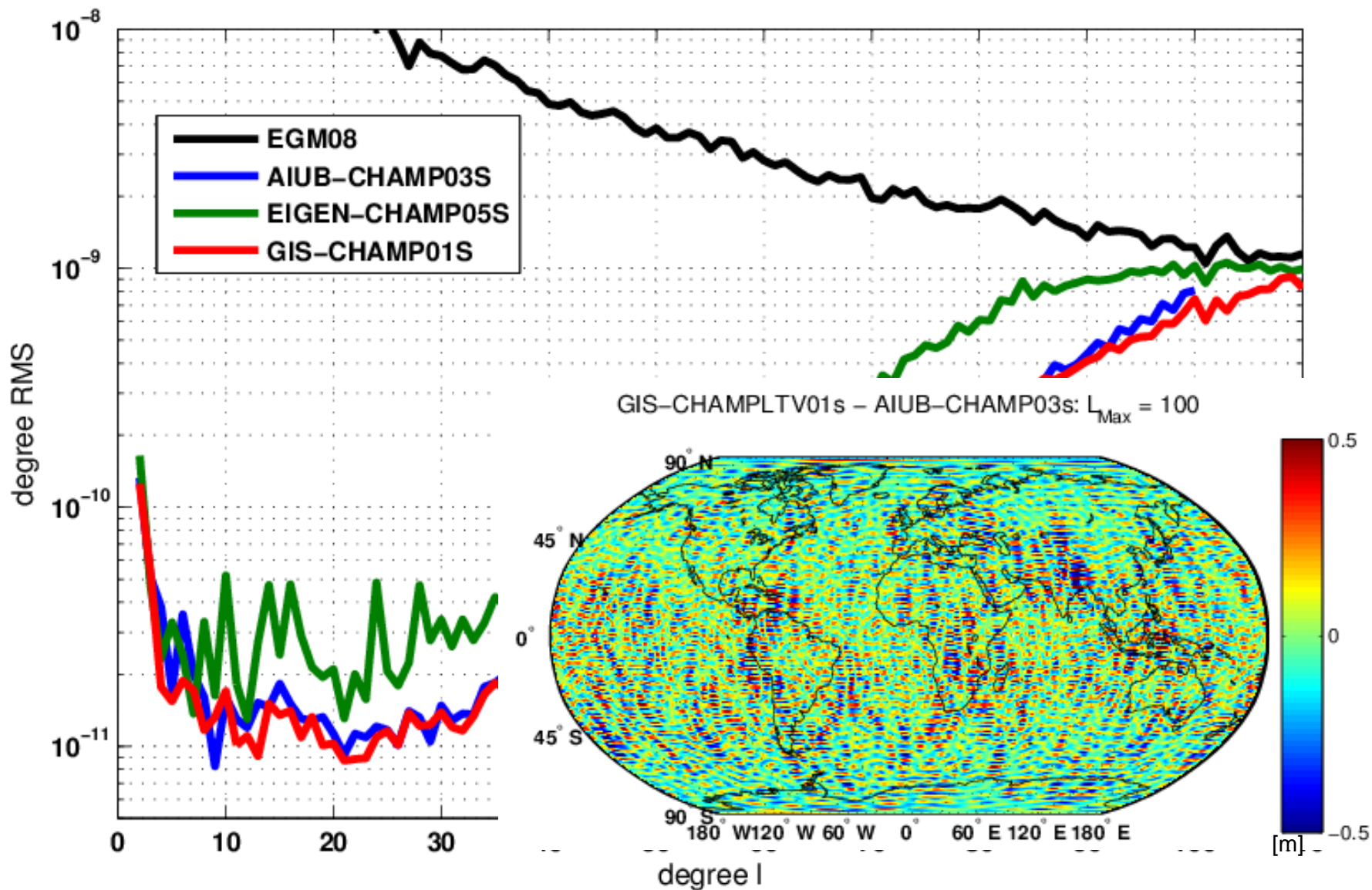
- Localizing outlier detection: moving windows (time and space domain)

Influence of outlier detection and covariance information



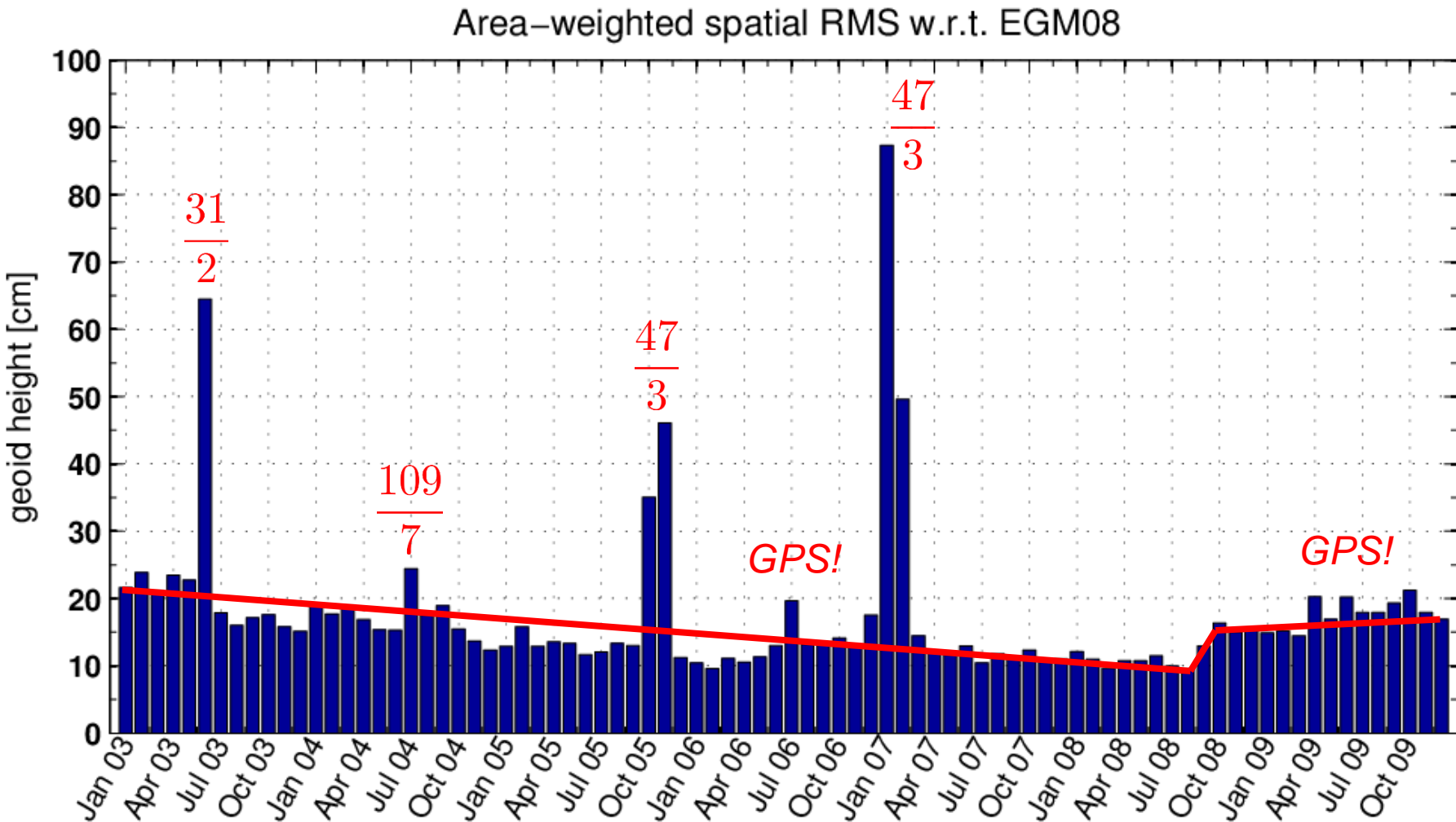
STATIC SOLUTION

CHAMP static gravity field

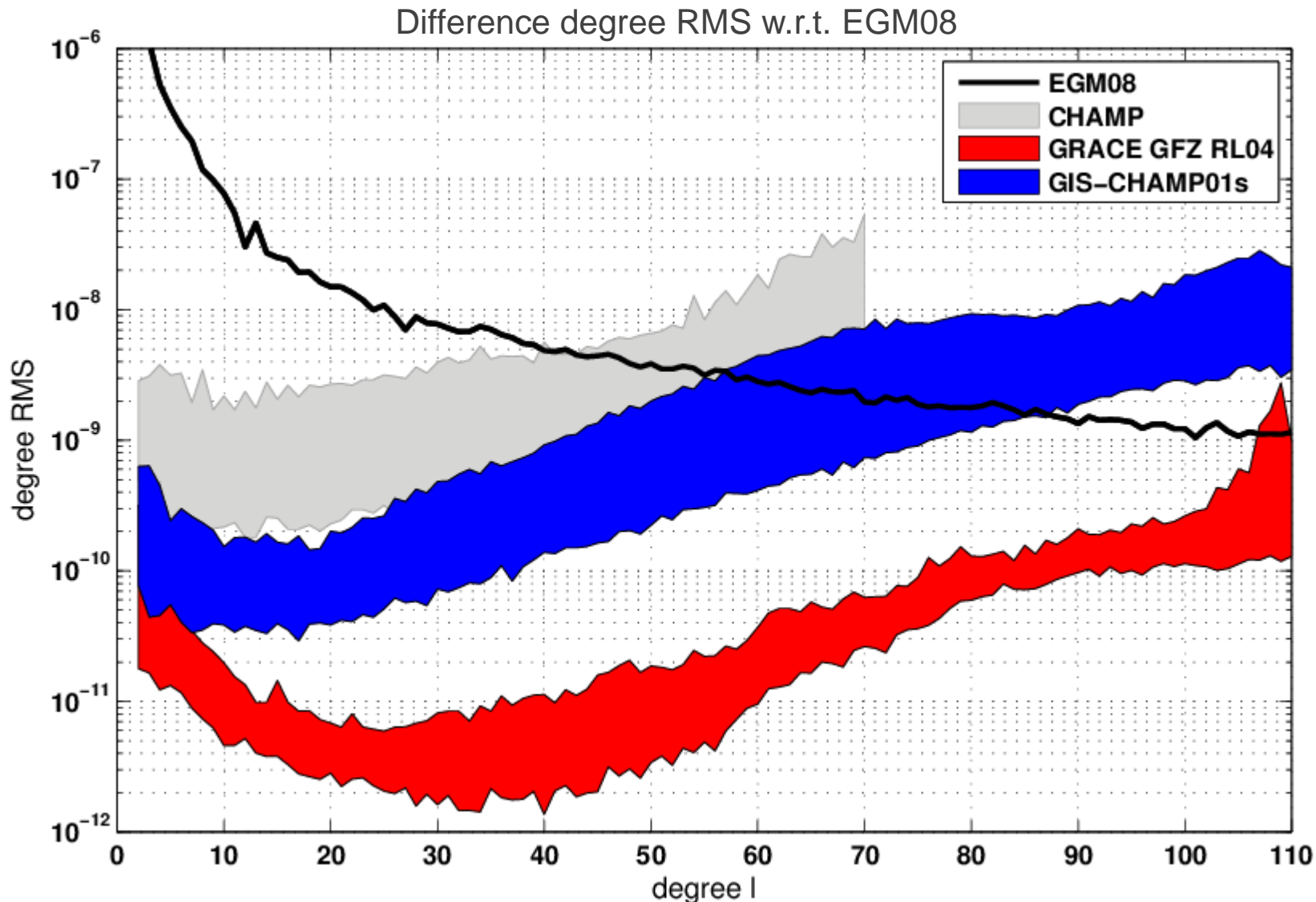


MONTHLY SOLUTIONS

CHAMP monthly gravity field solutions (1/4)

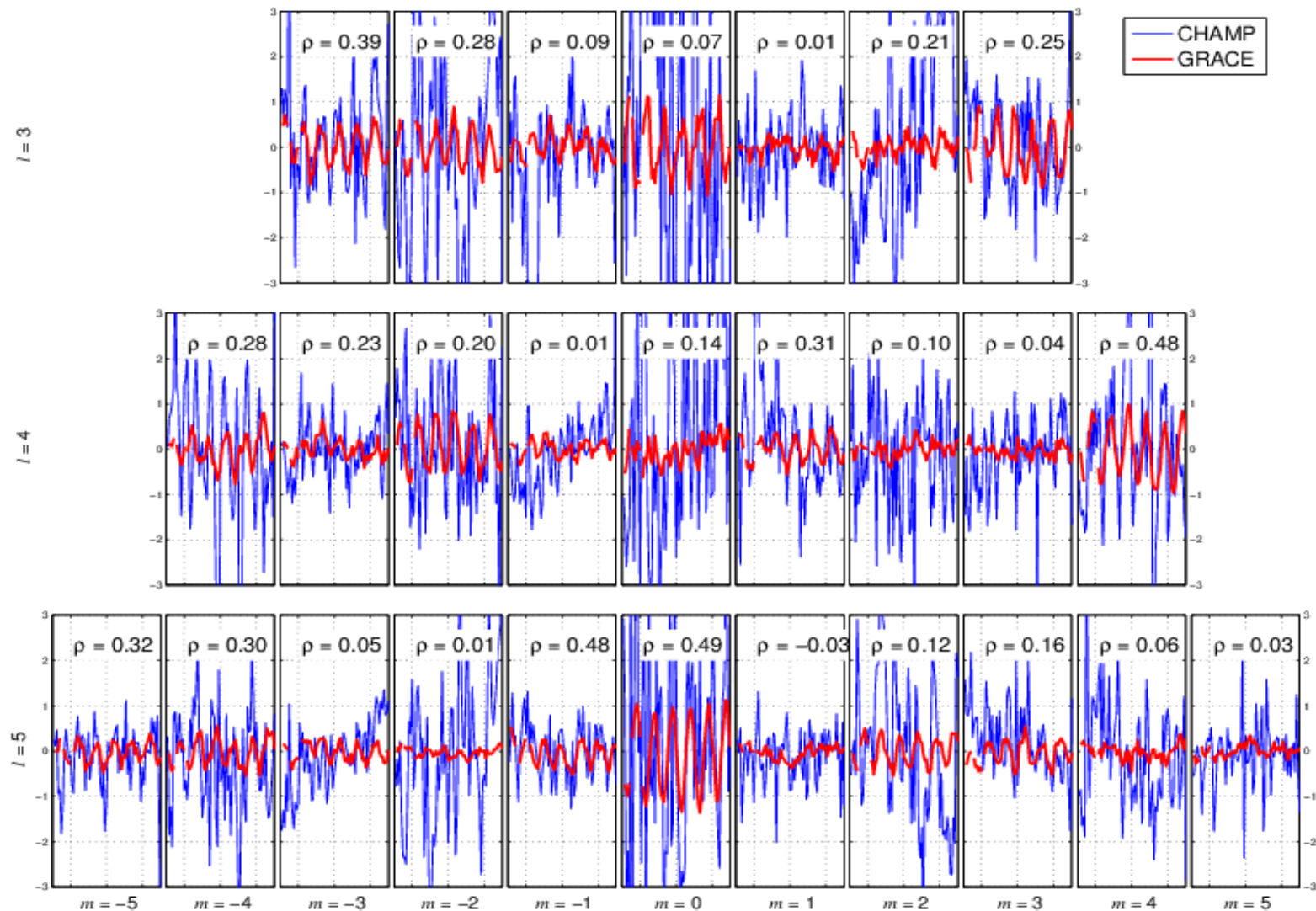


CHAMP monthly gravity field solutions (2/4)



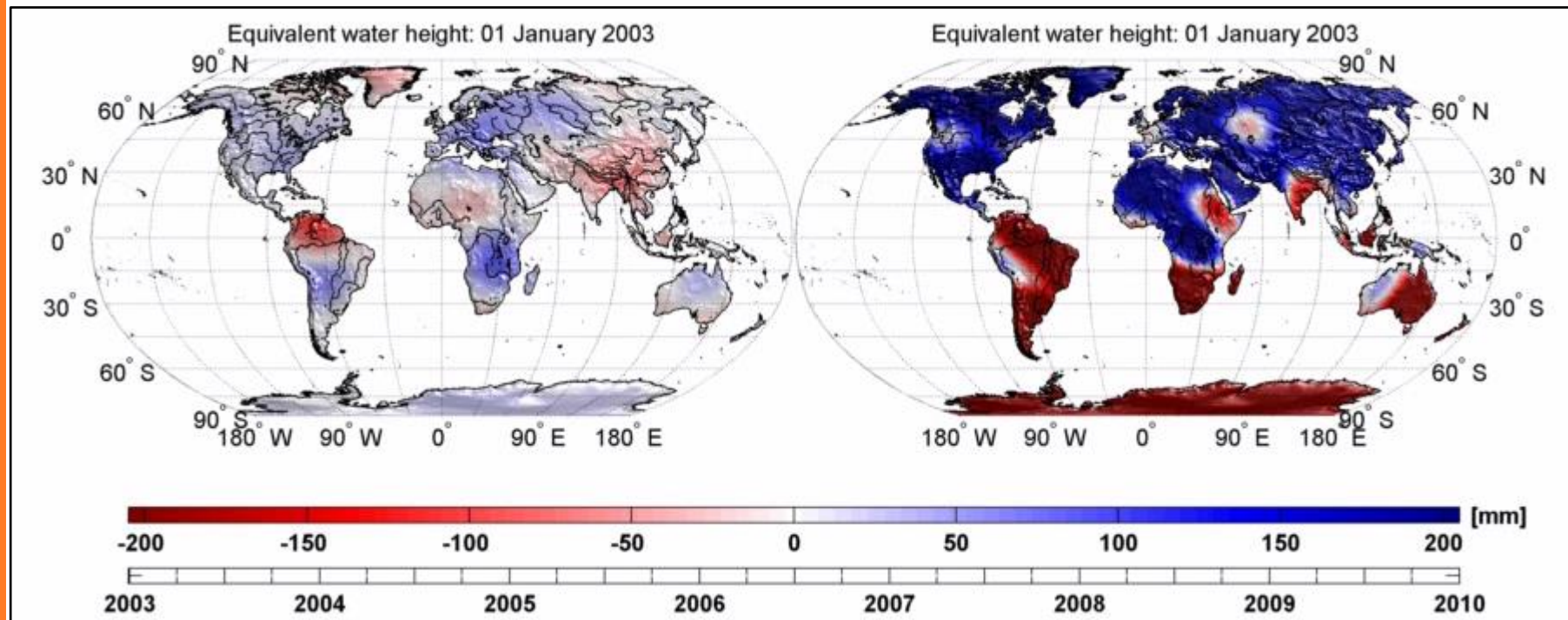
CHAMP monthly gravity field solution (3/4)

Time series of SH-coefficients: GRACE vs. CHAMP (annual) – scaled by 10^{10}



CHAMP monthly gravity field solutions (4/4)

GRACE GFZ Rel. 4



MODELING TIME VARIABILITY

Modeling time variability

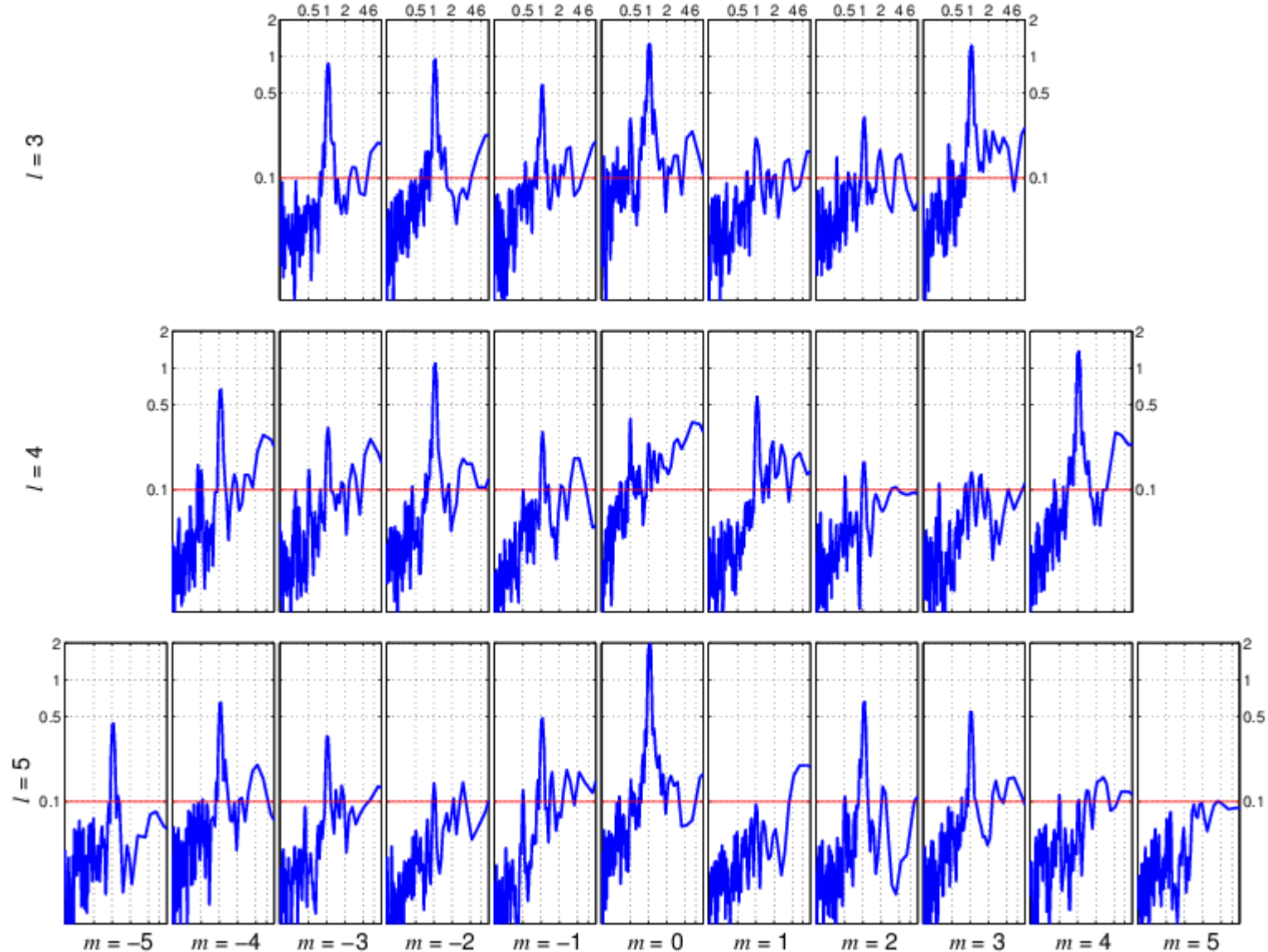
$$\bar{C}(t) = \bar{C}_0 + \dot{\bar{C}} \cdot t + \sum_{n=1}^N \bar{C}_n^{\cos} \cos(\omega_n t) + \bar{C}_n^{\sin} \sin(\omega_n t)$$

$$\bar{S}(t) = \bar{S}_0 + \dot{\bar{S}} \cdot t + \sum_{n=1}^N \bar{S}_n^{\cos} \cos(\omega_n t) + \bar{S}_n^{\sin} \sin(\omega_n t)$$

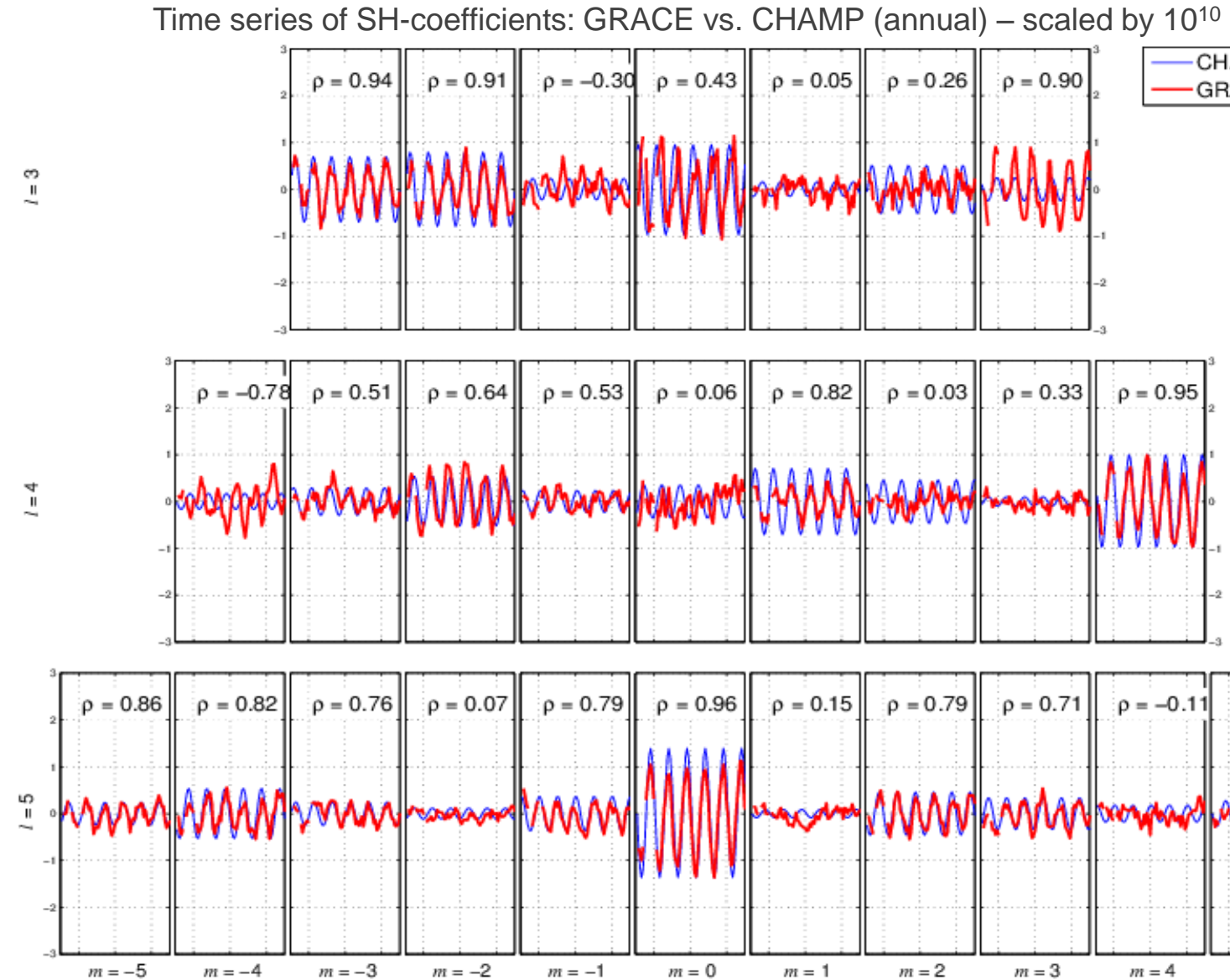
- Pro:
 - simple
 - considering spatial correlations between coefficients
- Con:
 - mean time-variable signal over the period of data
 - frequencies essentially unknown
 - variation of frequencies between coefficients
 - higher computational effort

Modeling time variability

Spectrum of time series of SH-coefficients: GRACE GFZ RL 04 – scaled by 10^9

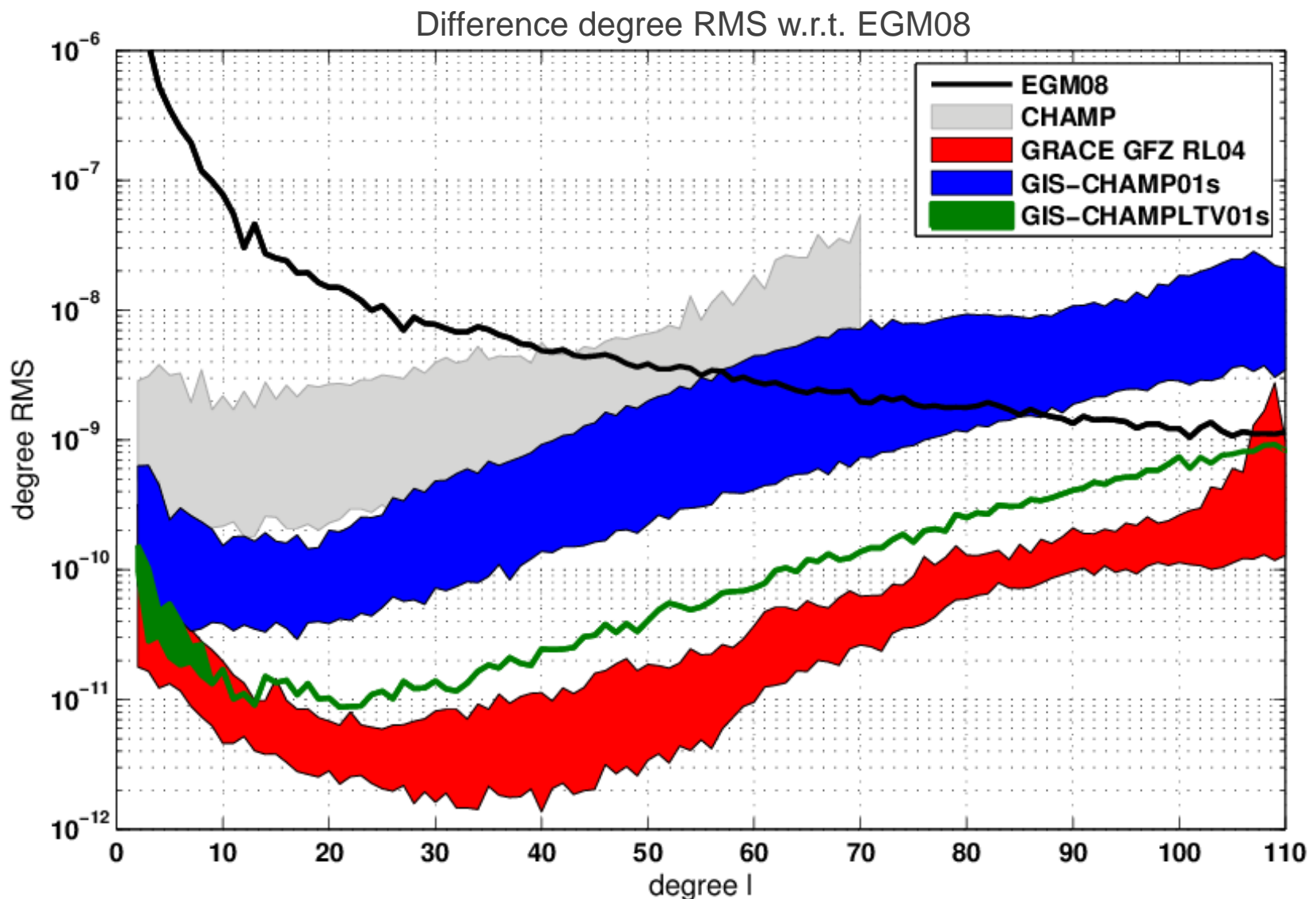


Modeled time-variable gravity field solution (1/4)



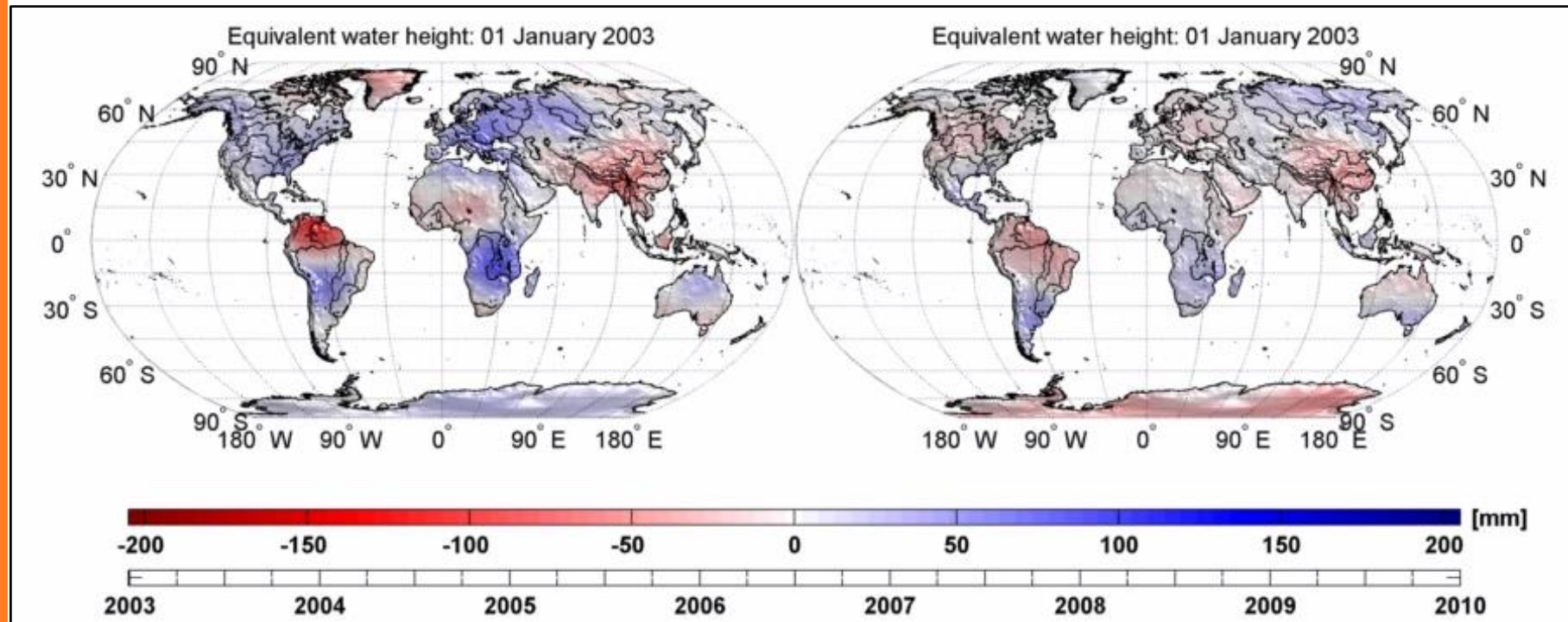
Modeled time-variable gravity field solution (2/4)

$$L_{Max} = 110$$
$$L_{Max}^{TV} = 8$$



Modeled time-variable gravity field solution (3/4)

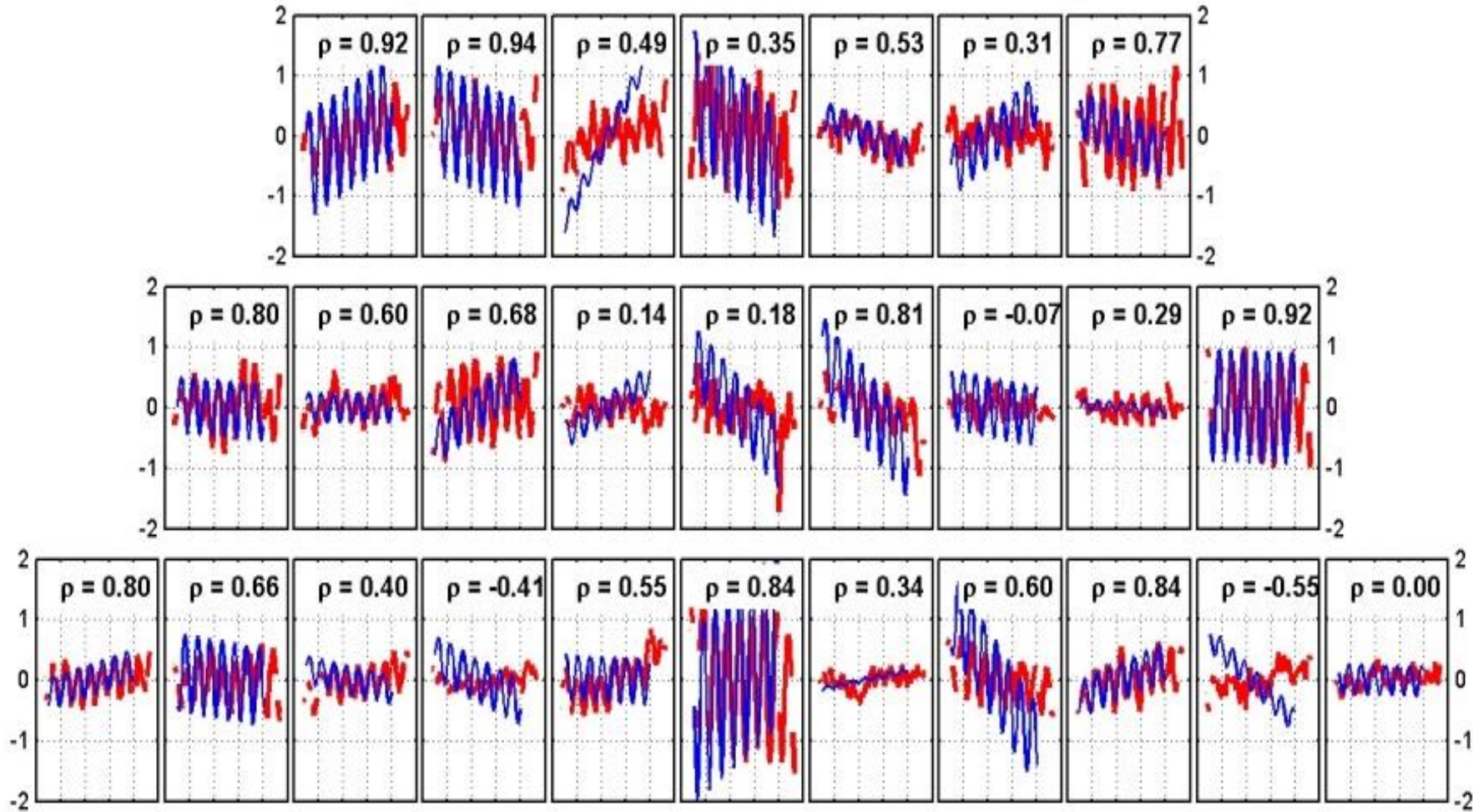
GRACE GFZ Rel. 4



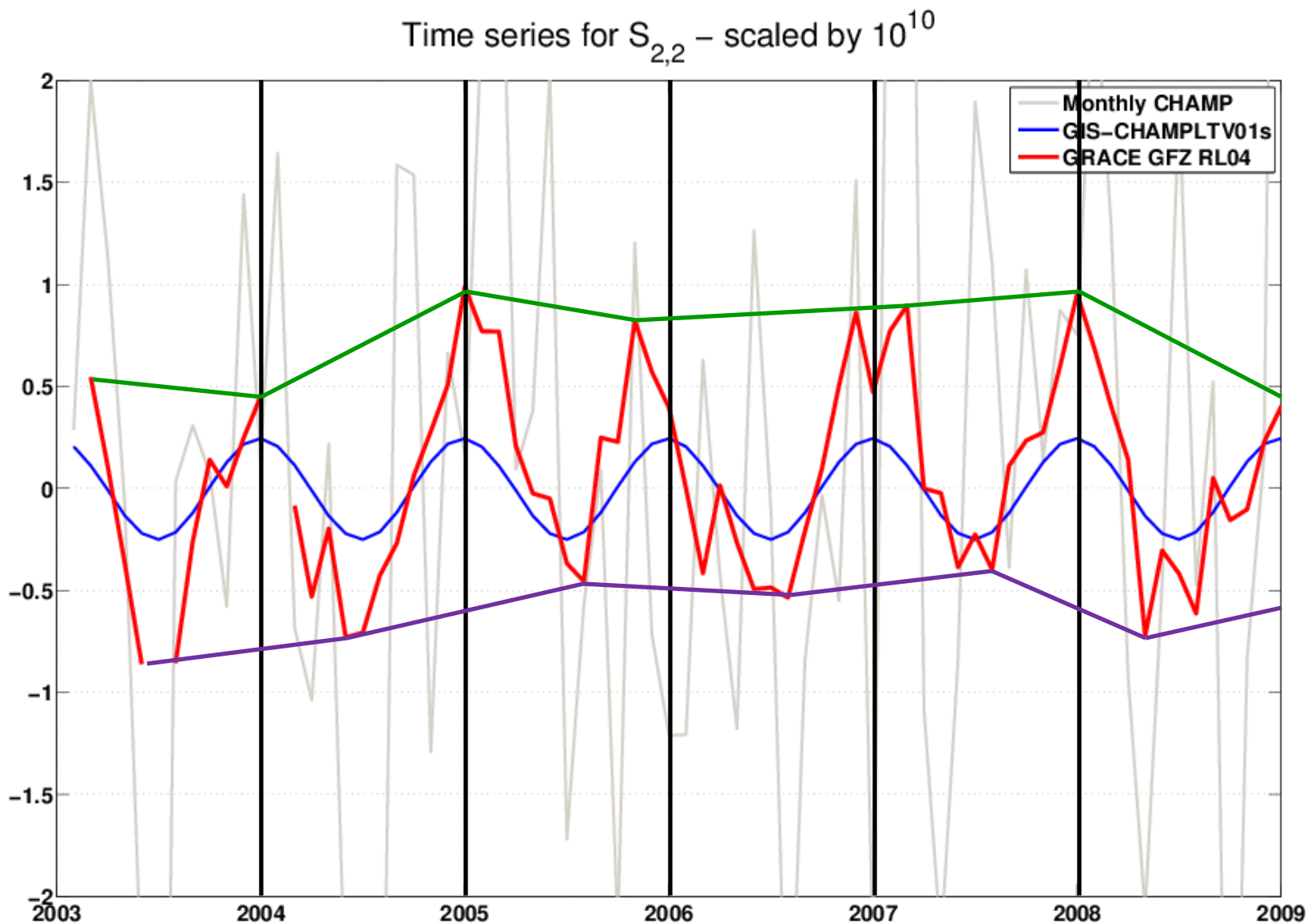
Modeled time-variable gravity field solution (4/4)

- additional trend estimation?

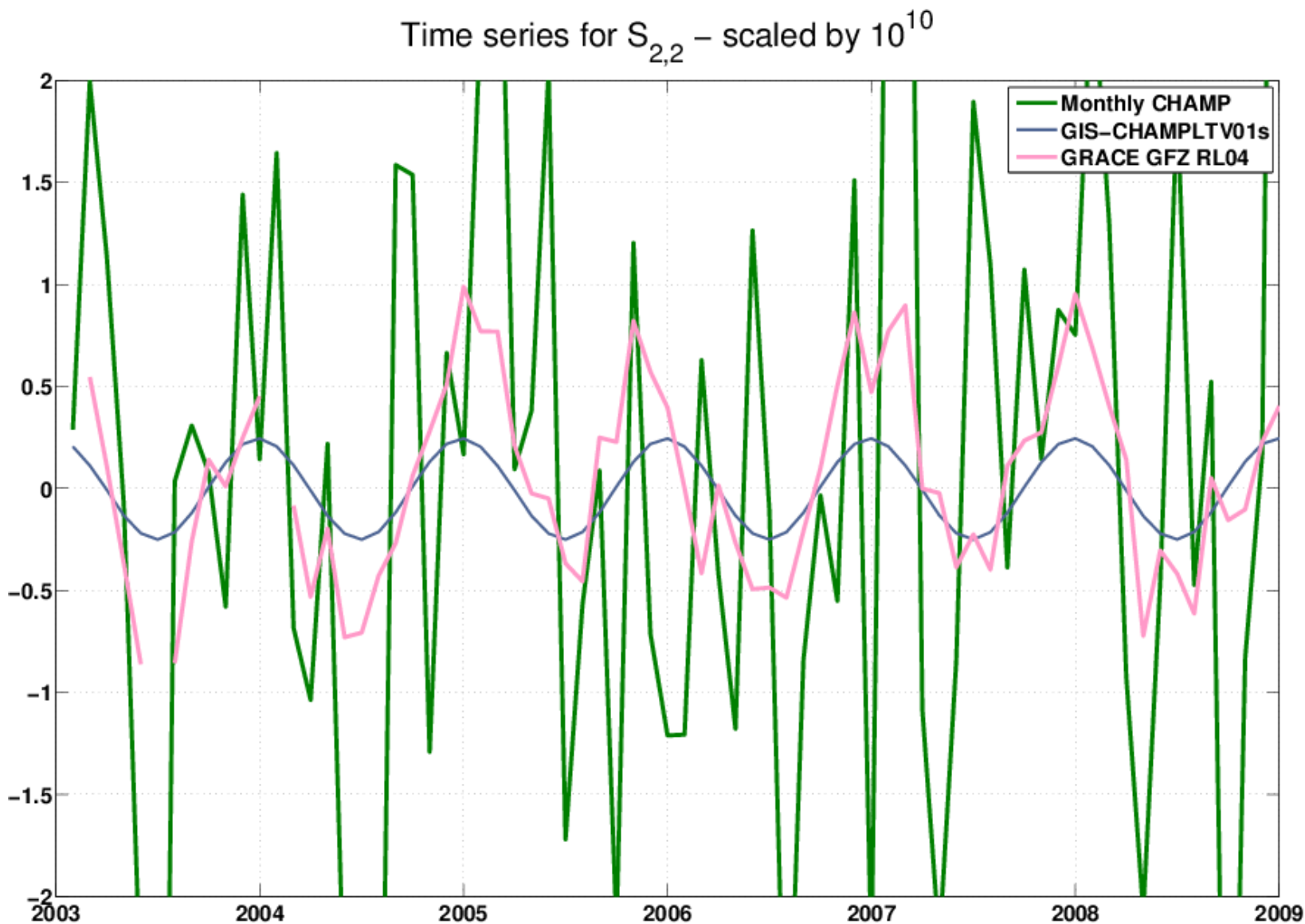
Time series of SH-coefficients: GRACE vs. CHAMP (annual + trend) – scaled by 10^{10}



Time series of a coefficient

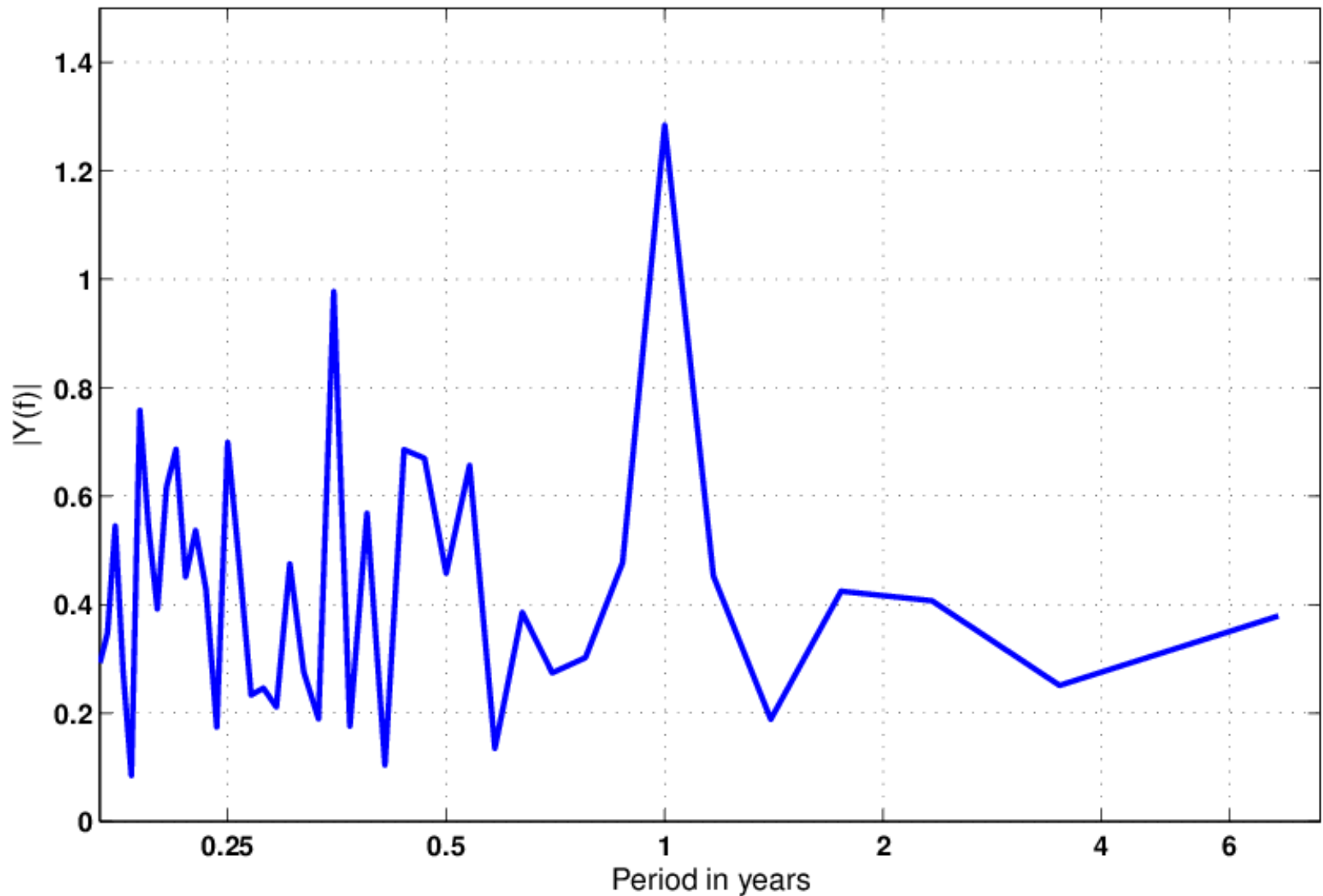


Time series of a coefficient



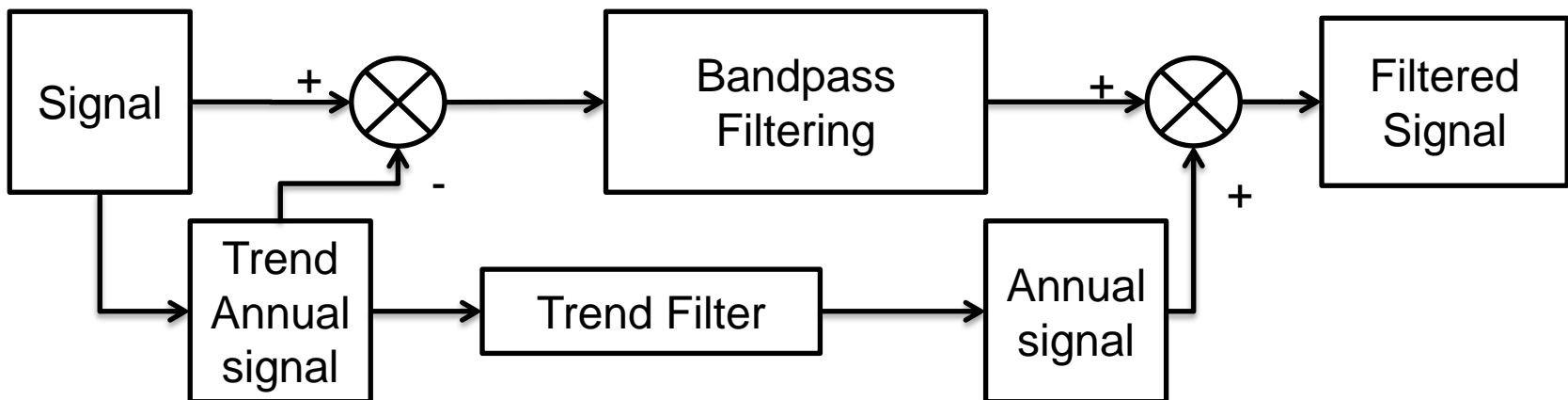
Spectrum of the time series

Single-Sided Amplitude Spectrum of $S_{2,2}$



FILTERED MONTHLY SOLUTIONS

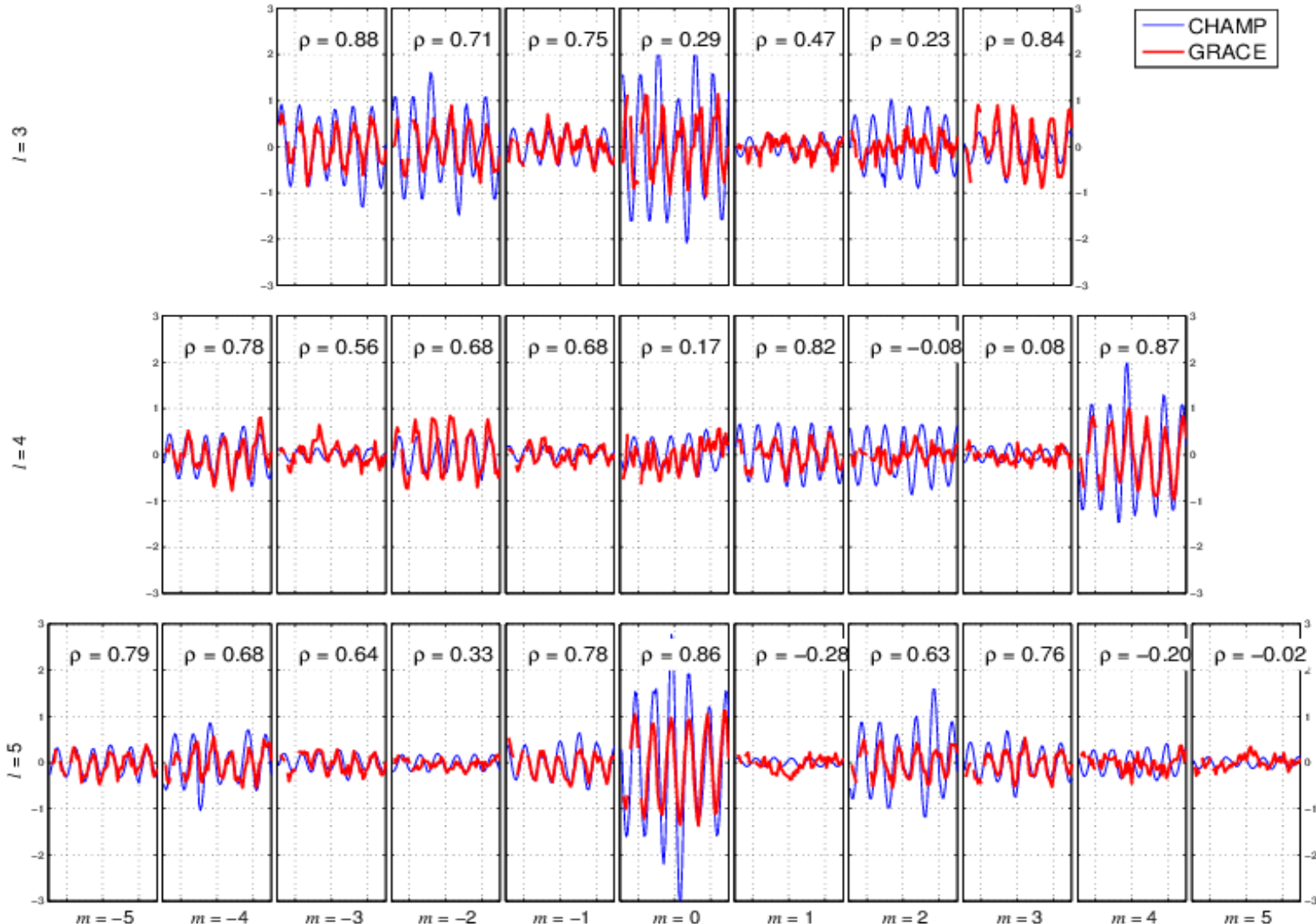
Filtering approach



- Pro:
 - variation of frequencies between coefficients possible (within passband)
 - applicable to all degrees and orders
 - filter design
- Con:
 - filter design
 - warmup
 - sophisticated outlier detection necessary
 - neglecting correlations between coefficients

Filtered monthly gravity field solutions (2/6)

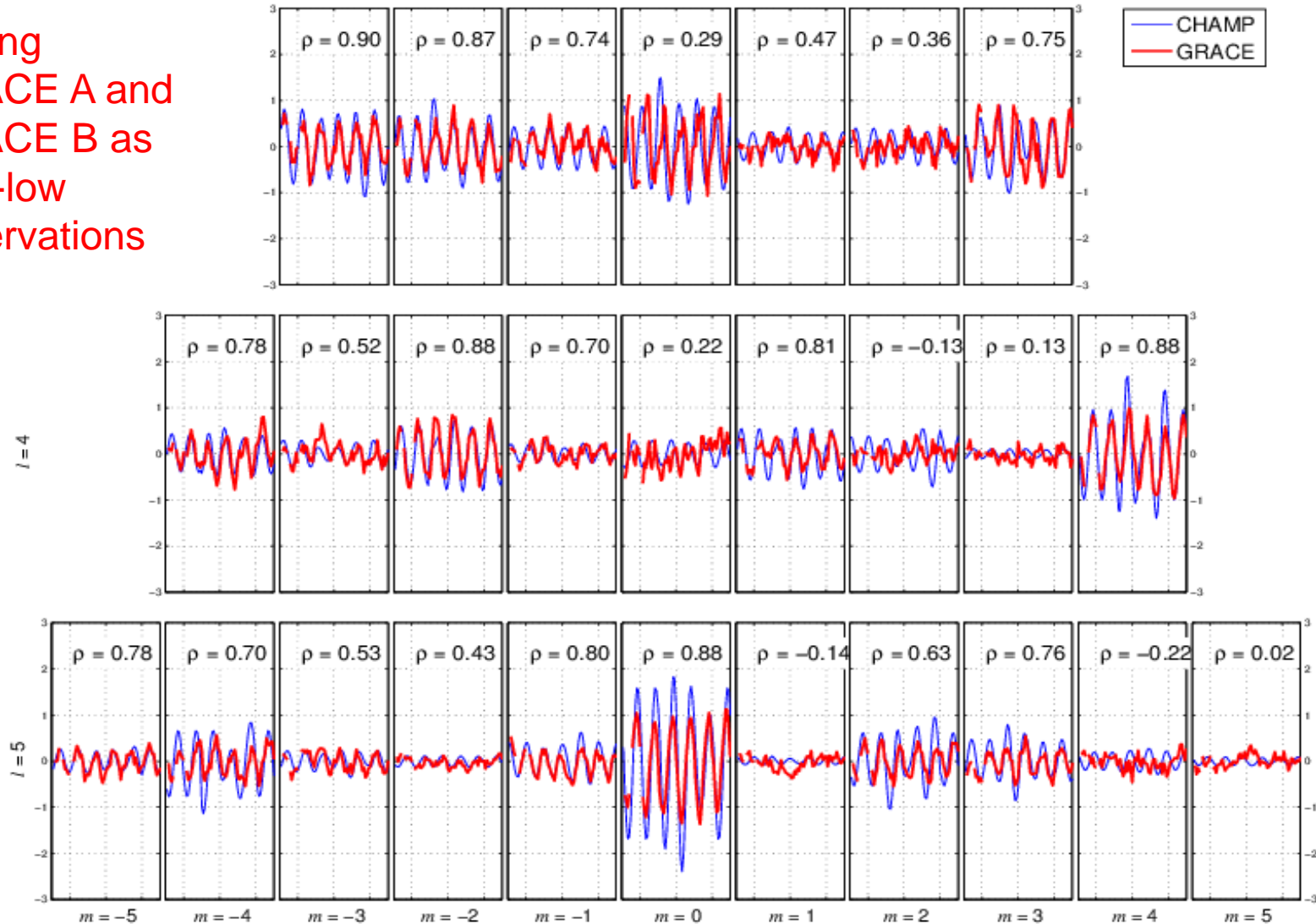
Time series of SH-coefficients: GRACE vs. CHAMP (filtered) – scaled by 10^{10}

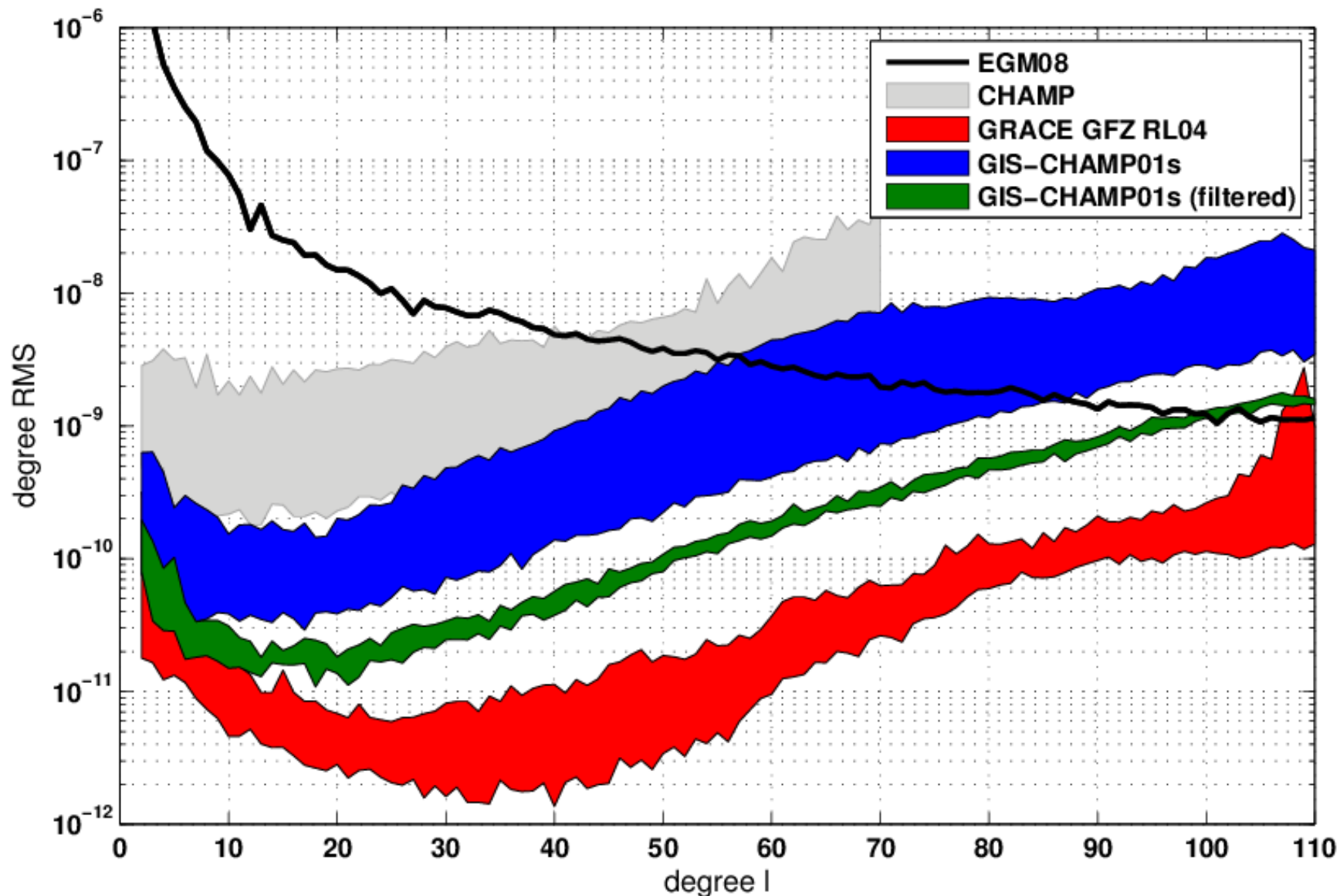


Filtered monthly gravity field solutions (3/6)

Time series of SH-coefficients: GRACE vs. High-Low (filtered) – scaled by 10^{10}

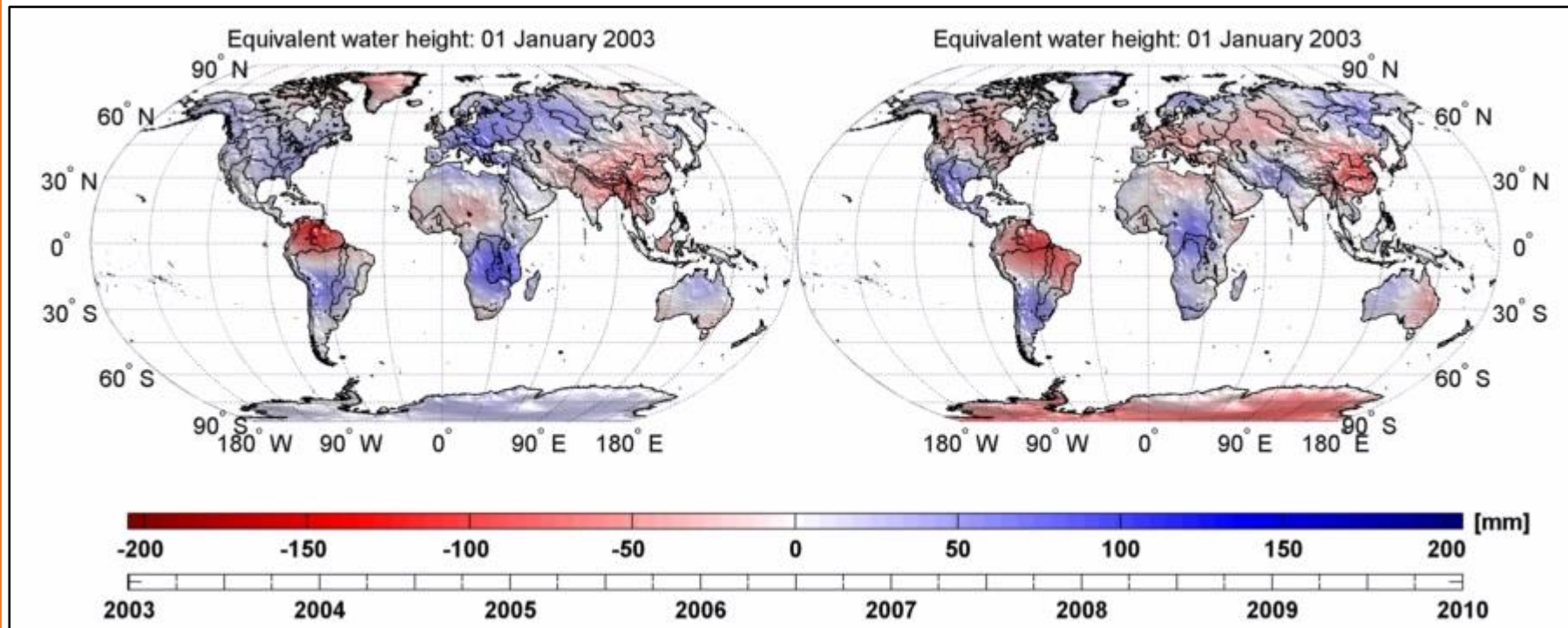
Adding
GRACE A and
GRACE B as
high-low
observations



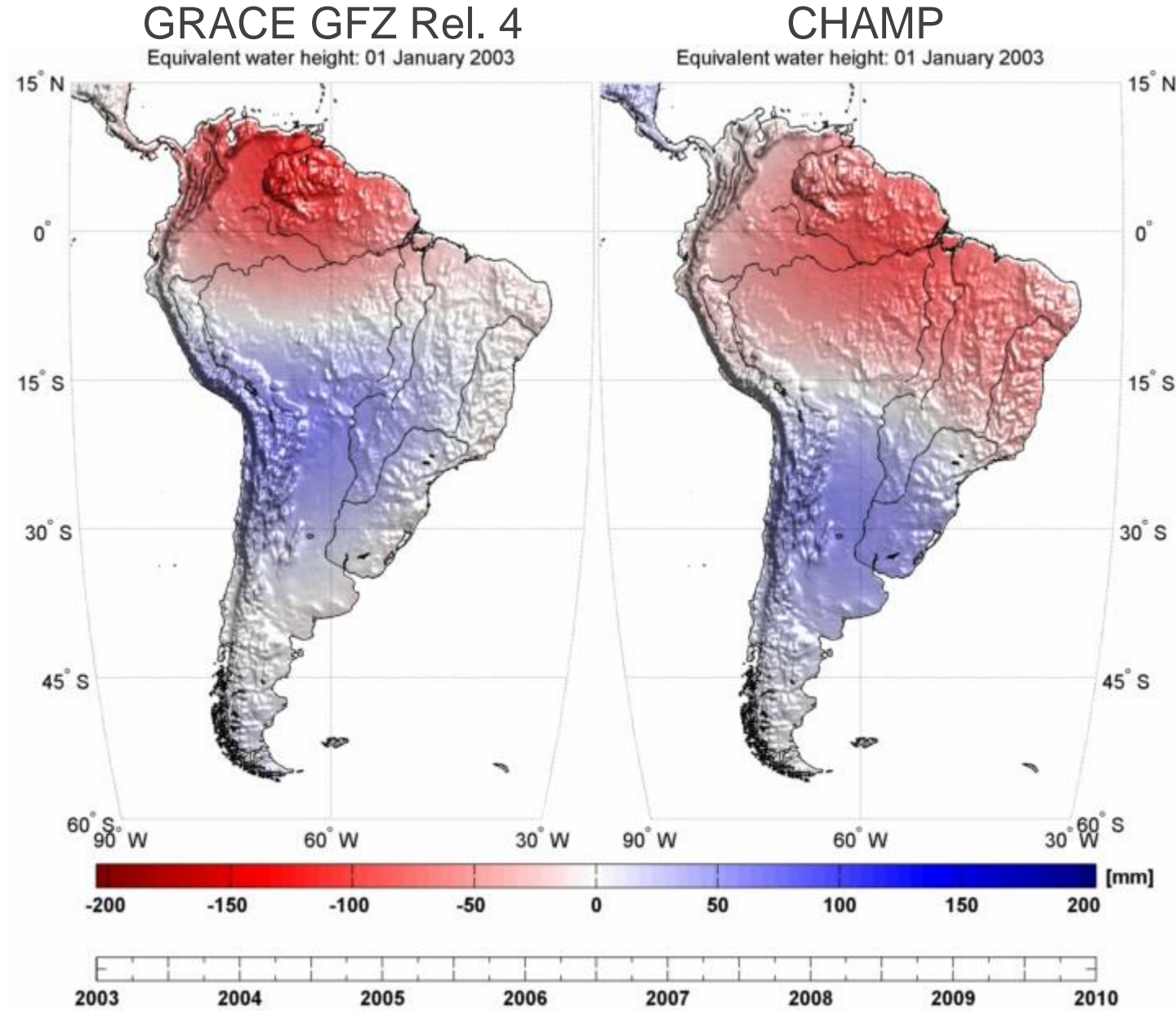
Filtered monthly gravity field solutions (1/6)

Filtered monthly gravity field solutions (4/6)

GRACE GFZ Rel. 4

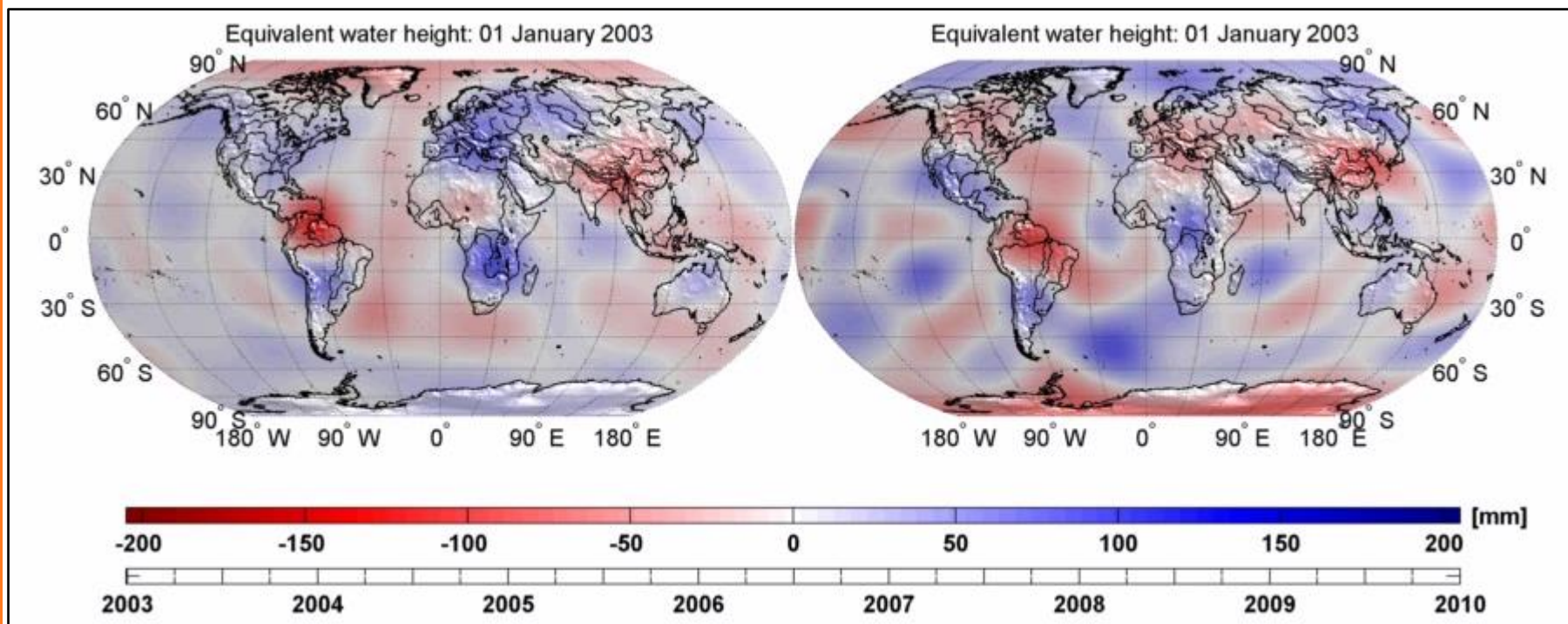


Filtered monthly gravity field solutions (5/6)



Filtered monthly gravity field solutions (6/6)

GRACE GFZ Rel. 4

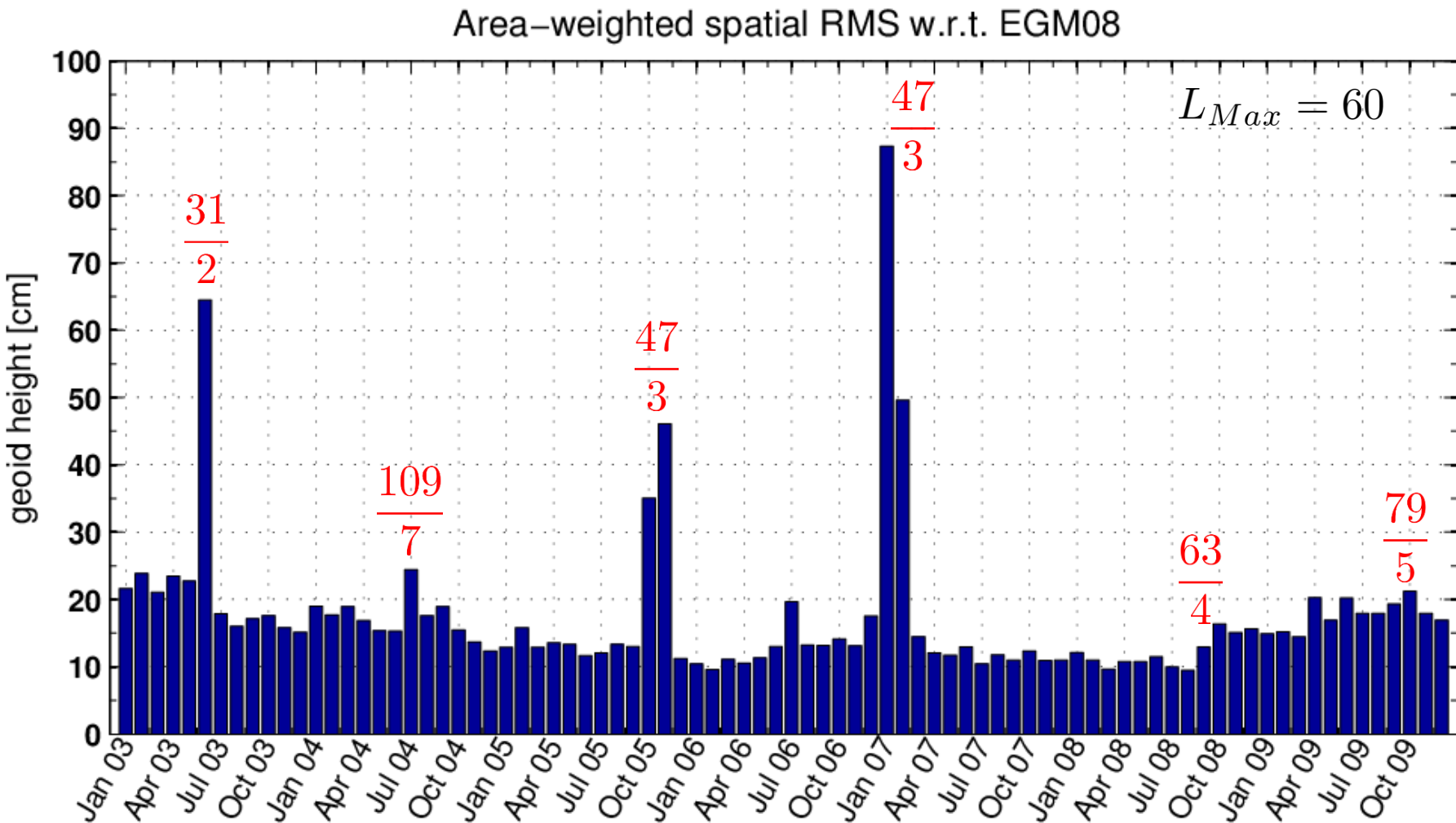


Summary Part I: CHAMP

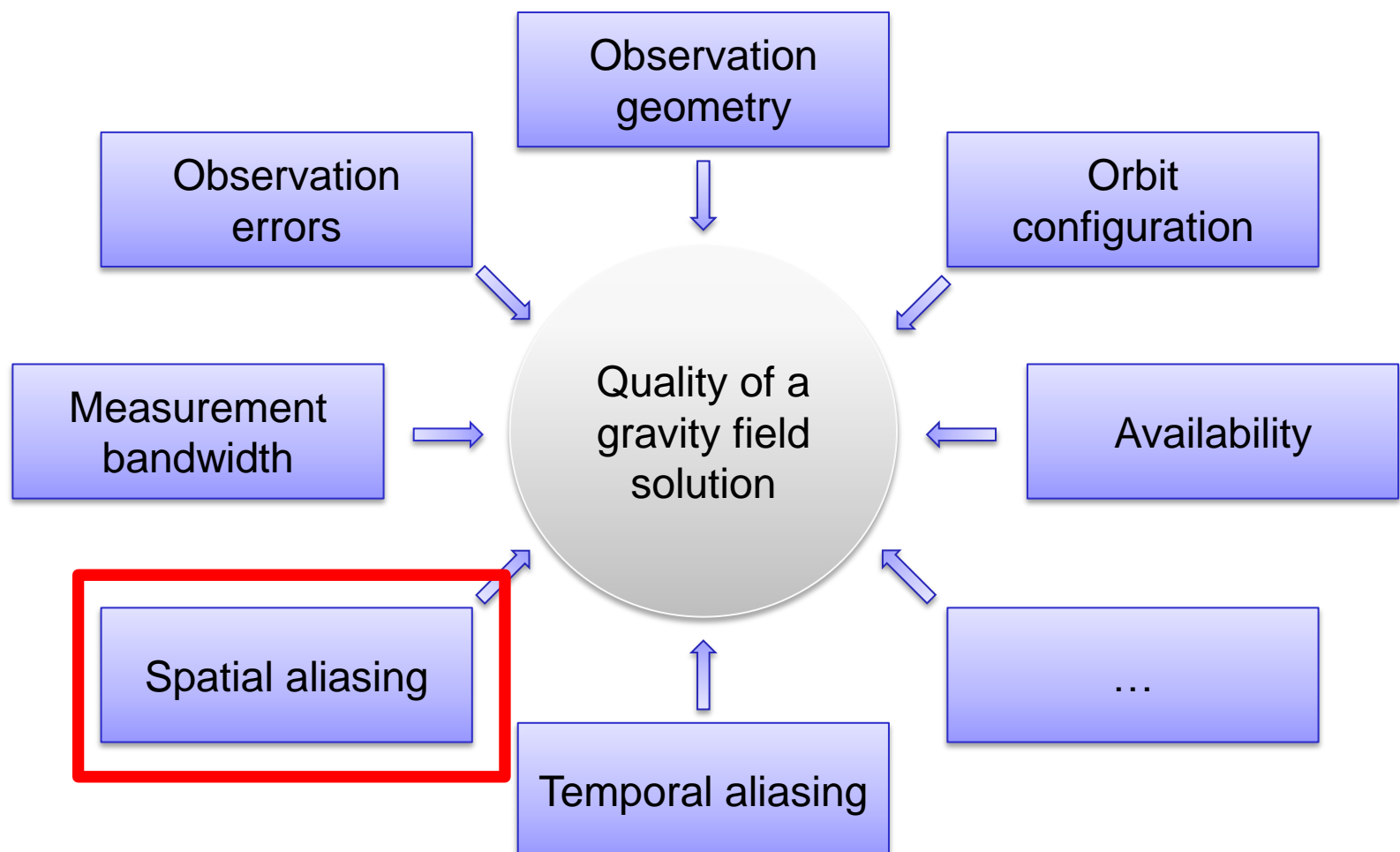
- Improved gravity field solution due AIUB - CHAMP position data including the time variability.
- Evaluation of the quality of time-variable solution necessary
- Processing refinements necessary (especially filtering)
- High-low SST is as a transitory technology till GFO (Swarm, Cosmic, Sentinel, ...)
- Acceleration approach also suitable to satellite missions without accelerometer data
- Other approaches ?

PART II: SPATIAL ALIASING

CHAMP monthly gravity field solutions (1/4)



Influences on accuracy



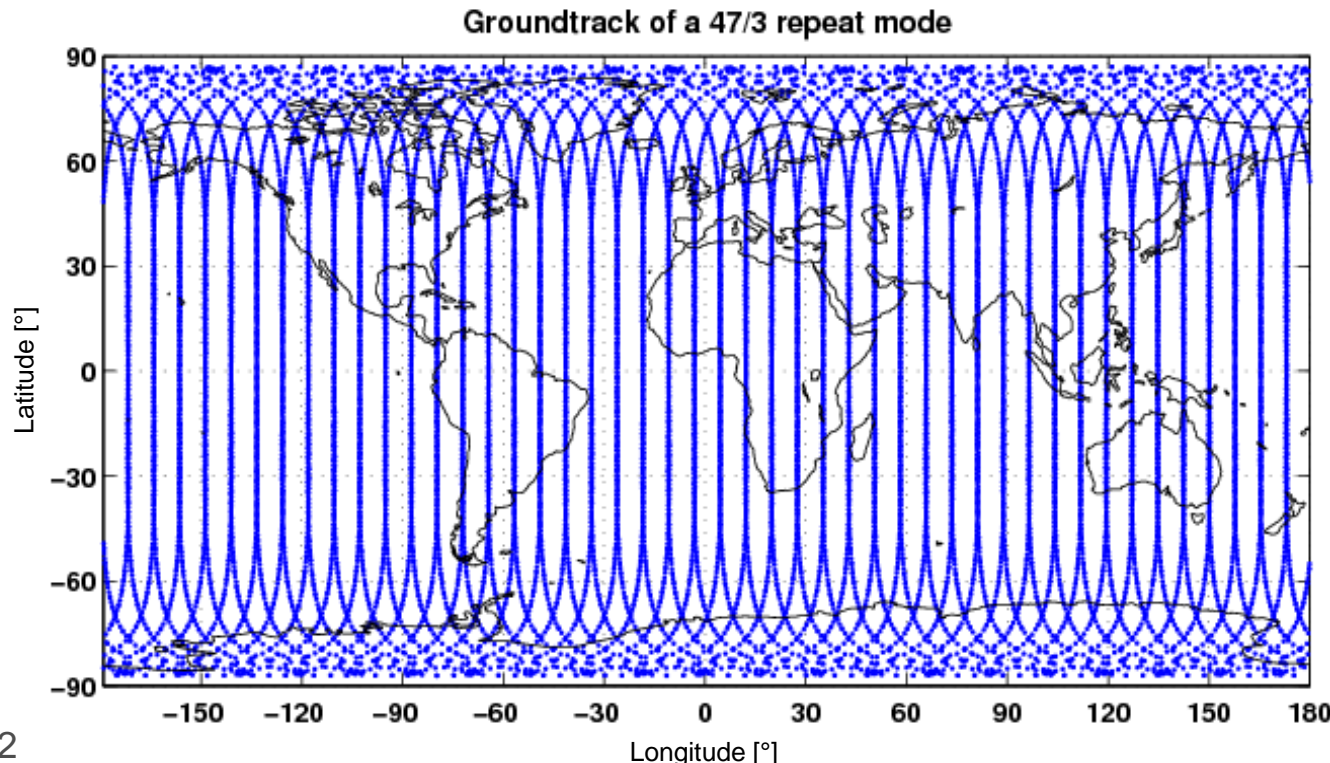
Colombo-Nyquist rule

$\frac{\beta}{\alpha}$ repeat orbit:

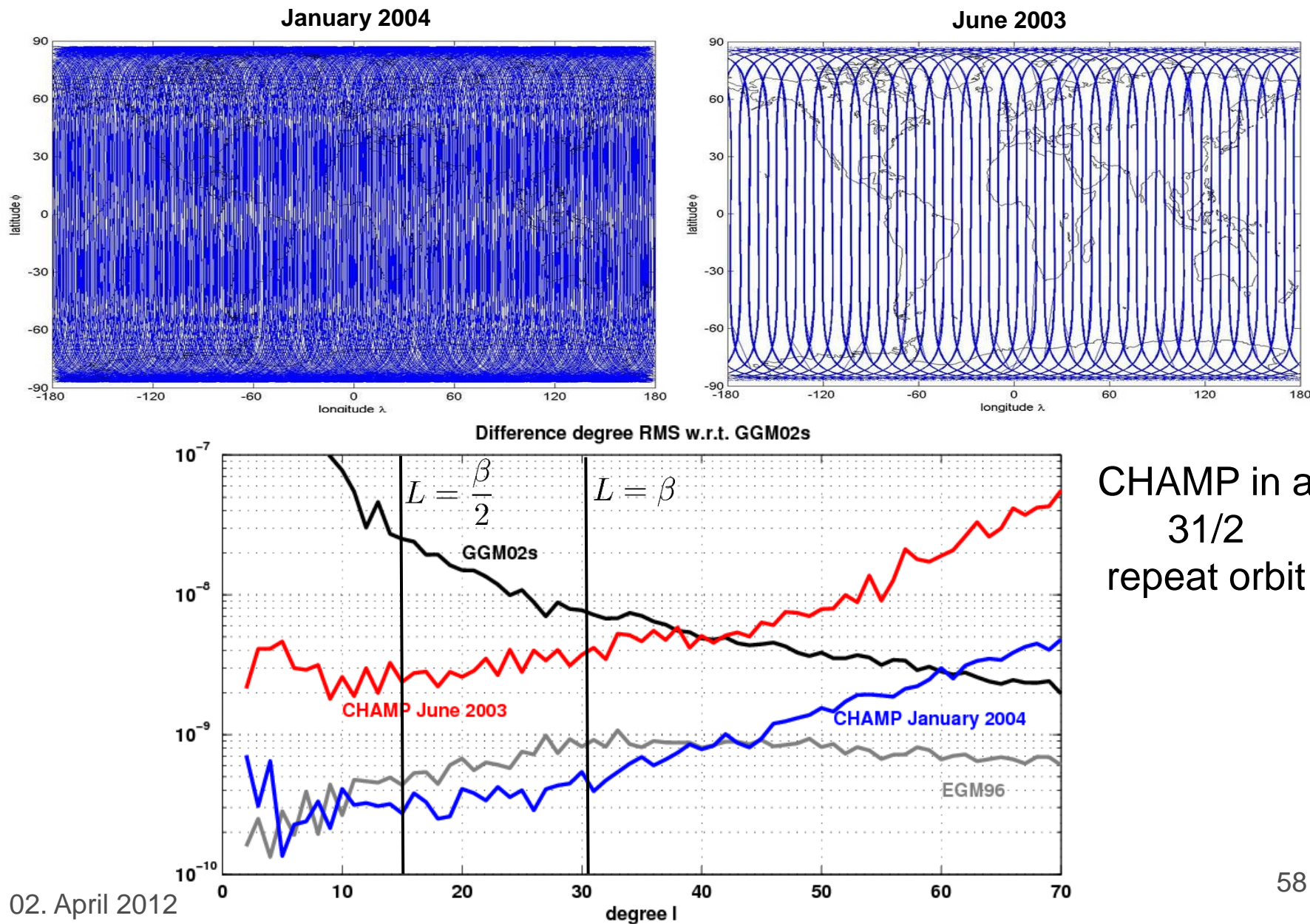
- β orbits
- α nodal days

⇒ maximum spatial resolution: $L = \frac{\beta}{2}$

Example: $\beta = 47, \alpha = 3 \Rightarrow L = 23$

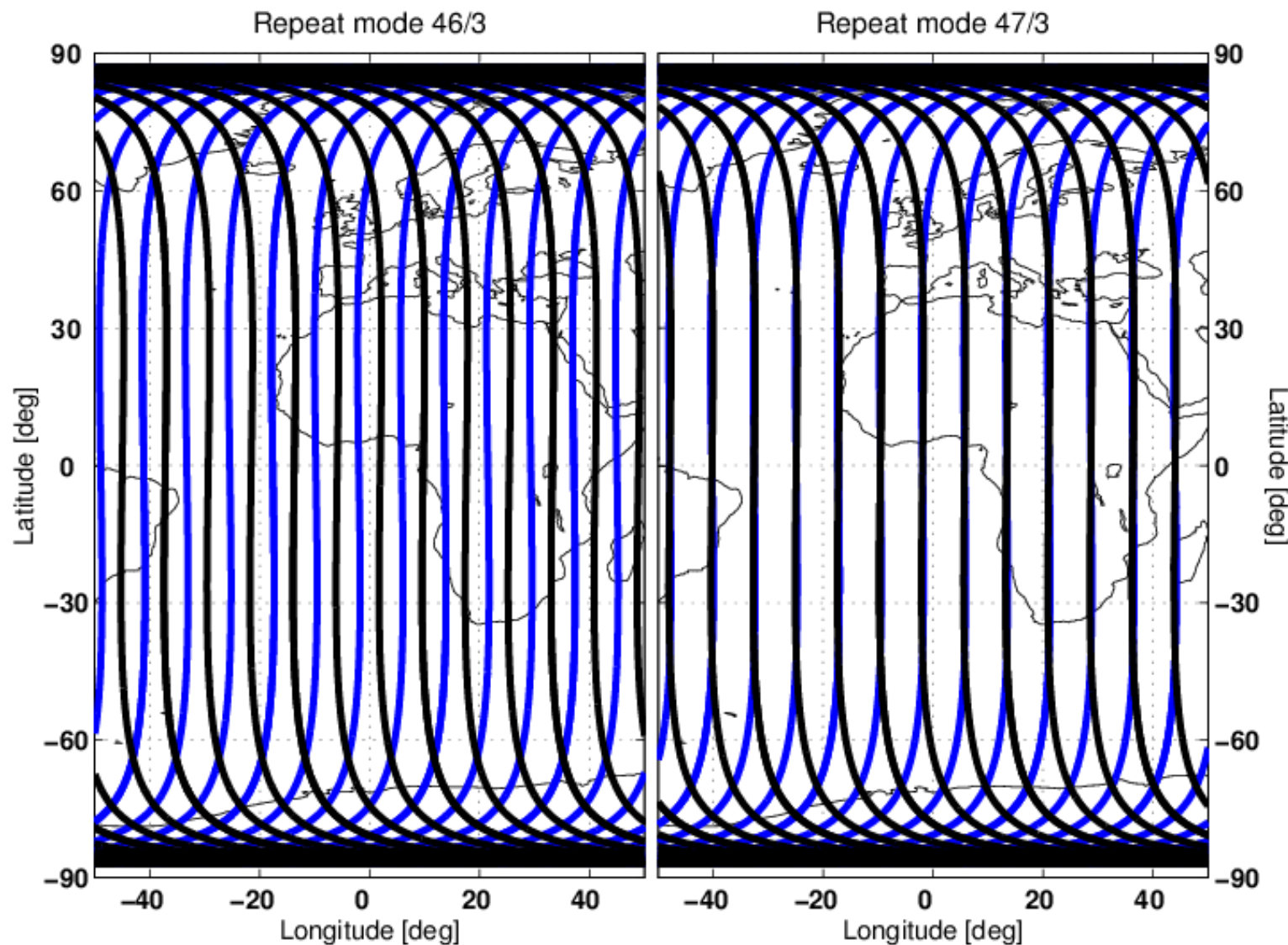


However...



NEW CRITERION?

Dependency on the parity (1/2)



Dependency on the parity (2/2)

Ascending equator crossings: $\lambda_p^a = \lambda_0^a + \frac{2\pi}{\beta}p$ with $p = 0 \dots \beta - 1$

First descending equator crossings: $\lambda_0^d = \lambda_0^a + \pi - \frac{1}{2}T_u\omega_E$

$$\lambda_0^d = \lambda_0^a + \pi - \pi \frac{\alpha}{\beta}$$

Condition: $\lambda_p^a - \lambda_0^d = 0$

$$\lambda_0^a + \frac{2\pi}{\beta}p - \lambda_0^a - \pi + \pi \frac{\alpha}{\beta} = 0$$

$$p = \frac{1}{2}(\beta - \alpha)$$

Solution only for $\beta - \alpha$ even, since all elements are integer.

Introducing the concept of unique equator crossings:

$$\chi = \begin{cases} 2\beta, & \text{for } \beta - \alpha \text{ odd} \\ \beta, & \text{for } \beta - \alpha \text{ even} \end{cases}$$

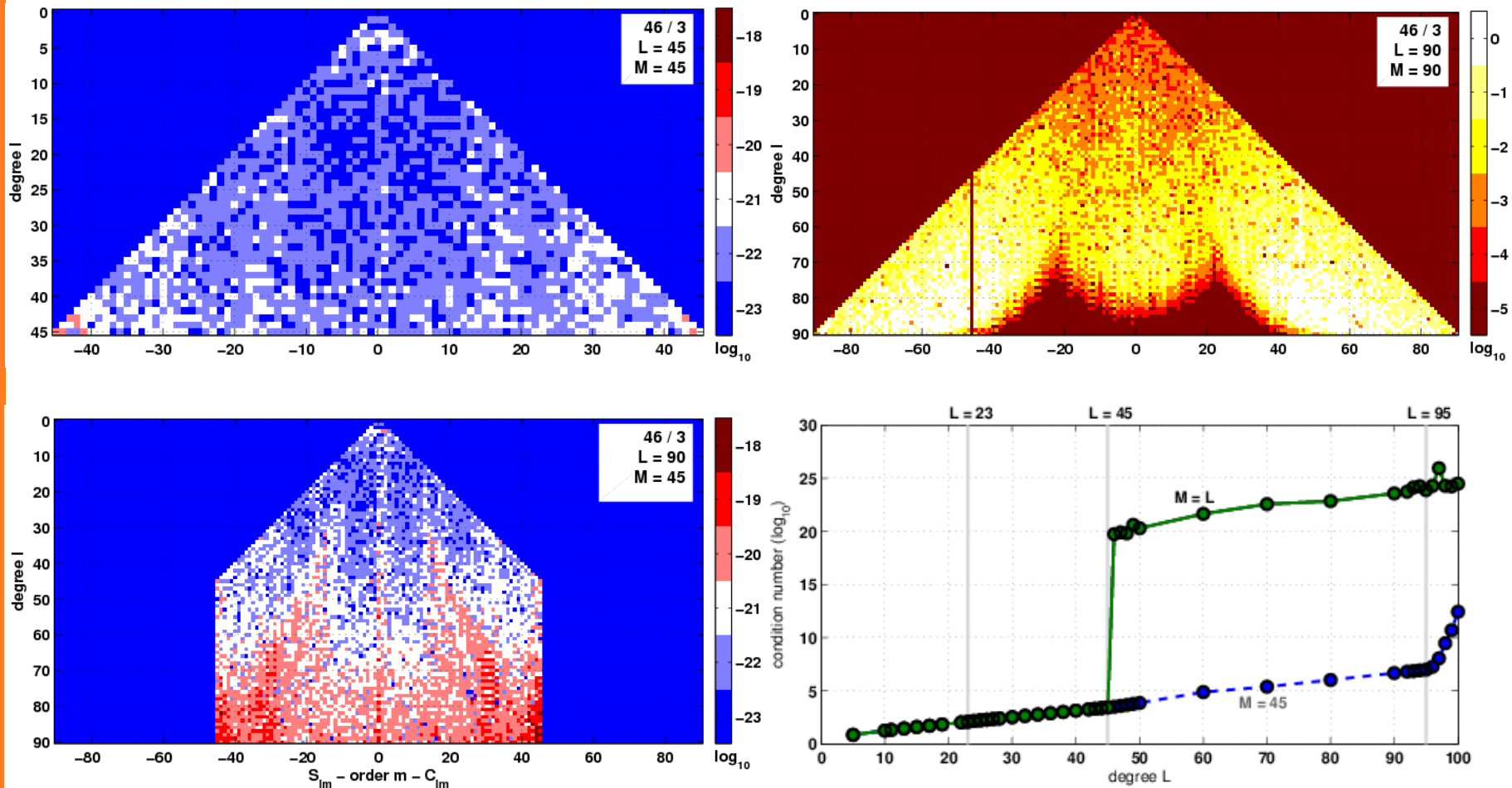
- Spatial representation:

$$V(r, \phi, \lambda) = \frac{GM}{R} \sum_{l=0}^{\infty} \left(\frac{R}{r} \right)^{l+1} \sum_{m=-l}^l \bar{K}_{lm} \bar{P}_{lm}(\sin \phi) e^{im\lambda}$$

SIMULATION STUDY

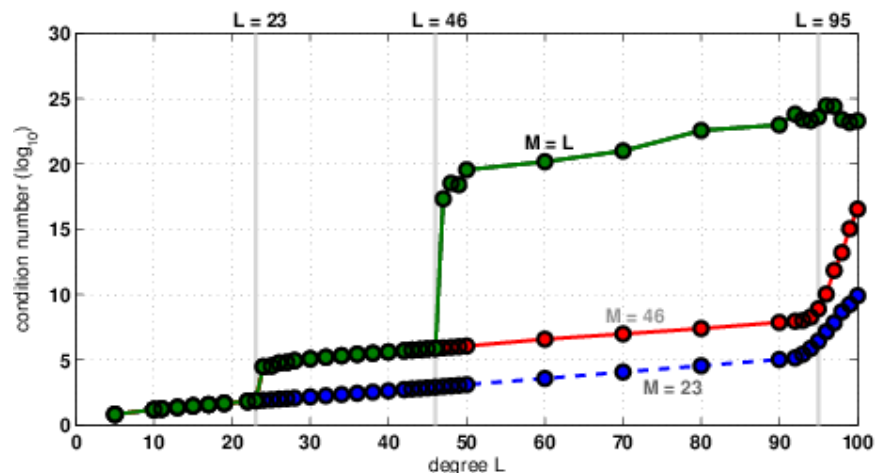
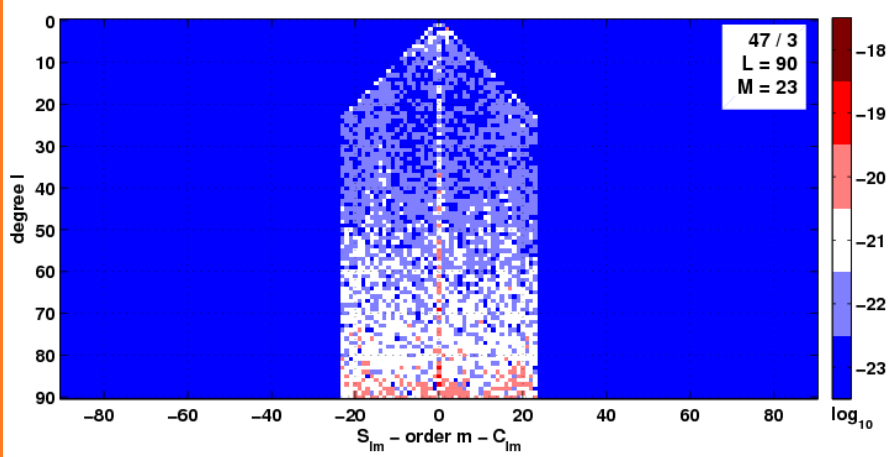
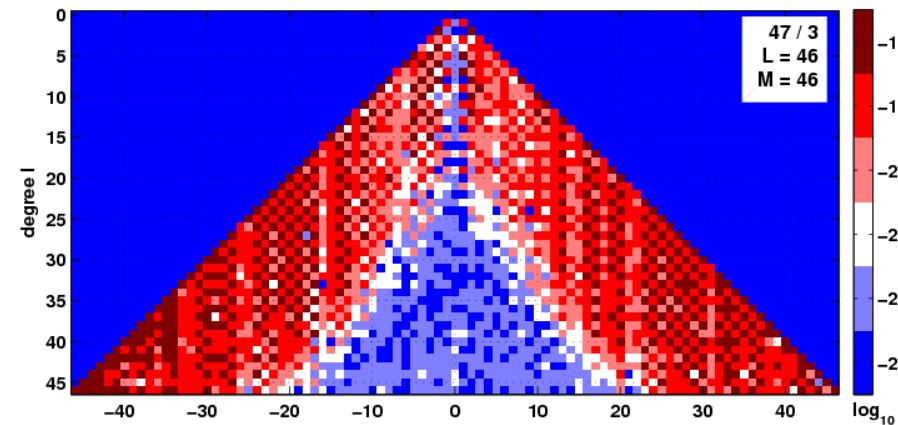
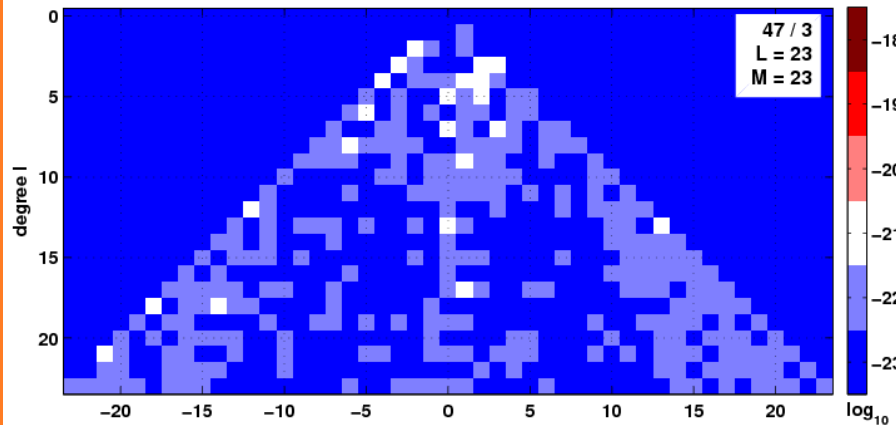
Simulation study: odd parity 46/3

$$M < \beta$$

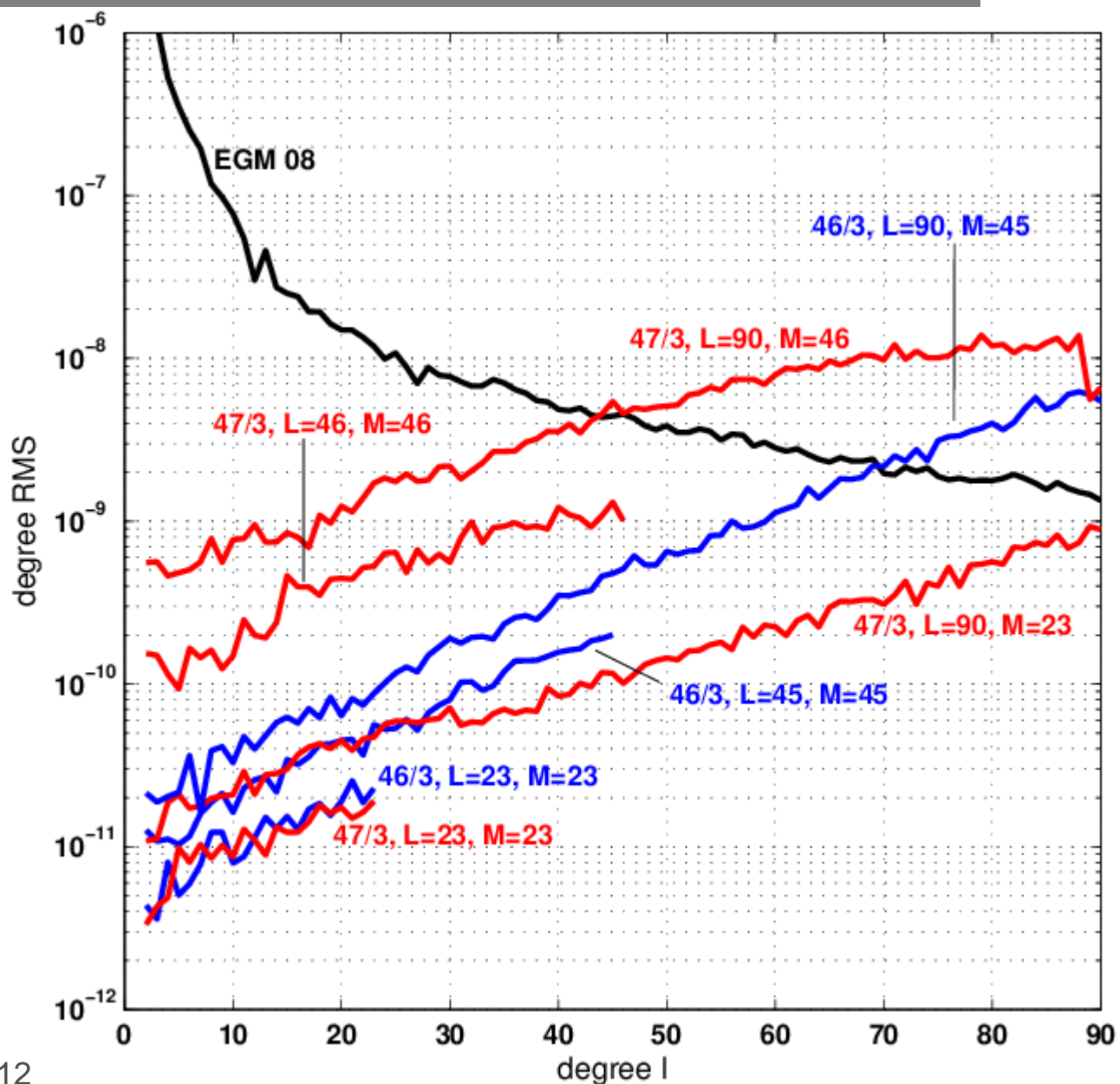


Simulation study: even parity 47/3

$$M < \frac{\beta}{2}$$



Noise impact

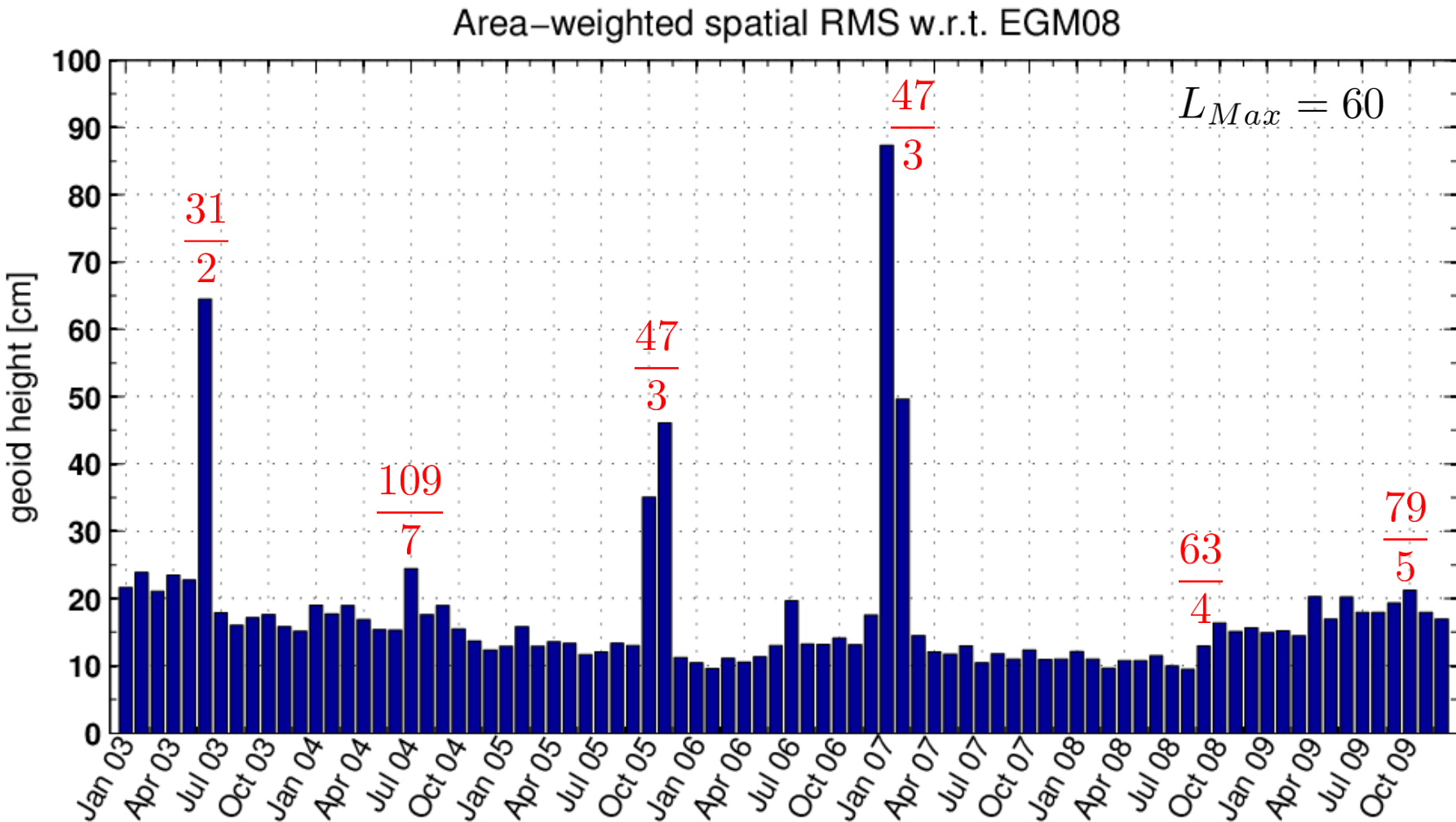


IMPACT ON CHAMP AND GRACE

CHAMP repeat cycles (1/2)

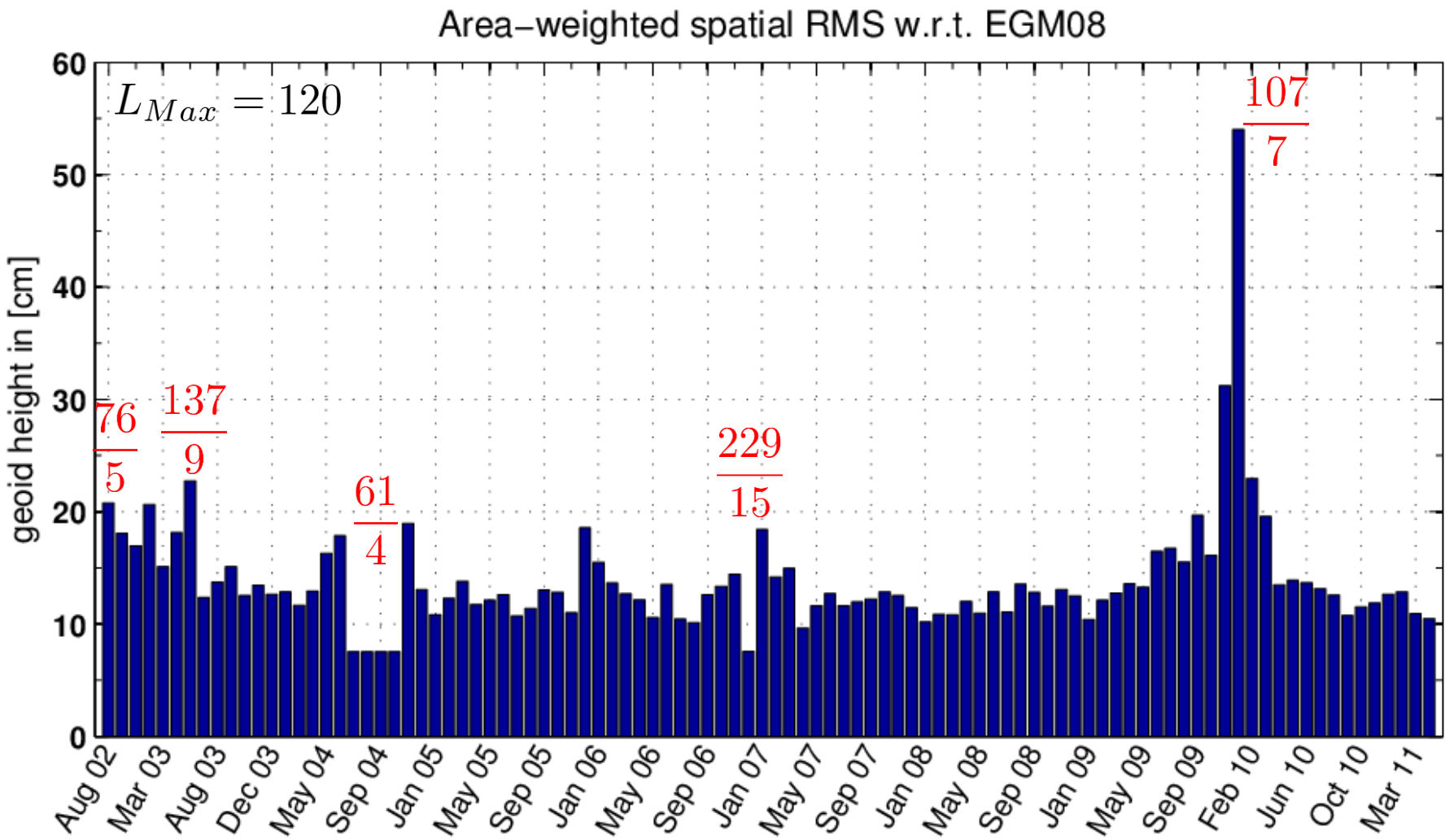
β	α	Time	Parity	h [km]	χ	M	Old: $L =$
139	9	January 2002	Even	409	139	69	69
31	2	May 2002	Odd	393	62	30	15
		October 2002					
		June 2003					
109	7	July 2004	Even	372	109	54	54
47	3	November 2005	Even	345	47	23	23
		January 2007					
63	4	September 2008	Odd	321	126	62	31
79	5	October 2009	Even	307	79	39	39

CHAMP repeat cycles (2/2)



β	α	Time	Parity	h [km]	χ	M	Old: $L =$
76	5	September 2002	Odd	485	152	75	37
137	9	April 2003	Even	478	137	68	68
61	4	September 2004	Odd	470	122	60	30
229	15	January 2006	Even	465	229	114	114
107	7	December 2009	Even	459	107	53	53
199	13		Even	453	199	99	99
46	3		Odd	445	92	45	22
169	11		Even	436	169	84	84
...	

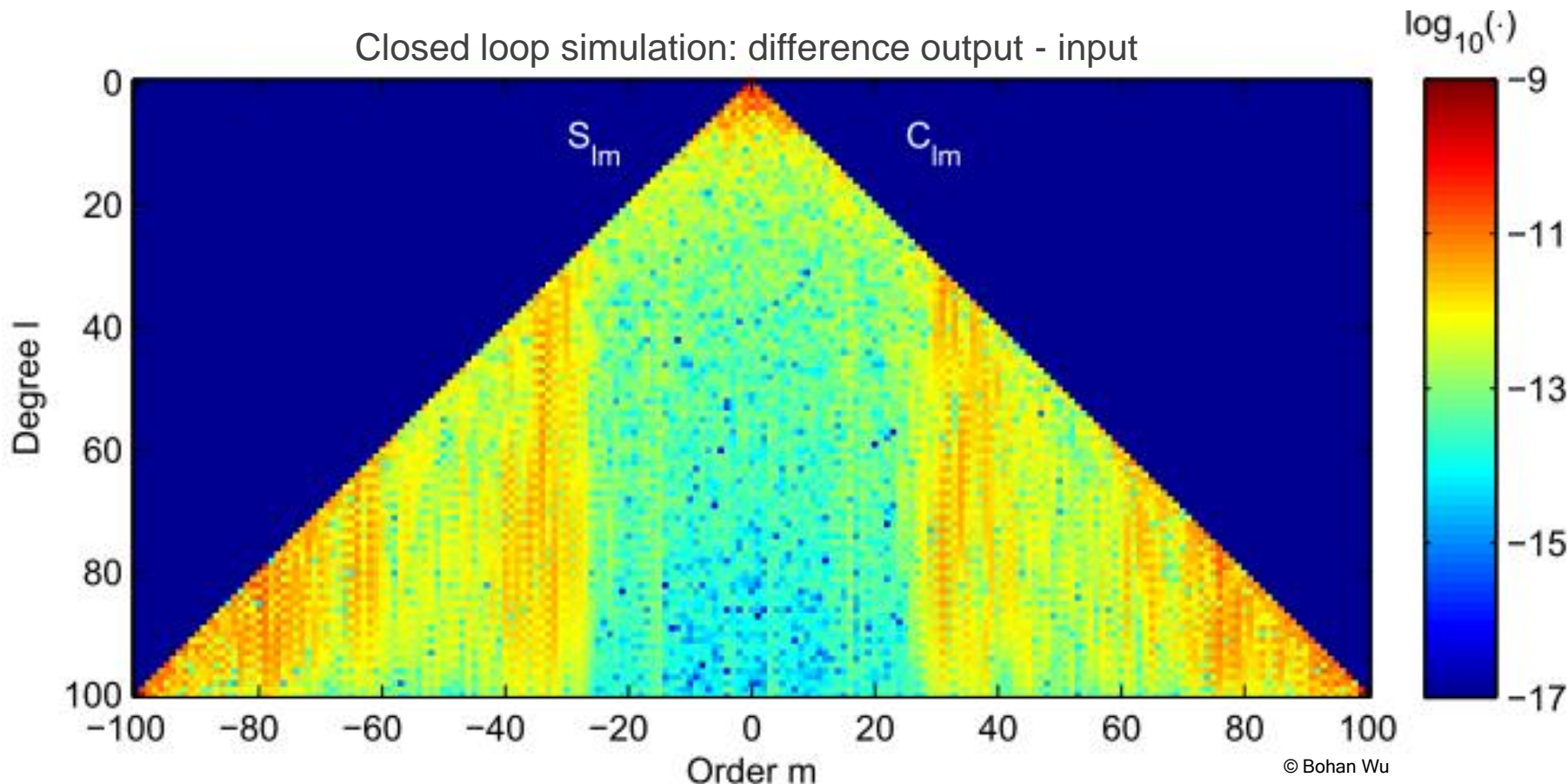
GRACE repeat cycles (2/2)



TEMPORAL ALIASING

Temporal aliasing?

- Closed loop simulation: GRACE
- Difference of ocean tide models (EOT10a –FES2004) as the only noise source

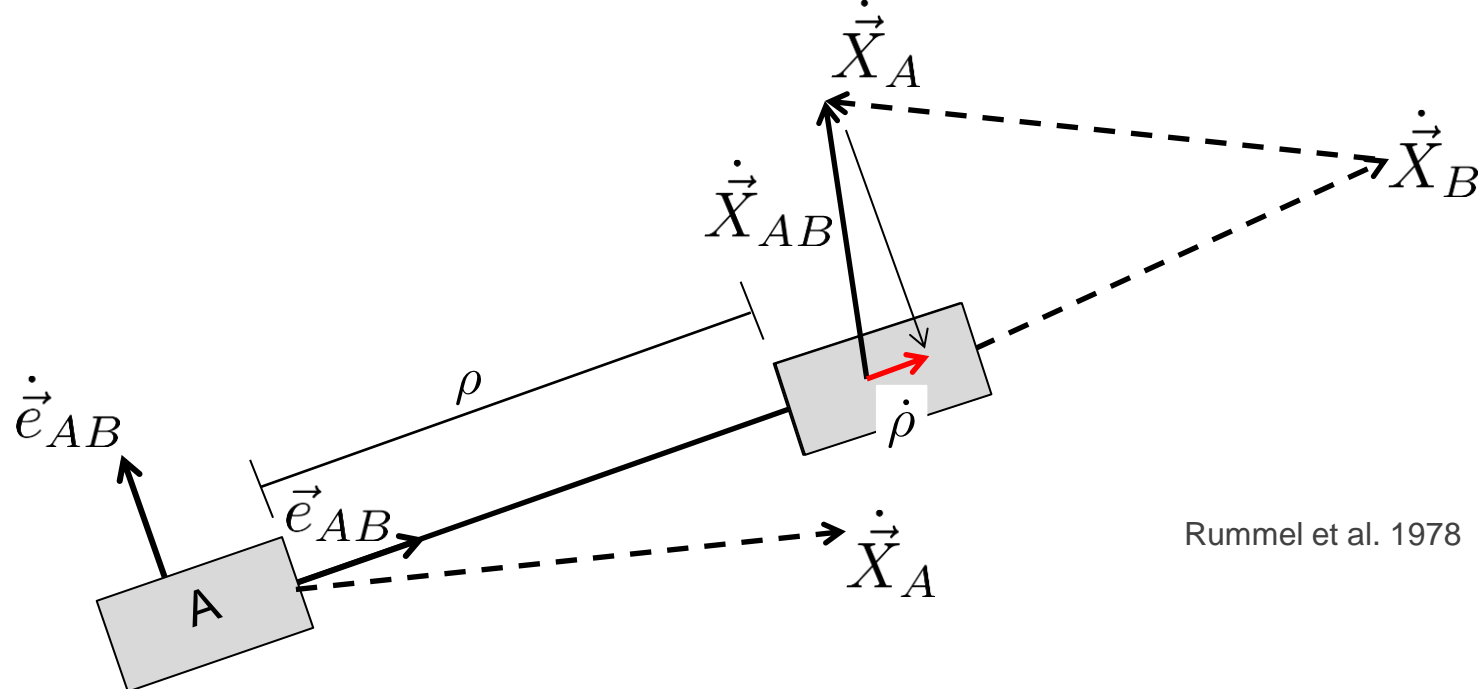


Summary Spatial Aliasing

- Refinement of Colombo-Nyquist rule necessary
- Nyquist criterion separately applicable to longitude and latitude direction due to near polar (limit?) orbits in gravity field missions
- Limitation practically on the maximum order M
- New rule of thumb describes only the influence due to the spatial aliasing of the static field.
- Signal higher than maximum order M ?
- Dependency on the observation quantity?
- Criterion?

PART III: GRACE and GRACE Follow-On

Geometry of the GRACE system



Rummel et al. 1978

Differentiation

Integration

$$\rho = \vec{X}_{AB} \cdot \vec{e}_{AB}$$

$$\dot{\rho} = \vec{X}_{AB} \cdot \vec{e}_{AB}$$

$$\ddot{\rho} = \vec{X}_{AB} \cdot \vec{e}_{AB} + \dot{\vec{X}}_{AB} \cdot \dot{\vec{e}}_{AB}$$

SOLUTION STRATEGIES

Solution strategies

Variational equations

$\rho, \dot{\rho}$ *Classical*
(Reigber 1989, Tapley 2004)

$\rho, \dot{\rho}, \Delta\rho$ *Celestial mechanics approach*
(Beutler et al. 2010, Jäggi 2007)

$\rho, \dot{\rho}$ *Short-arc method*
(Mayer-Gürr 2006)

...

In-situ observations

$\dot{\rho}$ *Energy Integral*
(Han 2003, Ramillien et al. 2010)

$\ddot{\rho}$ *Differential gravimetry*
(Liu 2010)

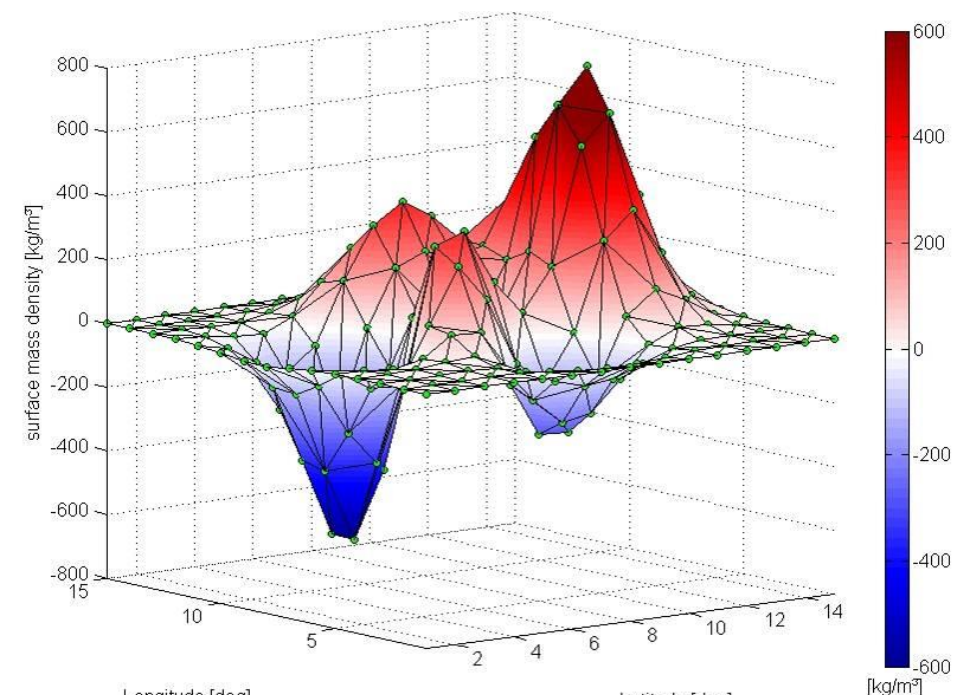
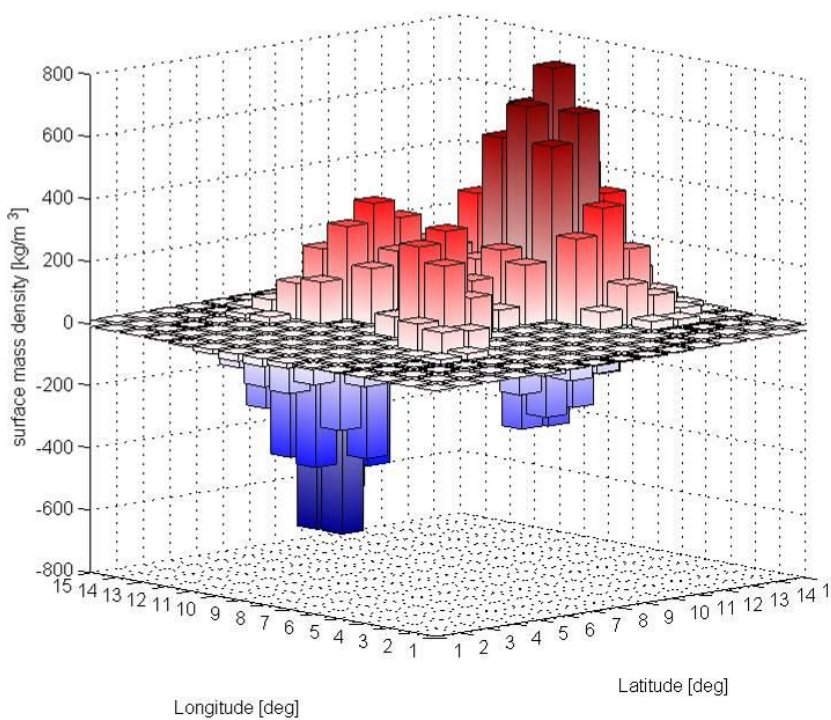
$\frac{\ddot{\rho}}{\rho}$ *LoS Gradiometry*
(Keller and Sharifi 2005)

...

Motivation for *in-situ* observations: local modeling

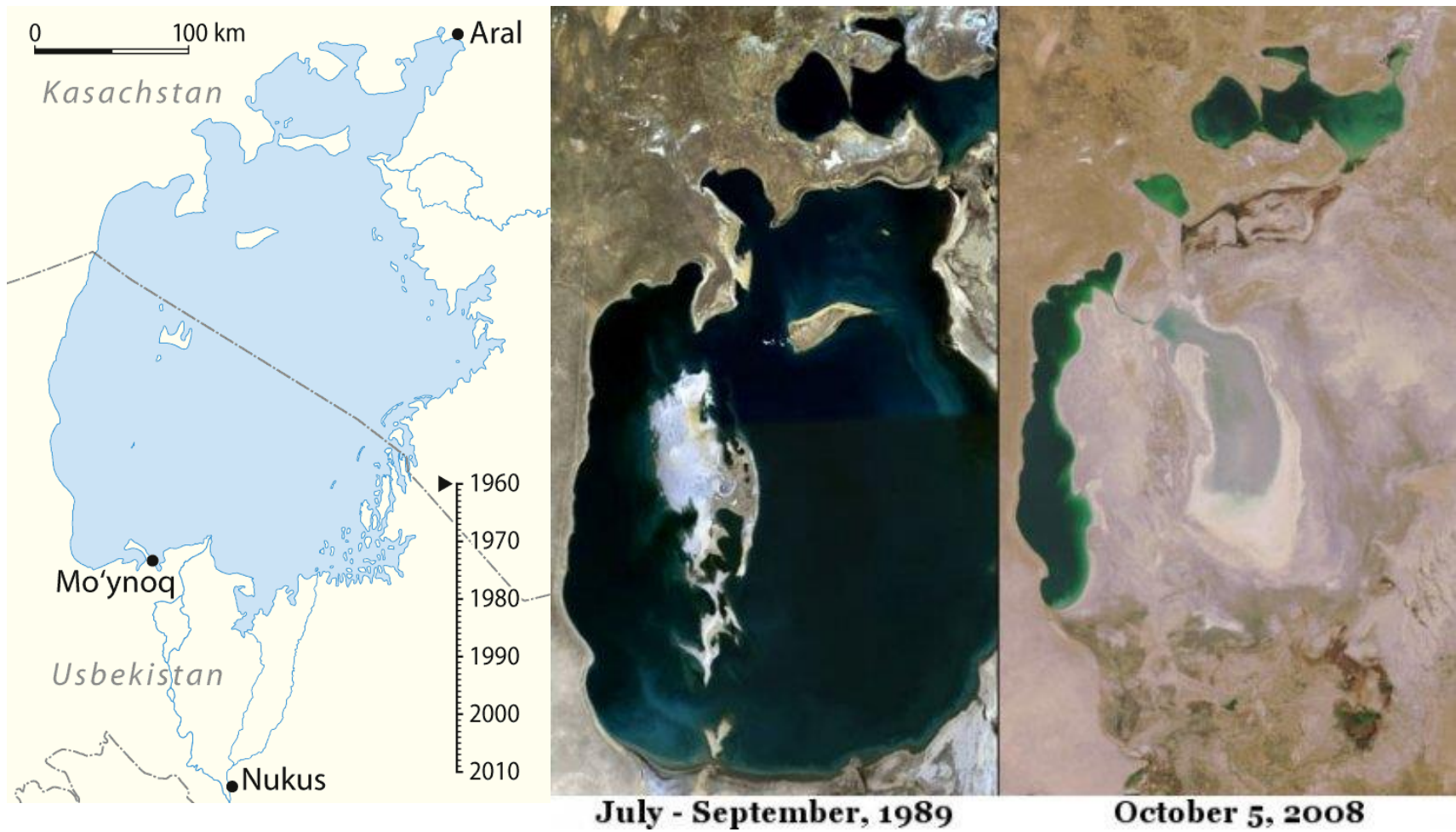
- Boundary element method

$$V = \int_{\Omega} \frac{\sigma(\vec{X}_Q)}{\|\vec{X} - \vec{X}_Q\|} d\vec{X}_Q = \sum_{i=1}^N \sigma_i \int_{\Omega_i} \frac{\Phi_i}{\|\vec{X} - \vec{X}_Q\|} d\Omega_i$$

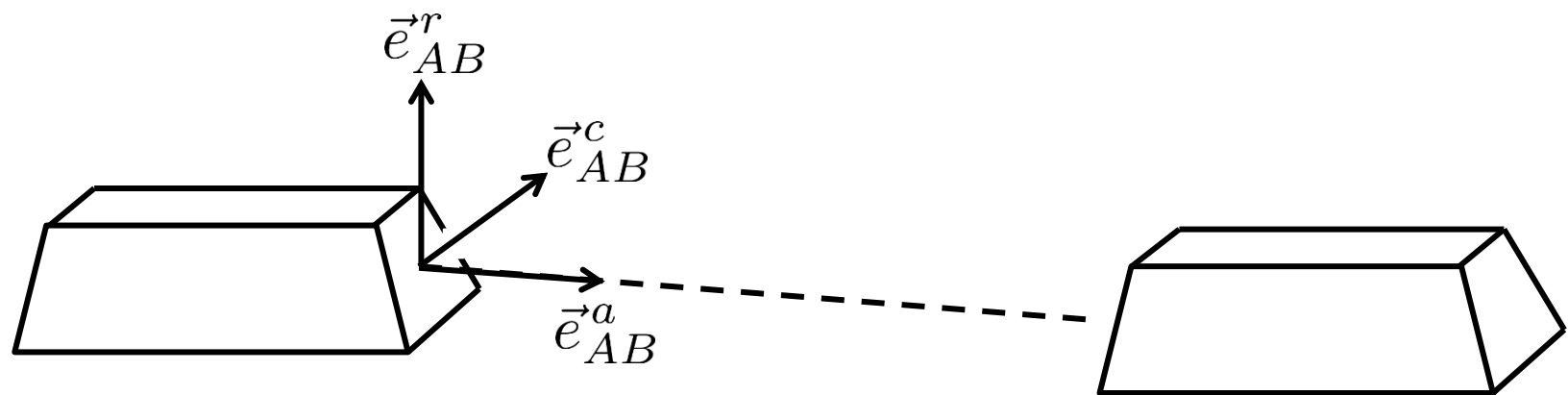


Motivation for *in-situ* observations: local modeling

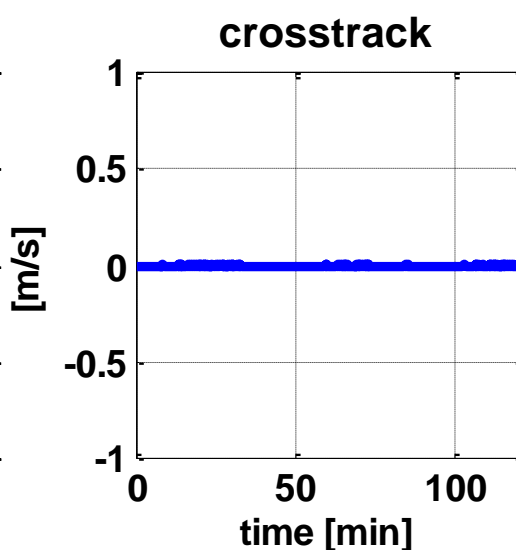
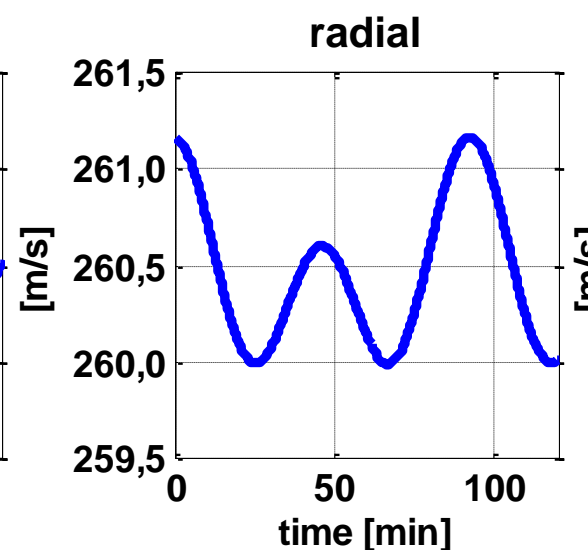
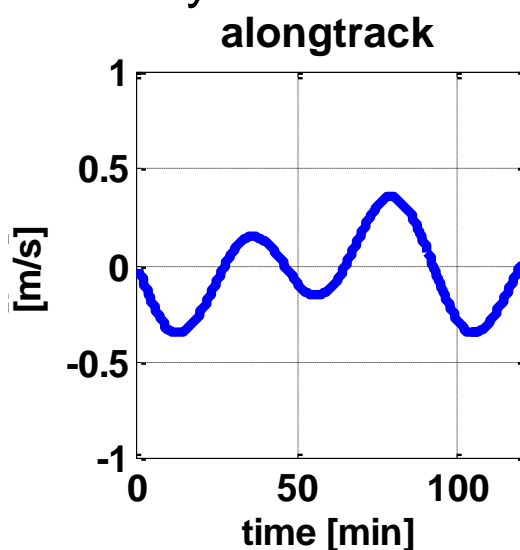
Water problems can only be solved on a basin scale.
(Robert Kandel – Water from Heaven)



IN-SITU OBSERVATIONS: DIFFERENTIAL GRAVIMETRY APPROACH



Velocity



Range observables:

$$\vec{X}_{AB} = \rho \cdot \vec{e}_{AB}^a$$

$$\dot{\vec{X}}_{AB} = \dot{\rho} \cdot \vec{e}_{AB}^a + \rho \cdot \dot{\vec{e}}_{AB}^a$$

$$\ddot{\vec{X}}_{AB} = \ddot{\rho} \cdot \vec{e}_{AB}^a + 2 \cdot \dot{\rho} \cdot \dot{\vec{e}}_{AB}^a + \rho \cdot \ddot{\vec{e}}_{AB}^a$$

Multiplication with unit vectors:

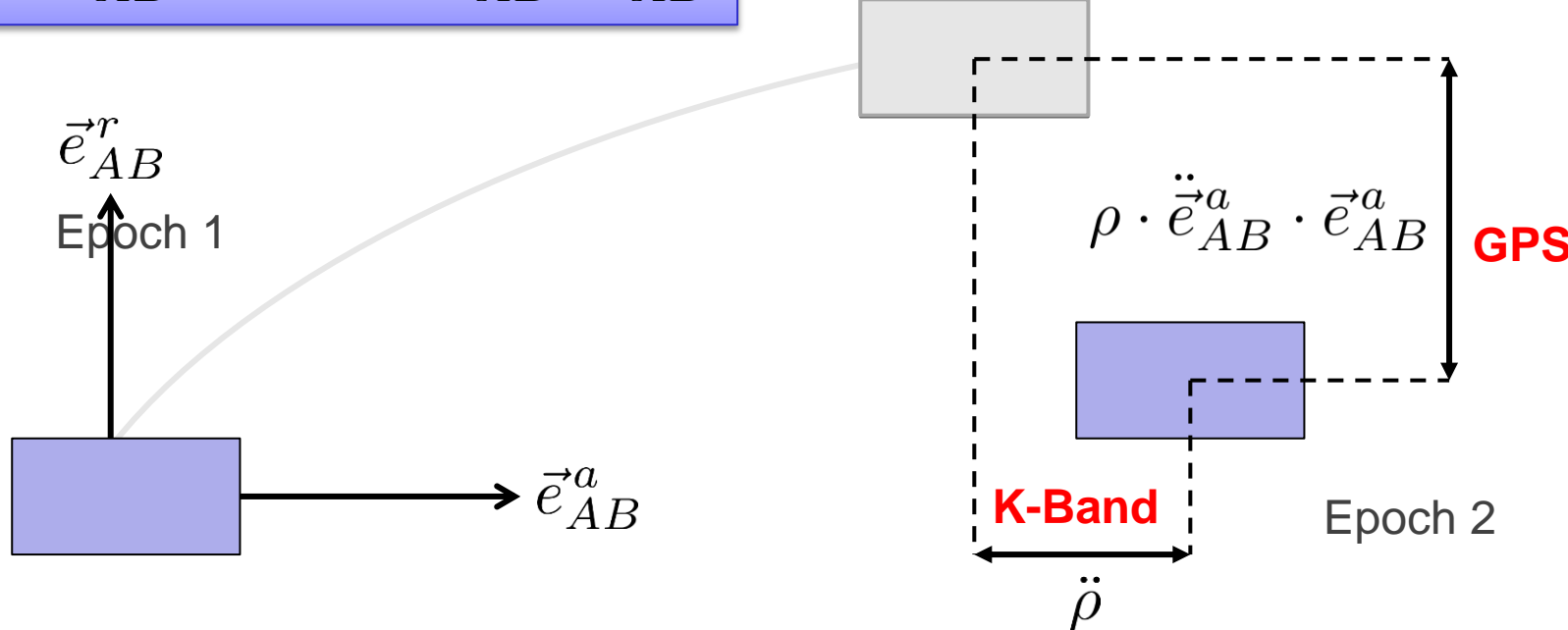
GRACE

$$\ddot{\vec{X}}_{AB} \cdot \vec{e}_{AB}^a = \ddot{\rho} + 0 + \rho \cdot \ddot{\vec{e}}_{AB}^a \cdot \vec{e}_{AB}^a$$

$$\ddot{\vec{X}}_{AB} \cdot \vec{e}_{AB}^r = 0 + 2 \cdot \dot{\rho} \cdot \|\dot{\vec{e}}_{AB}^a\| + \rho \cdot \ddot{\vec{e}}_{AB}^a \cdot \vec{e}_{AB}^r$$

$$\ddot{\vec{X}}_{AB} \cdot \vec{e}_{AB}^c = 0 + 0 + \rho \cdot \ddot{\vec{e}}_{AB}^a \cdot \vec{e}_{AB}^c$$

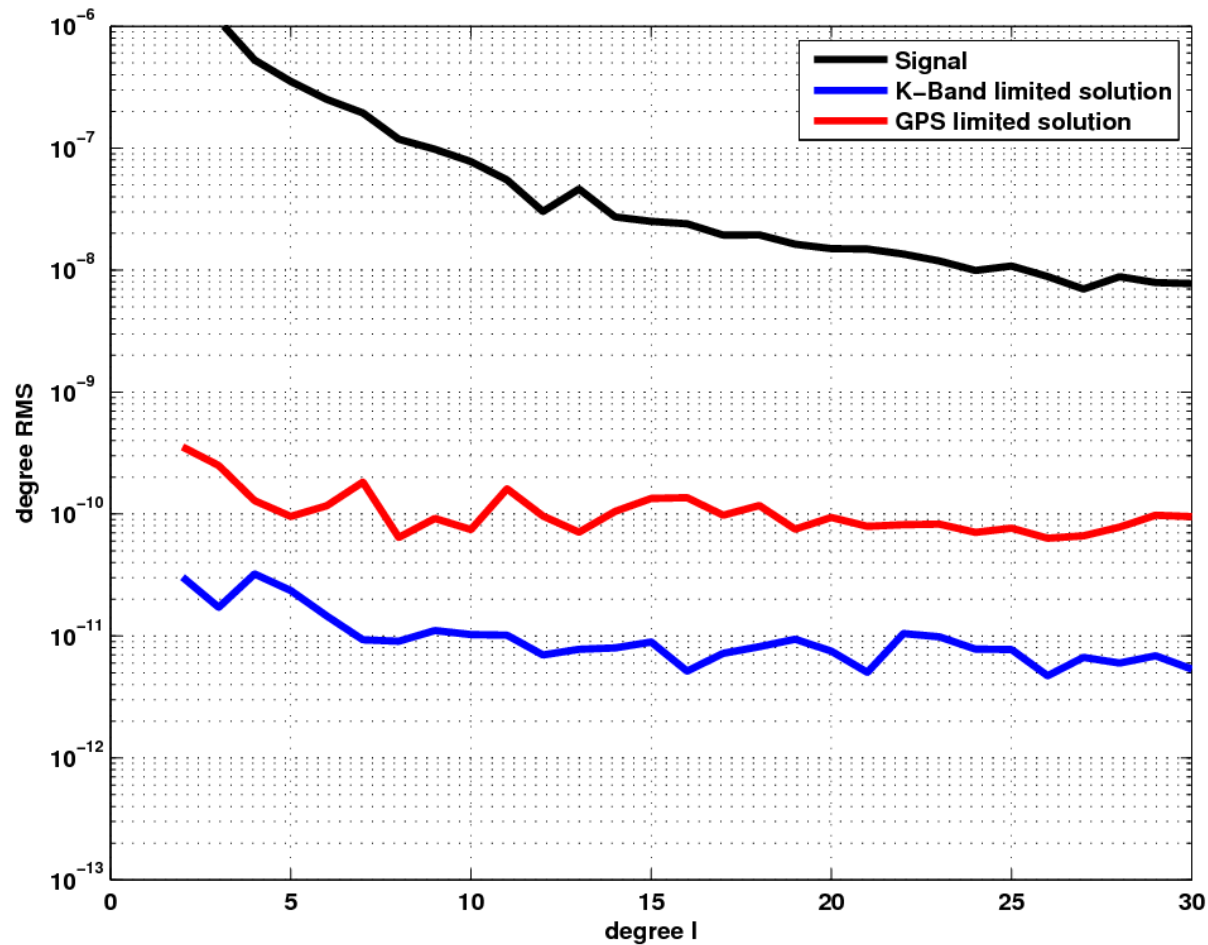
$$\ddot{\vec{X}}_{AB} \cdot \vec{e}_{AB}^a = \ddot{\rho} + \rho \cdot \ddot{\vec{e}}_{AB}^a \cdot \vec{e}_{AB}^a$$



$$\begin{aligned}
 \rho \cdot \ddot{\vec{e}}_{AB}^a \cdot \vec{e}_{AB}^a &= \vec{X}_{AB} \cdot \ddot{\vec{e}}_{AB}^a = -\dot{\vec{X}}_{AB} \cdot \dot{\vec{e}}_{AB}^a \\
 &= -\dot{\rho} \cdot \|\dot{\vec{e}}_{AB}^a\|^2 = -\frac{1}{\rho} \left(\dot{\vec{X}}_{AB} \cdot \dot{\vec{X}}_{AB} - \dot{\rho}^2 \right) \\
 &= -\rho \cdot \omega_c^2
 \end{aligned}$$

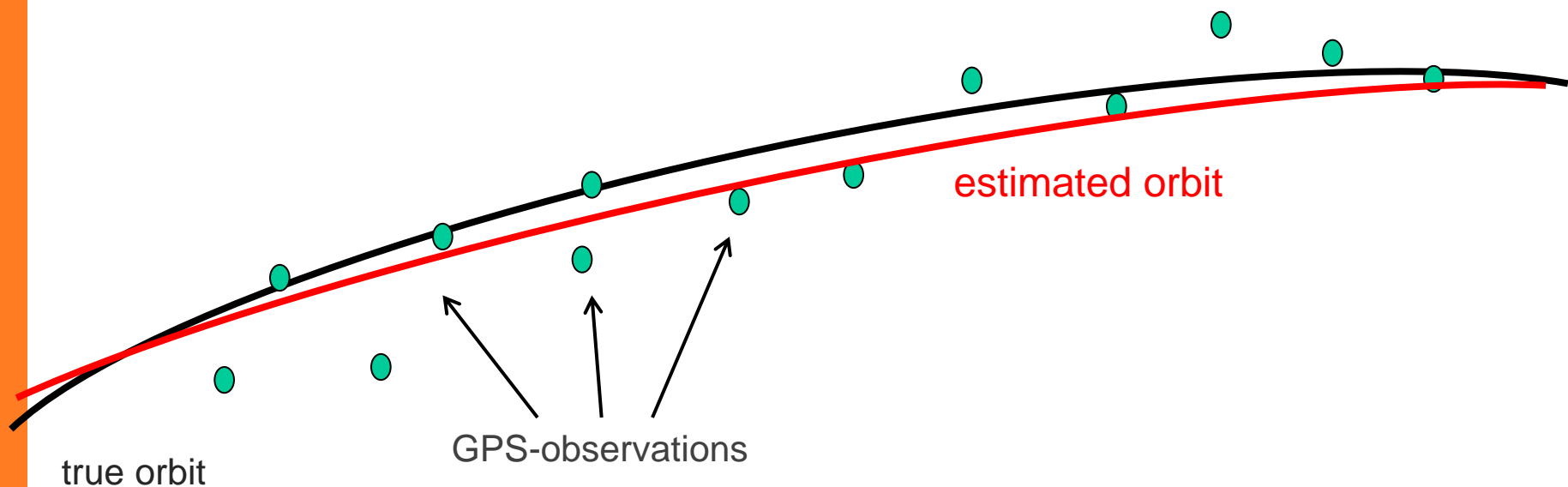
Limitation

Combination of highly precise K-Band observations with comparably low accurate GPS relative velocity



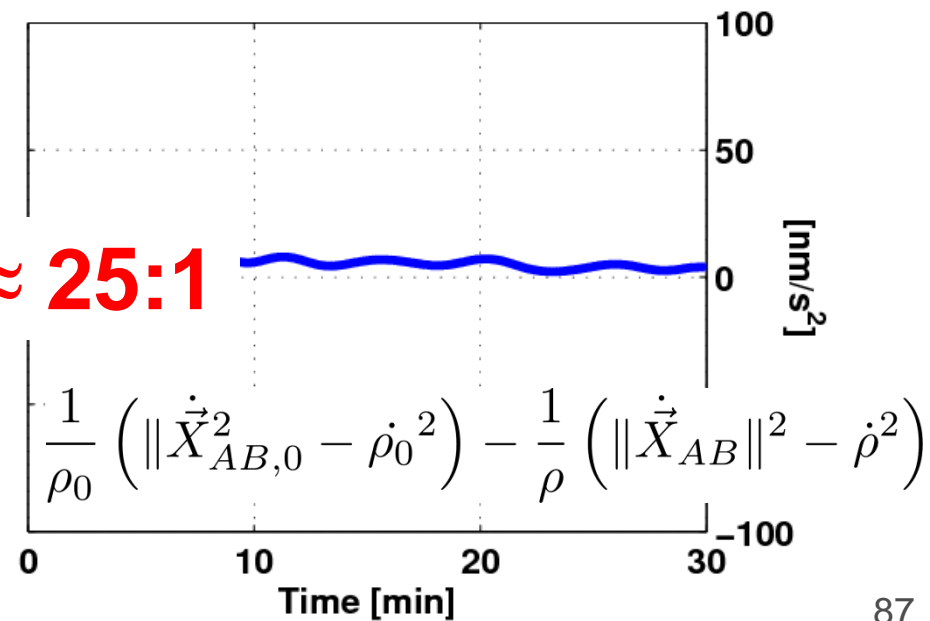
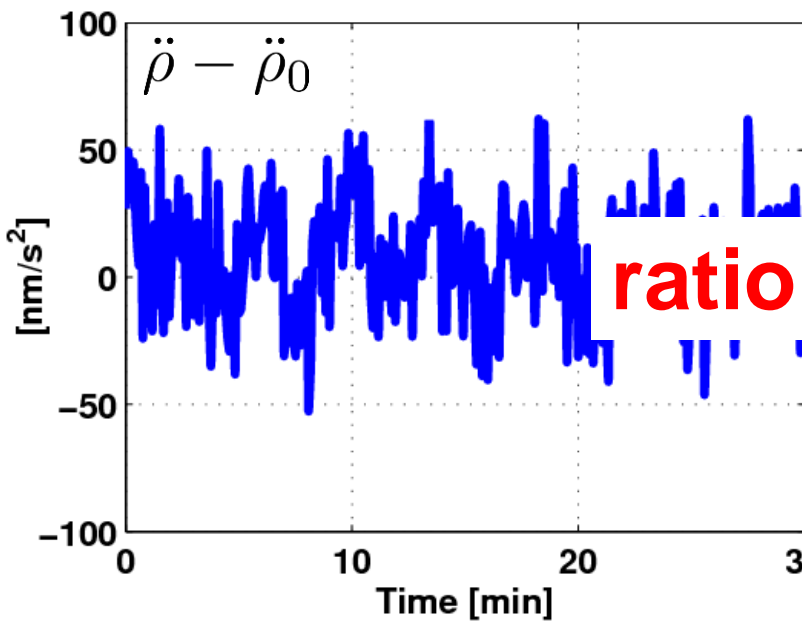
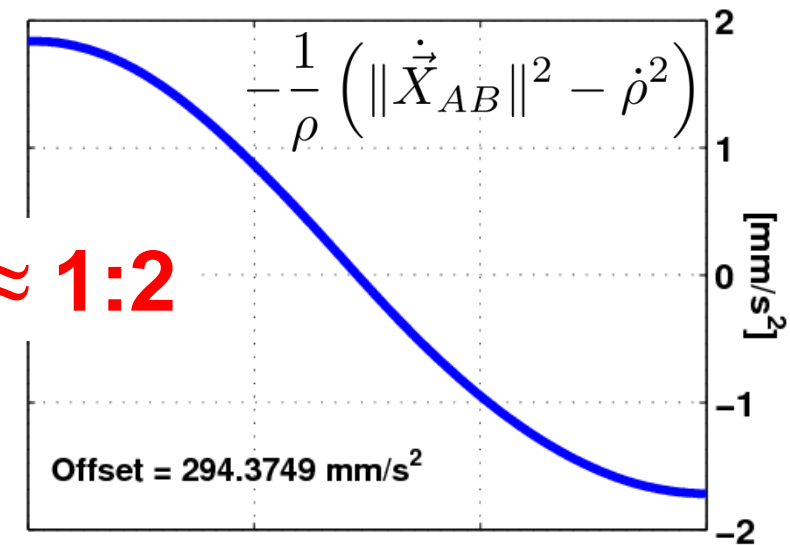
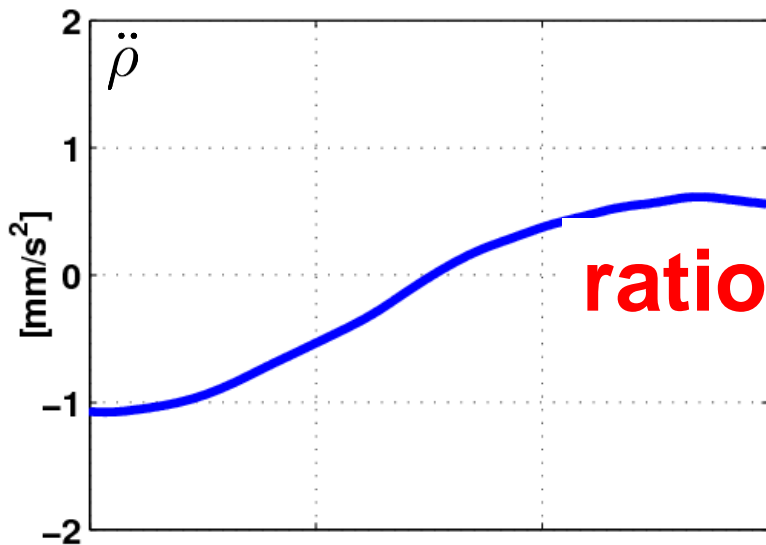
Residual quantities

- Orbit fitting using the homogeneous solution of the variational equation with a known a priori gravity field

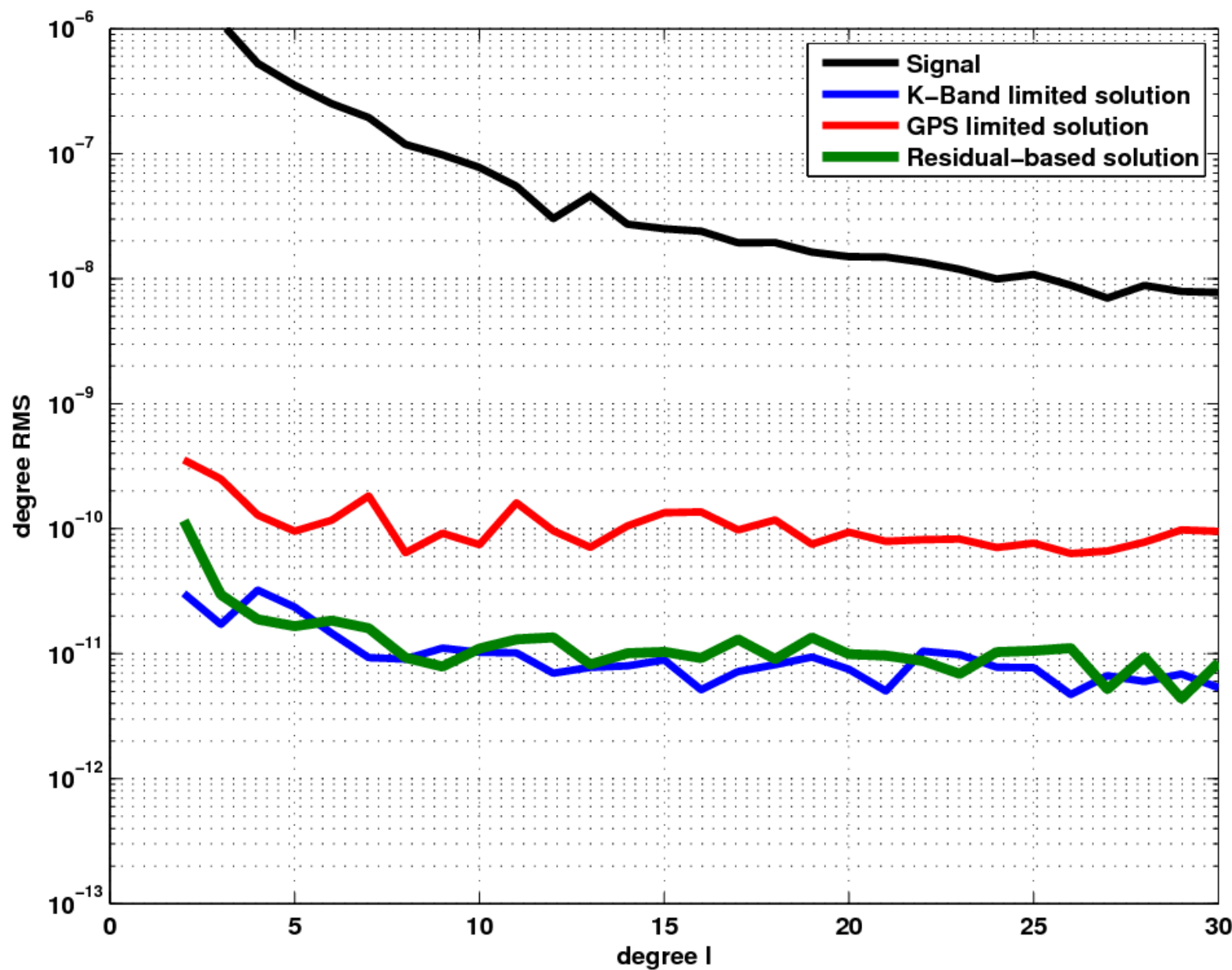


- Avoiding the estimation of empirical parameters by using short arcs

Residual quantities



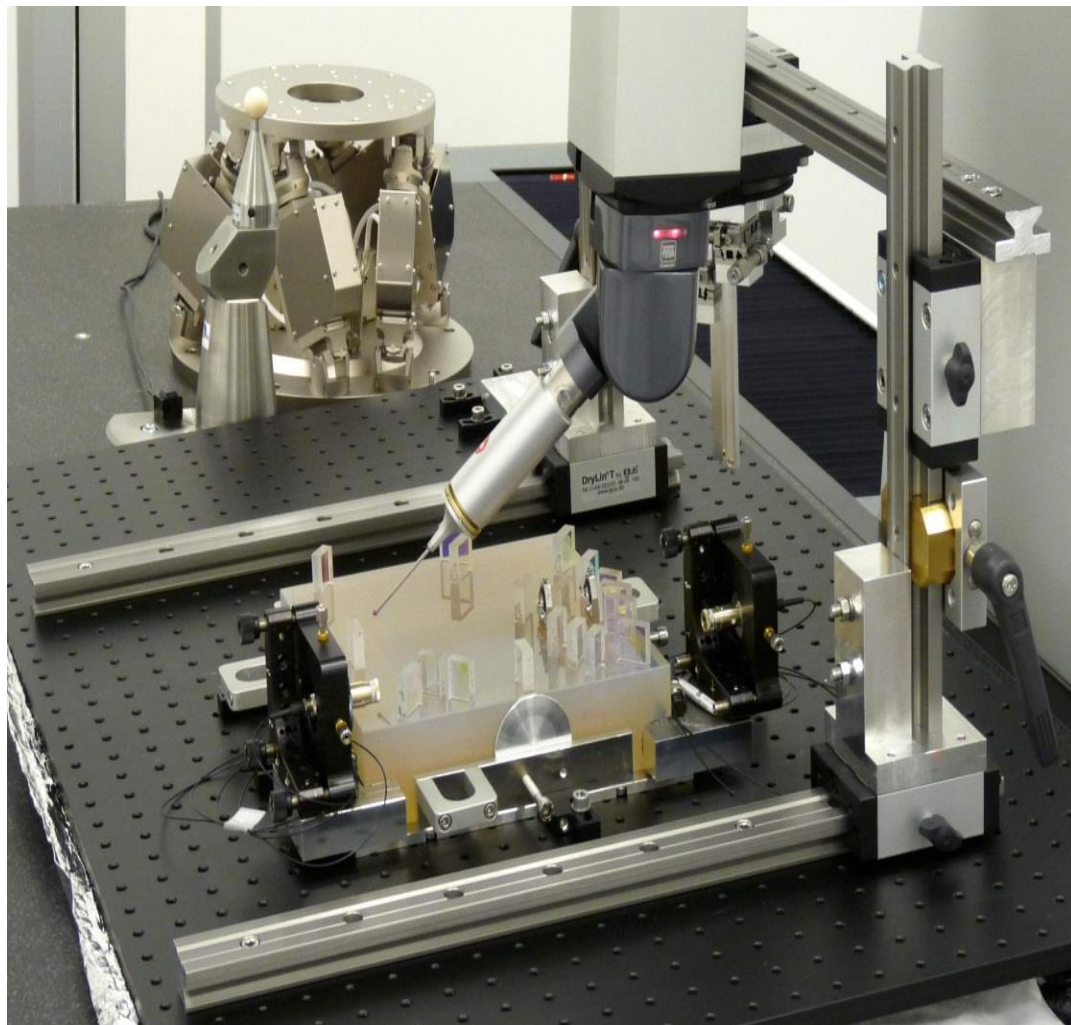
Approximated solution



GRACE FOLLOW-ON

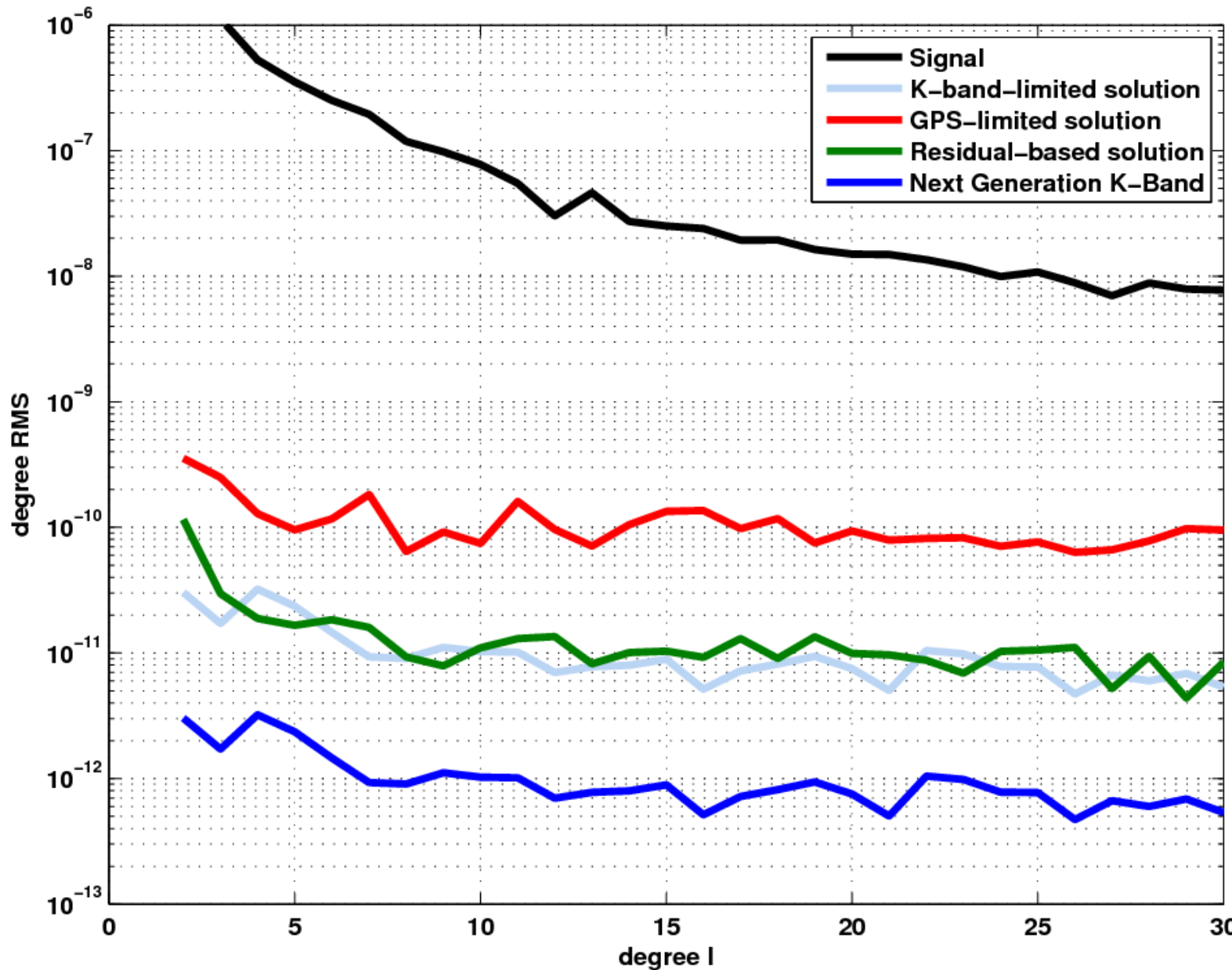
Next generation GRACE

- New type of inter-satellite distance measurement based on laser interferometry
- Noise reduction by factor 10 expected (factor 1000 possible)



M. Dehne, Quest

Solution for next generation GRACE



Variational equations for velocity term

- Reduction to residual quantity insufficient
- Modeling the velocity term by variational equations:

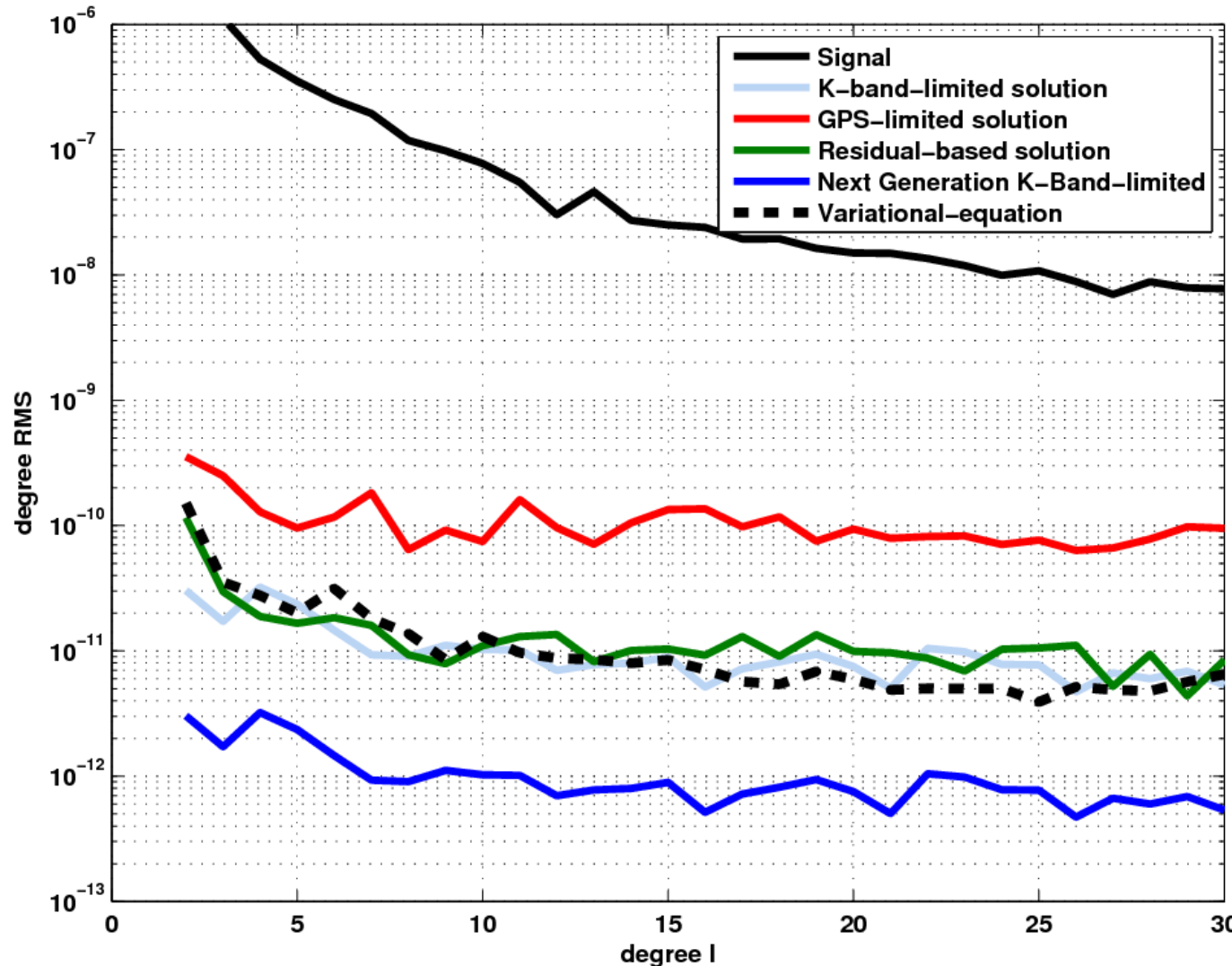
$$f = -\frac{1}{\rho} \left(\|\dot{\vec{X}}_{AB}\|^2 - \dot{\rho}^2 \right)$$

$$\frac{\partial f}{\partial p_i} = \frac{\partial f}{\partial x_A} \frac{\partial x_A}{\partial p_i} + \frac{\partial f}{\partial x_B} \frac{\partial x_B}{\partial p_i} + \dots + \frac{\partial f}{\partial \dot{z}_B} \frac{\partial \dot{z}_B}{\partial p_i}$$

- Application of the method of the variations of the constants
- Alternatively: application of the Hill equations

Results

- only minor improvements
- possibly the orbit fit to the GPS positions as a limiting factor



ICCT

Applicability of current GRACE solution strategies to the next generation of inter-satellite range observations

Chair: Matthias Weigelt

Co-Chair: Adrian Jäggi

The objectives of the study group are to:

- investigate each solution strategy, identify approximations and linearizations and test them for their permissibility to the next generation of inter-satellite range observations,
- investigate the interaction with global and local modeling,
- extend the applicability to planetary satellite mission, e.g. GRAIL
- establish a platform for the discussion and in-depth understanding of each approach and provide documentation.

**It is not the idea,
to find the best approach!**

Example: sensitivity to non-gravitational error sources

- Calibration of the accelerometer:

- Calibration model for GRACE:

$$\tilde{\vec{f}} = (1 + S_1) \vec{f} + \vec{b}$$

- Full calibration model for an accelerometer

$$\tilde{\vec{f}} = (1 + S_1) \vec{f} + S_2 \vec{f}^2 + N \vec{f} + \vec{b}$$

with: \vec{b} bias

S_1 linear scale matrix

S_2 non-linear scale matrix

N misalignment matrix

- Calibration with GPS-positioning!

Interaction between approaches and modeling

In collaboration with JSG 0.3:

Comparison of methodologies for regional gravity field modeling

Chair: M. Schmidt, Co-Chair: Ch. Gerlach

Users interest in **regional mass variations**, e.g. floodings:

Requirements are:

- **enhanced spatial resolution**,
- **arbitrary regions** of interests (river basins, etc.),
- **combinations of measurement techniques** (space gravity missions, airborne, terrestrial, altimetry, other remote sensing, etc.).

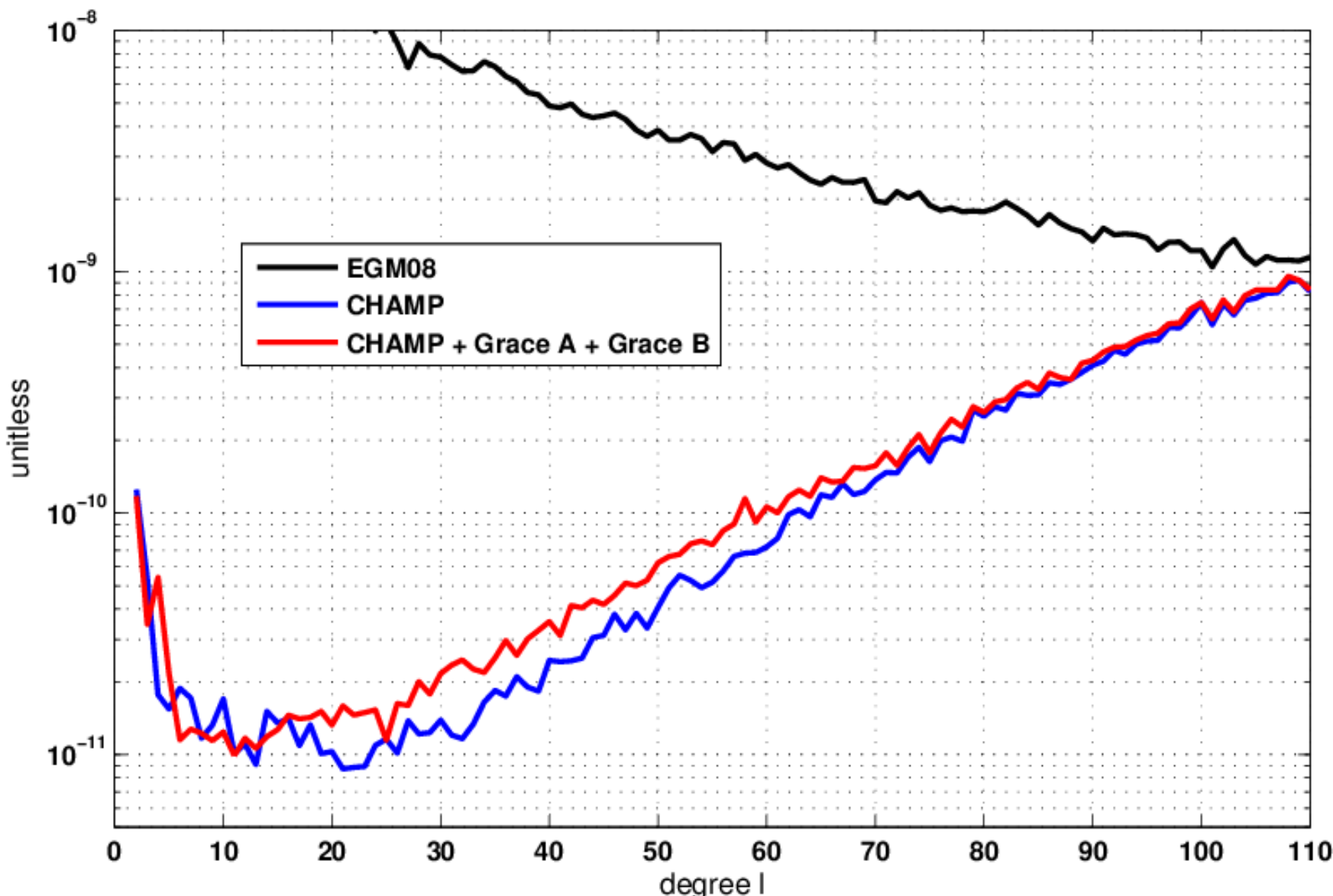
- Simulation

Are we prepared for future satellite missions?

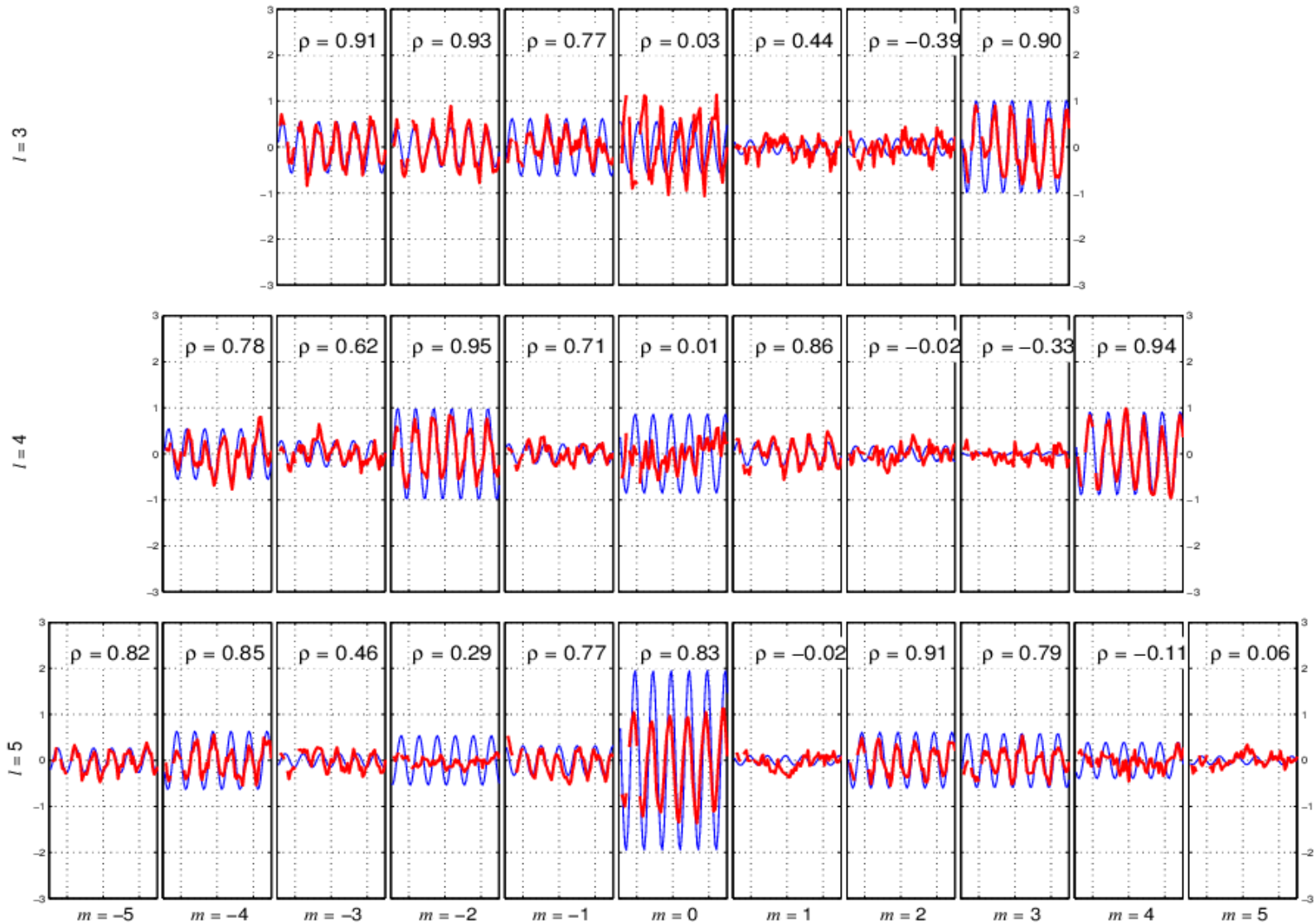
- *Yes, but we should also make use of the time.*
 - e.g. applicability of approaches to GFO
- *Satellite systems (...) need to be better understood.*
 - e.g. spatial aliasing
- *Thinking outside of the box*
 - e.g. high-low SST as transitory technology

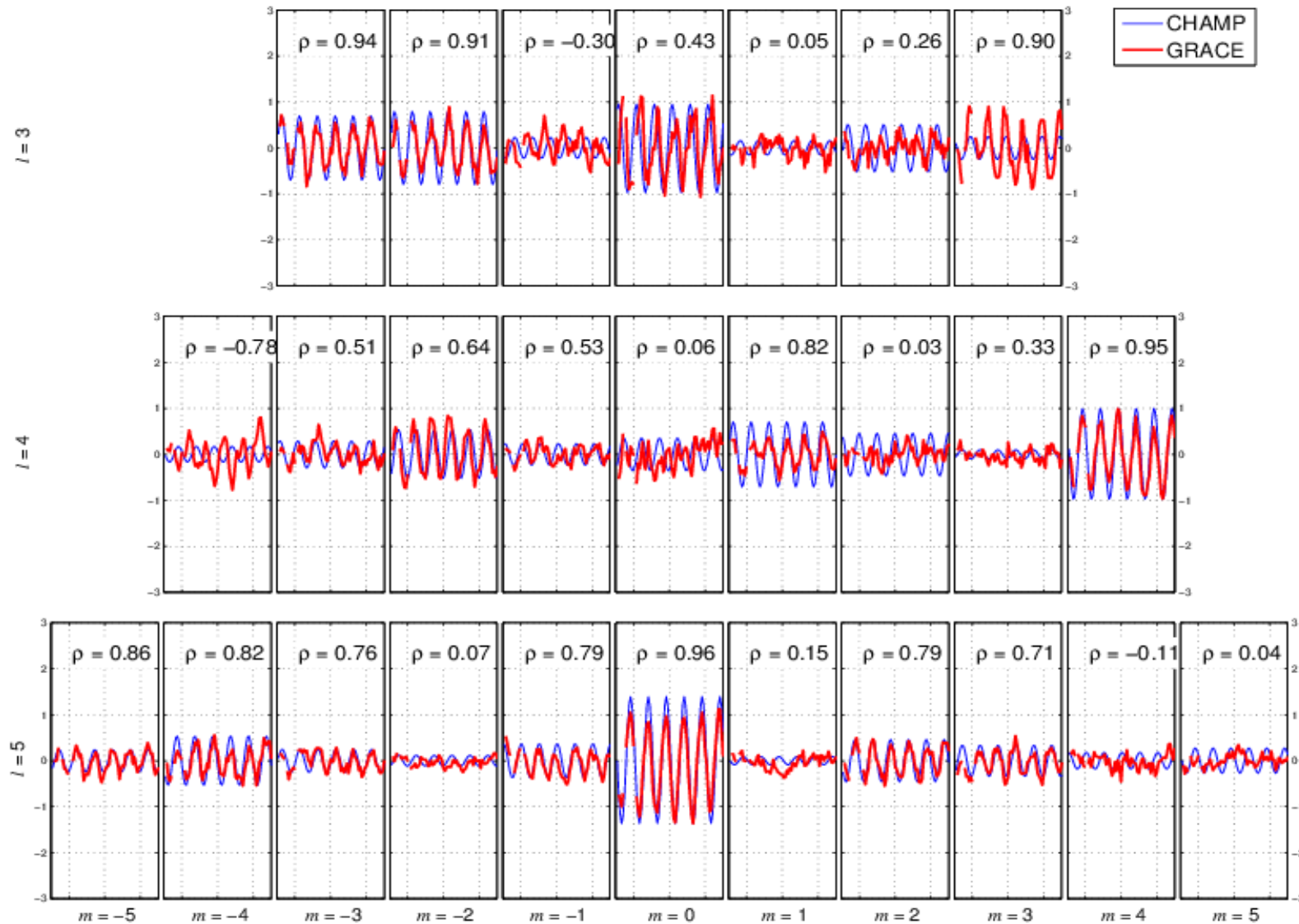
BACKUP

CHAMP + GRACE A + GRACE B

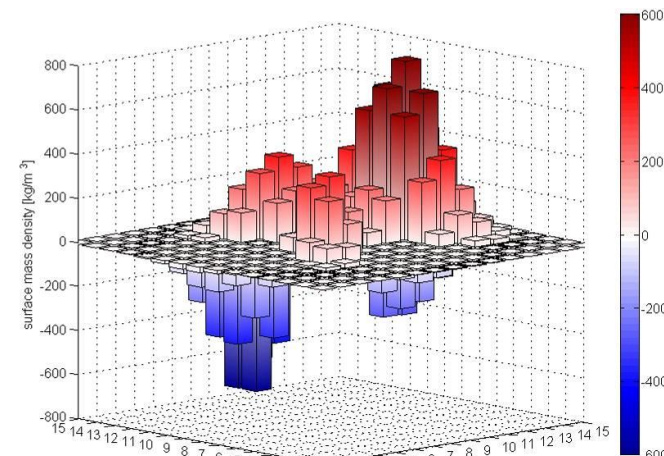
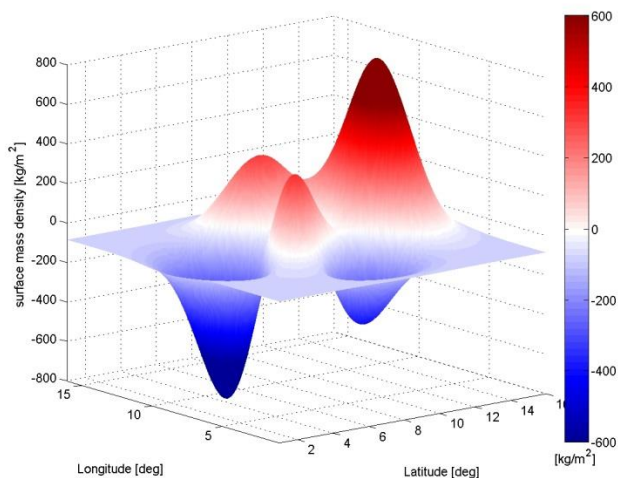


Time series of SH-coefficients: GRACE vs. CH+GA+GB (annual) – scaled by 10^{10}

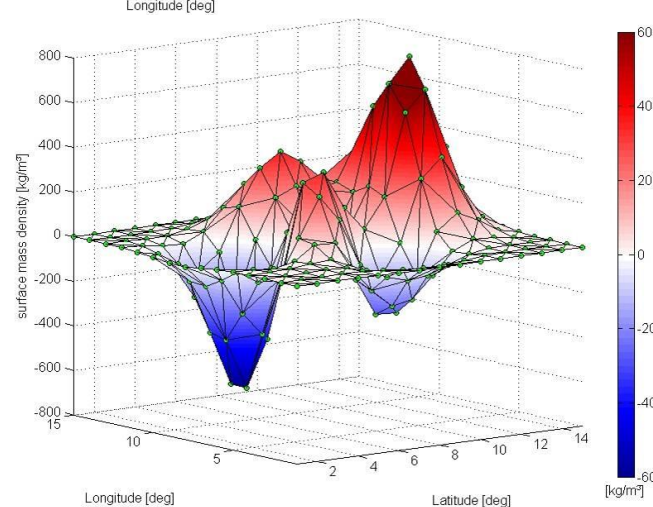


Time series of SH-coefficients: GRACE vs. CHAMP (annual) – scaled by 10^{10} 

*Decomposition of the surface into elements with finite extend
(boundary elements)*



e.g. blocks



e.g. triangles

Example: Consider the single layer potential

$$V = \int_{\Omega} \frac{\sigma(\vec{X}_Q)}{\|\vec{X} - \vec{X}_Q\|} d\vec{X}_Q$$

Separation of the surface into elements: $\Omega = \sum_{i=1}^N \Omega_i$

Assumption:

$$\vec{X} = \sum_{k=1}^K \Phi_{i,k}^{\vec{X}} \vec{X}_{i,k}$$

$$\sigma_i(\vec{X}_Q) = \sum_{k=1}^K \Phi_{i,k}^{\sigma} \sigma_{i,k}(\vec{X}_{i,k})$$

*The boundary elements are called **isoparametric** if $\Phi_{i,k}^{\vec{X}} = \Phi_{i,k}^{\sigma}$*

Example: Consider the single layer potential

Including transformation to the normal triangle and spherical integration

$$V = \frac{GR^2}{4\pi} \sum_{i=1}^N \sum_{k=1}^K \sigma_{i,k} \int_{-1}^1 \int_{-1}^{-\xi} \frac{J_i(\xi, \eta) \cdot \Phi_{i,k}(\xi, \eta) \cdot \cos \phi(\xi, \eta)}{\|\vec{X}(r, \phi, \lambda) - \vec{X}(R, \phi(\xi, \eta), \lambda(\xi, \eta))\|} d\eta d\xi$$

Integration by Gaussian quadrature

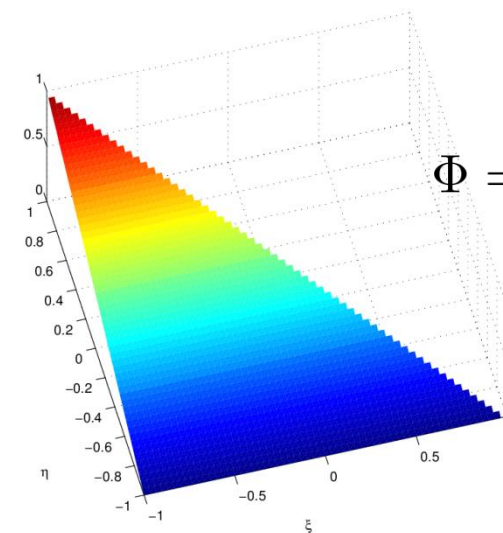
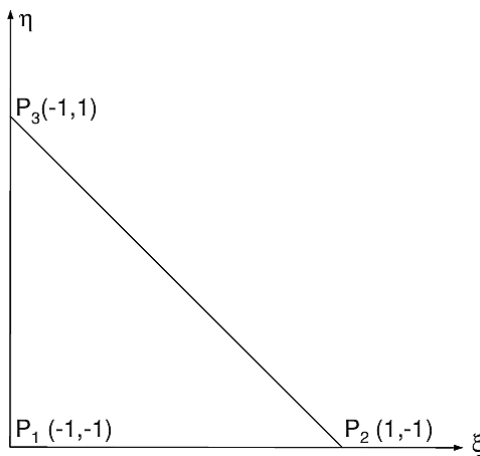
$$\int_{-1}^1 \int_{-1}^{-\xi} \dots d\eta d\xi \Rightarrow \sum_{l=1}^L \sum_{m=1}^L w_l w_m \dots \quad \text{with } w_l w_m = 0 \text{ for } m > l$$

Integration is exact for a polynomial of order $2L$.

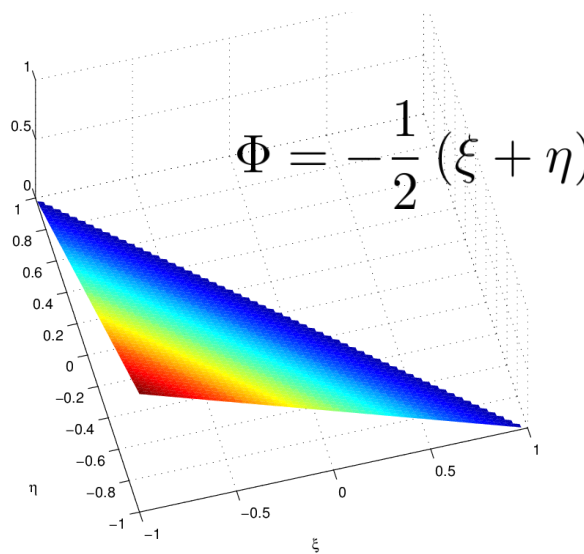
Base functions are

- *strictly space-limited (i.e. band-unlimited)*
- *compact*
- *continuous but not differentiable at the edges*
- *singular if the point of interest lies inside or on the corner of the element*
 - *Weak singularity for potential* $\left(\frac{1}{r}\right)$
 - *Strong singularity for gradient* $\left(\frac{1}{r^3}\right)$

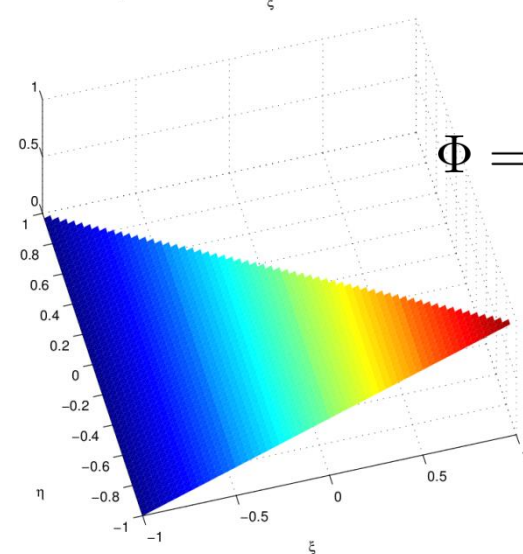
Example: linear triangle



$$\Phi = \frac{1}{2} (\eta + 1)$$

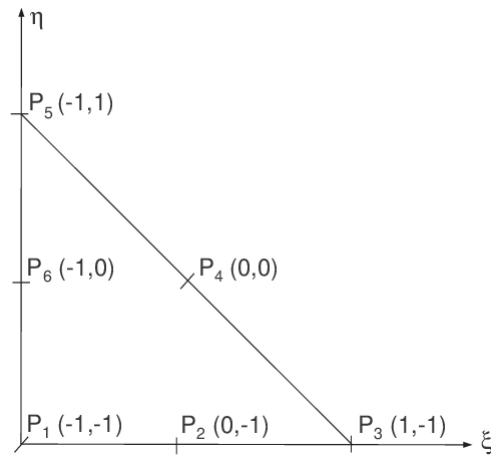


$$\Phi = -\frac{1}{2} (\xi + \eta)$$

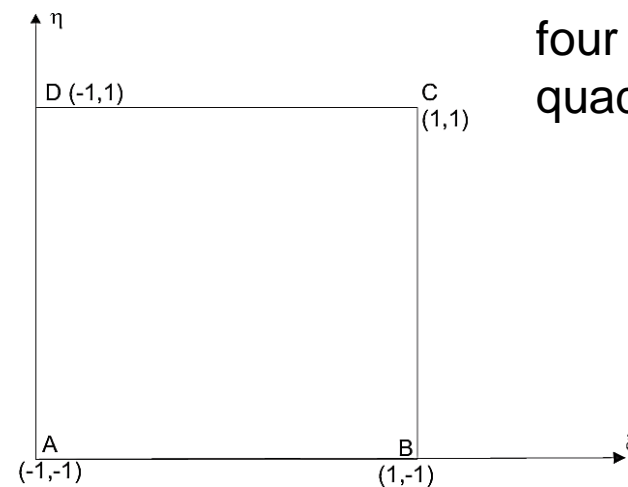


$$\Phi = \frac{1}{2} (\xi + 1)$$

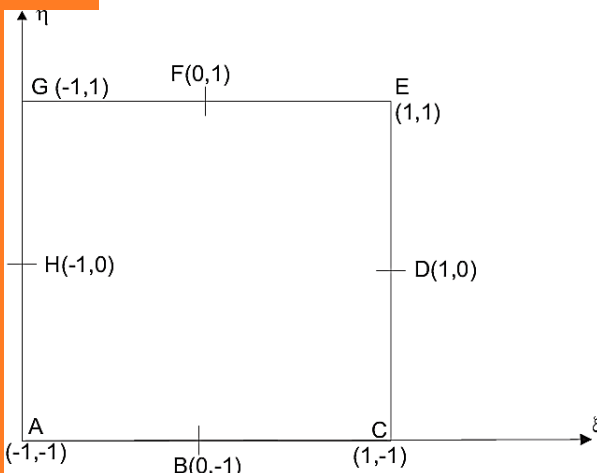
six node triangle



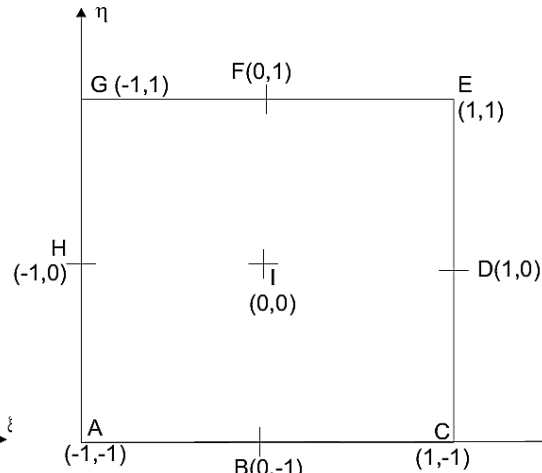
four node quadrilateral



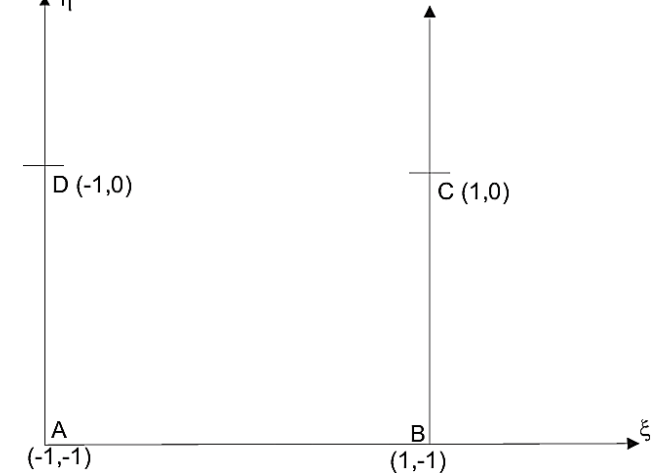
eight node quadrilateral:



nine node quadrilateral:

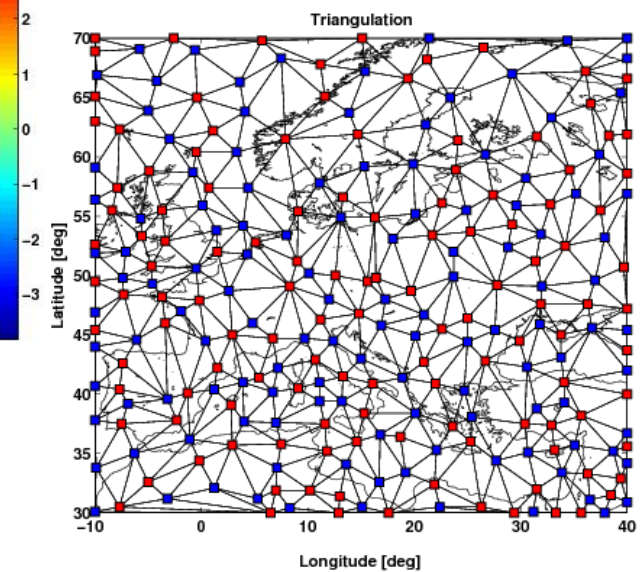
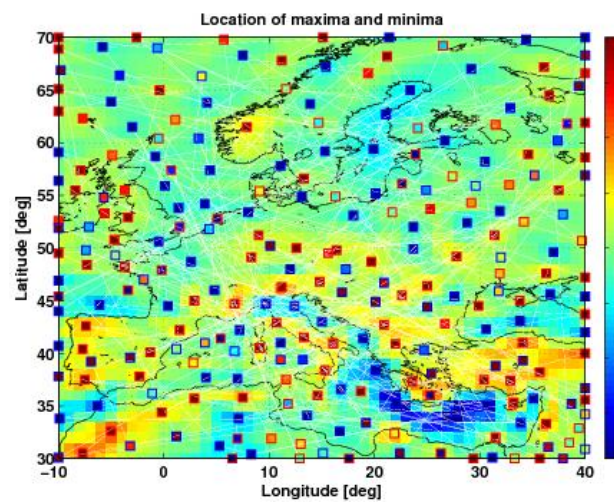
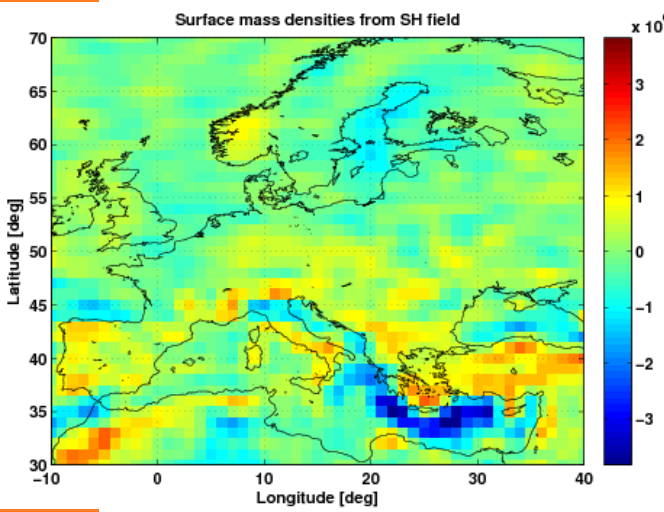


infinite quadrilateral:

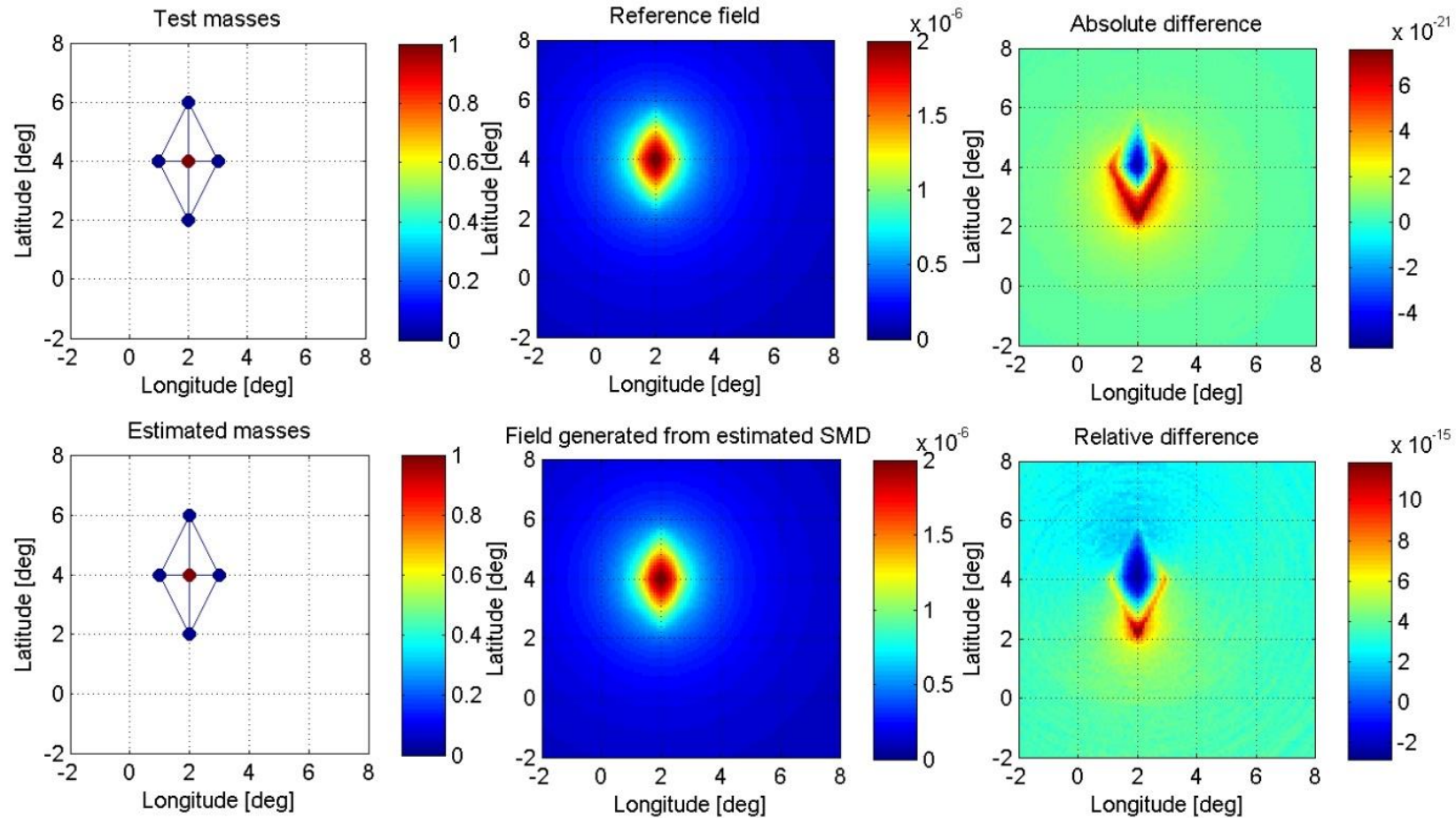


Point grid: any (as long as a proper tessellation is possible)

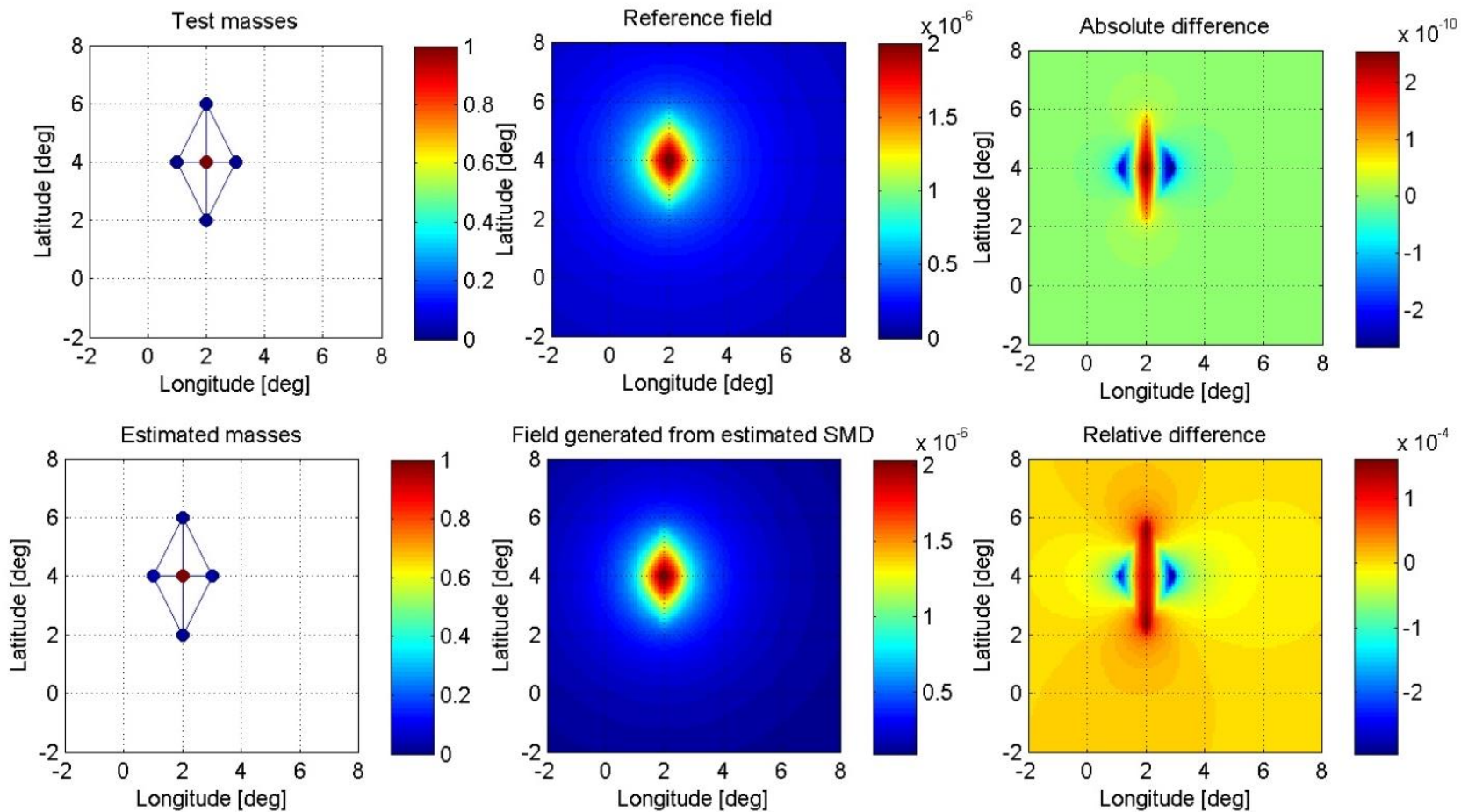
Currently based on the maxima and minima of an a priori field



- *Search for maxima and minima of an a priori field*
- *Triangulation by Delaunay tessellation*
- *Least-squares adjustment*
 - *brute-force*
 - *assembly of the normal matrix (singularity!)*
 - *full consideration of the stochastic information*
- *No regularization*
 - *objective: avoid regularization by proper grid*
 - *iterative search for vertices*

Closed loop simulation: noisefree and $h=0\text{km}$ 

Closed loop simulation: noise=1% and h=400km



Simulation study

